Title

Assessing the threat of two deadly fungal pathogens (Batrachochytrium dendrobatidis and Batrachochytrium salamandrivorans) to amphibian biodiversity and the impacts of human-mediated movement of an invasive carrier species and climate change

Author

Yap, Tiffany

Publication Date

2016

Peer reviewed|Thesis/dissertation

UNIVERSITY OF CALIFORNIA

Los Angeles

Assessing the threat of two deadly fungal pathogens (*Batrachochytrium dendrobatidis* and *Batrachochytrium salamandrivorans*) to amphibian biodiversity and the impacts of human-mediated movement of an invasive carrier species and climate change

A dissertation submitted in partial satisfaction

of the requirements for the degree of

Doctor of Environmental Science and Engineering

by

Tiffany Ann Yap

2016

Abstract of the Dissertation

Assessing the threat of two deadly fungal pathogens (*Batrachochytrium dendrobatidis* and *Batrachochytrium salamandrivorans*) to amphibian biodiversity and the impacts of human-mediated movement of an invasive carrier species and climate change

by

Tiffany Ann Yap

Doctor of Environmental Science and Engineering

University of California, Los Angeles, 2016

Professor Richard F. Ambrose, Co-Chair

Professor Vance T. Vredenburg, Co-Chair

Batrachochytrium dendrobatidis (*Bd*), a fungal pathogen that causes chytridiomycosis in amphibians, has infected >500 species and caused declines and extinctions in >200 species. Recently, a second deadly fungal pathogen that also causes chytridiomycosis*, Batrachochytrium salamandrivorans* (*Bsal*) was discovered. The presence of these lethal pathogens in international trade threatens amphibian diversity. In this dissertation, I use a novel modeling approach to predict disease risk from *Bd* and/or *Bsal* to amphibian populations in North America and Asia by incorporating pathogen habitat suitability, host availability, the potential presence of an invasive carrier species, and pathogen invasion history. First I identify *Bsal* threat to North American salamanders to be greatest in the Southeast US, the West Coast, and highlands of Mexico. I then

investigate the compounded risk of *Bd* and *Bsal* in North America and find highest relative risk in those same areas and in the Sierra Nevada Mountains and the northern Rocky Mountains. However, when I incorporate the historical context of *Bd* into the model by treating the eastern US as the native range of *Bd*, I find invasive *Bd* risk to be highest in the mountain ranges of the western US and Mexico, which could influence how amphibians in these areas respond to *Bsal*. I also uncover a pattern that suggests the translocation of the American bullfrog (*Rana catesbeiana*) to western North America may have facilitated *Bd* spread. Last, I investigate the threat of *Bd* in Asia and find that mountain forests in China, Southeast Asia, and the Pacific Islands have the highest relative *Bd* risk, and the potential presence of *R. catesbeiana* and amphibian richness may have a strong influence on *Bd* risk. I also predict that climate change may lead to a 3-23% decrease in total area of *Bd* risk in Asia by 2070. These findings provide helpful guidance for conservation planning and management by further highlighting the role of *R. catesbeiana* in *Bd* spread and identifying areas at highest risk to prioritize for surveillance, monitoring, and species susceptibility studies needed to enhance our understanding of the pathogen invasion history, disease dynamics, and potential interactions of *Bd* and *Bsal*.

The dissertation of Tiffany Ann Yap is approved.

Thomas Welch Gillespie

James O. Lloyd-Smith

Richard R. Vance

Richard F. Ambrose, Committee Co-Chair

Vance T. Vredenburg, Committee Co-Chair

University of California, Los Angeles

2016

Dedication

To my parents, Drs. Celia and Sisenando Yap.

Table of Contents

List of Figures

List of Tables

List of Appendices

Acknowledgements

Deep gratitude goes to my UCLA co-advisor, Rich Ambrose, an extraordinary mentor who has advised and guided me with patience, wisdom, and open flexibility, always emphasizing the process and looking out for my best interests. And a major thank you to my San Francisco State University co-advisor, Vance Vredenburg, whose enthusiasm and trust helped me power through and complete this work.

I am thankful to the faculty and staff of the ESE Program, especially Keith Stolzenbach, Arthur Winer, Mel Suffet, and Myrna Gordon, for their dedication to the program and their constant encouragement. I have extreme appreciation for my collaborators at the Museum of Vertebrate Zoology at UC Berkeley, Michelle Koo and David Wake, who were generous with their time and knowledge of bioinformatics and the amphibian world. I am thankful to my committee members, Tom Gillespie, Jamie Lloyd-Smith, and Rick Vance, for their guidance, support, and enthusiasm for science and exploration. And I thank undergraduate research apprentices at UC Berkeley and San Francisco State University that helped with data collection and data mining. Some of my graduate expenses were funded through the William and Flora Hewlett Foundation and the Charles F. Scott Fellowship.

This work would not be possible without the availability of private and public data. Private disease data (occurrences of *Batrachochytrium dendrobatidis*) were provided by Vredenburg Lab collaborators from all over the world, and I am thankful for their generosity in sharing these data. Public data from Amphibiaweb (http://www.amphibiaweb.org), VertNet (http://www.vertnet.org), the IUCN (http://www.iucnredlist.org), WorldClim, (http://www.worldclim.org), the US Geological Survey, the US Fish and Wildlife Service, the Center for International Earth Science Information Network (http://www.ciesin.org), and the

Consortium for Spatial Information (http://www.cgiar-csi.org/data) were invaluable, and I am thankful to these collections and organizations for sharing their data.

Chapter 2 is a version of Yap et al. (2015)[1], published in July 2015 in *Science*. It was coauthored by Vance Vredenburg, Michelle Koo, Rich Ambrose, and David Wake. Vance and Michelle co-developed the study and, with Rich, substantially contributed to the concepts presented. David provided expertise and oversight regarding salamander ecology and editorial insight. I feel extremely lucky to have had the opportunity to work with these amazing scientists and share this publication with them.

Chapters 3 and 4 are in preparation for publication. They were both coauthored by Vance Vredenburg, Michelle Koo, and Rich Ambrose. Similar to Chapter 2, Vance and Michelle co-developed the studies and, with Rich, substantially contributed to the concepts presented.

Finally, I am thankful to my family and friends for their unconditional love and support as I continue on my life journey.

[1] Yap, TA, Koo, MS, Ambrose, RF, Wake DB, Vredenburg, VT (2015) Averting a North American biodiversity crisis. *Science* 349(6247):481–482. doi:10.1126/science.aab1052

Vita

Education and Employment

2001	B.A. Integrative Biology, with Minor in Education University of California, Berkeley
2002	Curatorial Assistant Museum of Vertebrate Zoology University of California, Berkeley
2002-2004	Staff Research Associate Northern California Institute of Research and Education/University of California, San Francisco
2005-2007	Staff Research Associate/Lab Manager University of California, Los Angeles
2008-2011	Graduate Student Researcher University of California, Los Angeles
2009	Research Assistant Southern California Coastal Water Research Project
2009	M.S. Environmental Health Sciences with a Certification in Leaders in Sustainability University of California, Los Angeles
2011-Present	Environmental Scientist III AECOM

Publications

2015	**Yap, TA**, Koo, MS, Ambrose, RF, Wake, DB, Vredenburg, VT (2015) Averting a North American biodiversity crisis. *Science* 349(6247):481–482. doi:10.1126/science.aab1052
2016	**Yap, TA,** Gillespie L, Ellison S, Flechas SV, Koo MS, Martinez AE, Vredenburg VT (2016) Invasion of the fungal pathogen *Batrachochytrium dendrobatidis* on California Islands. *Ecohealth* 13(1):145-150. doi: 10.1007/s10393-015- 1071-y

Presentations and Invited Lectures

2011	**Yap, TA**, Ambrose, RF (2011) "Linking the Motile and Sessile Organisms Data." Annual Multi-Agency Rocky Intertidal Network (MARINe) workshop
2012	**Yap, TA**, Ambrose, RF (2012) "Investigating Rockweed Abundances in the Rocky Intertidal of the West Coast of the USA." Annual MARINe workshop
2015	**Yap, TA** (12 May 2015) "A new chytrid fungal pathogen threatens North American salamander biodiversity." Colloquium in Ecology, Evolution, and Conservation Biology, San Francisco State University
2015	Koo, MS, **Yap TA**, Vredenburg VT, Catenazzi A, Spencer CL, Wake DB (1 Aug 2015) "Averting a biodiversity crisis: AmphibiaWeb addresses the new *Bsal* threat." Society for the Study of Amphibians and Reptiles Meeting, University of Kansas
2015	Koo, MS, **Yap TA**, Vredenburg VT, Catenazzi A, Spencer CL, Wake DB (11 Aug 2015) "Averting a biodiversity crisis: AmphibiaWeb addresses the new *Bsal* threat." Southern Appalachia *Bsal* Meeting, Asheville, NC
2015	**Yap, TA** (2 December 2015) "Salamander vulnerability to *Bsal*, a lethal chytrid fungus." EcoINFORMA Workshop: Promoting Synergy in the innovative use of environmental data. Washington DC
2016	**Yap, TA** (16 April 2016) "Emerging infectious disease and amphibian mass extinction: how research can guide biodiversity conservation policy." Our Changing Planet Lecture Series, Cal Day, University of California, Berkeley

1. CHAPTER 1: Introduction

In the midst of an ongoing sixth mass extinction, amphibians are the most impacted vertebrate group with approximately 200 species collapsing to or near extinction since the 1970s (Alroy 2015; Wake & Vredenburg 2008; Stuart et al. 2004). According to the IUCN, approximately 41% of assessed species are considered threatened, meaning their conservation status is vulnerable, endangered, or critically endangered (IUCN 2015). Amphibians are important in many ecosystems because they play key roles in trophic dynamics and the carbon cycle, and they are often considered ecosystem health indicators due to their permeable skin and sensitivity to environmental disturbances. Therefore, it is important to assess the potential threats to these vulnerable species to guide conservation management plans and protect biodiversity and environmental health.

Emerging infectious diseases (EIDs) in wildlife are causing drastic declines across multiple taxa around the world, including in amphibians. Chytridiomycosis, an EID caused by the fungal pathogen *Batrachochytrium dendrobatidis* (*Bd*), has severely impacted amphibian biodiversity globally, infecting over 500 species (Olson et al. 2013) and causing declines and extinctions in at least 200 species (Alroy 2015; Fisher et al. 2009; Skerratt et al. 2007). *Bd* has been recorded in all three Orders of Amphibia (Anura, Caudata, Gymnophiona), though the majority of declines and extinctions due to *Bd* have occurred in frogs. There is a variety of strains of *Bd* with ranging virulence and pathogenicity, and the strain associated with epizootics (i.e. epidemics in wildlife) is the Global Panzootic Lineage of *Bd* (*Bd*-GPL) (Farrer et al. 2011).

Recently, a new infectious chytrid fungal pathogen closely related to *Bd*, *Batrachochytrium salamandrivorans* (*Bsal*), was discovered in the Netherlands and is causing mass die-offs in wild European fire salamander (*Salamandra salamandra*) populations (Martel et

al. 2013). *Bsal* is hypothesized to have evolved in Asia, seems to only infect salamanders (Martel et al. 2014), and has spread to Europe via the international pet trade (Martel et al. 2014; Cunningham et al. 2015; Sabino-Pinto et al. 2015). Global trade likely played a role in the current *Bd* pandemic (Hanselmann et al. 2004; Garner et al. 2006; Fisher & Garner 2007; Schloegel et al. 2012; Liu et al. 2013), and now a second deadly pathogen present in trade threatens the already-struggling amphibian populations.

For my dissertation, I used predictive models to assess the vulnerability of amphibians to chytridiomycosis. Models are important tools that can predict pathogen invasions, even when data are limited or incomplete. They allow for scientists to identify regions where a species is likely to be present but not yet discovered or where it may become established once it spreads. I incorporated a combination of both private and publicly available data that include abiotic and biotic factors that likely influence the ability of *Bd* and/or *Bsal* to establish. In addition, I investigated local historical context of pathogen invasion, which, to my knowledge, has not been done in previous *Bd* studies. I also assess human influences on the amphibian chytrid disease system, particularly international amphibian trade and climate change. I created disease risk models at a continental scale that identify areas most vulnerable to pathogen establishment that should be prioritized for conservation management as well as *Bd* and *Bsal* studies.

In Chapter 2, which was published in Science on 31 July 2015, my colleagues and I assessed the threat of *Bsal* to the salamanders of North America. We focused on North America because it is the world's salamander diversity hotspot with almost 50% of all salamander species. This was urgent for several reasons. First, *Bsal* has not yet been documented in North America, though few studies have been published in the short time since *Bsal* was described (Bales et al. 2015; Muletz et al. 2014). Second, *Bsal* is present in the international pet trade (Martel et al.

2014; Cunningham et al. 2015; Sabino-Pinto et al. 2015) and could easily spread to North America from Asia, its proposed area of origin (Martel et al. 2014), or Europe, where it has already spread to wild and captive salamander populations (Martel et al. 2014; Cunningham et al. 2015; Sabino-Pinto et al. 2015). Third, Martel et al. (2014) found that *Bsal* is extremely lethal to two North American newts, the rough-skinned newt (*Taricha granulosa*) and the red-spotted newt (*Notopthalmus viridescens*), both of which have large, vagile populations with expansive ranges that overlap with many localized, endemic species. And fourth a rapid management response could prevent the introduction of *Bsal* to wild salamander populations in North America, but at the time no institution had yet responded to the *Bsal* threat. Our goal was to catalyze conservation policy by determining the potential for *Bsal* to be introduced to North America and identifying the most vulnerable regions and species. We did this by investigating US trade data, potential habitat suitability for *Bsal*, and host availability.

In Chapter 3 we continued to investigate the threat of chytridiomycosis in North America, this time focusing on both *Bd* and *Bsal*. Evidence of the presence of *Bd* in North America dates back to the 1880s (Ouellet et al. 2005; Talley et al. 2015); however, the eastern US has exhibited patterns of an enzootic state with no known declines due to *Bd* and a prevalence of about 20% (Talley et al. 2015), whereas epizootics have been documented in California (Padgett-Flohr & Hopkins 2009; Vredenburg et al. 2010; Vredenburg et al. 2013; Huss et al. 2013), Colorado (Muths et al. 2003), and Mexico (Cheng et al. 2011). In addition, the American bullfrog (*Rana catesbeiana*), a known *Bd* carrier implicated in the global spread of *Bd* through trade (Hanselmann et al. 2004; Garner et al. 2006; Fisher & Garner 2007; Schloegel et al. 2012; Liu et al. 2013), is native to the eastern US and now has established, invasive populations in the western US. While this has not been previously tested or investigated, it is possible that the

translocation of *R. catesbeiana* outside of its native range may have played a role in *Bd* spread in North America. And if *Bd*-GPL (or its preceding strain) coevolved with *R. catesbeiana* and originated in the eastern US, this could explain the differing *Bd* dynamics within the US, as populations naïve to a given pathogen are at greater risk of experiencing an epizootic (Rachowicz et al. 2005; Lips et al. 2006; Vredenburg et al. 2010) compared to those that have existed with the pathogen in an enzootic state (Rodriguez et al. 2014; Talley et al. 2015).

The potential introduction of *Bsal* could also influence disease risk in North America. We currently do not know how interactions between these two closely related pathogens may influence species susceptibility and disease risk. Surviving individuals could incur sub-lethal effects from infection (or from fighting off infection), such as immunosuppression or reduced fitness (Parris & Cornelius 2004; Parris & Beaudoin 2004; Davidson et al. 2007; Bielby et al. 2015; Fites et al. 2013), which could compound their risk to disease and reduce their chances of surviving infection from a second deadly pathogen. On the other hand, species or populations previously exposed to a similar pathogen may benefit from cross immunity, in which a host acquires immunity or partial immunity to one pathogen because of previous infection from a closely related pathogen (McMahon et al. 2014). Thus, it is important to investigate the various potential scenarios and disease risk outcomes of these multi-host, multi-pathogen interactions.

In our study, we created models that incorporate habitat suitability, host availability, and pathogen invasion history to help predict which areas in North America have the highest relative risk of *Bd*/*Bsal* exposure. We investigated the role of pathogen invasion history and the translocation of *R. catesbeiana* in disease dynamics and spread, and we assessed the potential impacts of pathogen interactions. We also estimated the

potential threat of *Bd* and/or *Bsal* to all 263 threatened amphibian species in North America (IUCN 2016).

In Chapter 4 we focused on the threat of *Bd* in Asia, where there have been no documented declines or die-offs due to *Bd*. Unlike areas of endemism in the US and Brazil, where *Bd* prevalence has been found to be about 20% (Talley et al. 2015; Rodriguez et al. 2014), *Bd* has been found at a prevalence of less than 6% (Goka et al. 2009; Swei et al. 2011; Bai et al. 2012; Zhu et al. 2014; Zhu et al. 2016), and recent increases have been seen in Korea (Bataille et al. 2013) and the Philippines (Vredenburg et al. unpublished). This suggests that *Bd* may be newly emerging in Asia. The continuous introduction of various *Bd* strains, including *Bd*-GPL, by the commercial trade of *R. catesbeiana* is alarming because, while *Bd* was previously thought to only reproduce asexually, there is evidence of hybridization among the *Bd* strains (Schloegel et al. 2012). Therefore, trade could facilitate intercontinental *Bd* gene flow and potentially lead to more epizootics from *Bd*-GPL itself or through the hybridization of the different *Bd* strains. In this chapter we predicted the areas most vulnerable to *Bd* in Asia by integrating habitat suitability, host availability, the potential presence of the highly traded and farmed *Bd* carrier *R. catesbeiana*, and future climate change. We also showed the potential threat of *Bd* to the 410 threatened amphibian species in Asia (IUCN 2016).

Ultimately, my goal for my dissertationiss three-fold. By demonstrating the high threat of disease on amphibian populations and how human activities are strongly linked to ecosystem health, I hope to drive conservation policy and management. I also hope to aid researchers to conduct targeted studies, surveillance, and monitoring. And by highlighting the limitations of available data, I hope to promote a more comprehensive, innovative approach to addressing and combatting EIDs in wildlife. There are still many unanswered questions regarding the disease

ecology and host-pathogen dynamics of *Bd* and *Bsal*. More studies investigating disease transmission, species susceptibility, pathogen interactions, pathogen invasion history, and human influences would help inform conservation planning and management and improve future predictions of disease risk.

2. CHAPTER 2: Averting a North American biodiversity crisis – a newly described pathogen poses a major threat to salamanders via trade[1]

In the midst of an ongoing sixth mass extinction (Wake & Vredenburg 2008), more than 40% of all amphibians are threatened (Stuart et al. 2004). Chytridiomycosis, an emerging infectious disease (EID) caused by the fungal pathogen *Batrachochytrium dendrobatidis* (*Bd*), has been more devastating than any infectious wildlife disease recorded, with >200 amphibian species collapsing to or near extinction (Skerratt et al. 2007). Recently, a new infectious chytrid fungal pathogen from Asia and specific to salamanders (Martel et al. 2014), *Batrachochytrium salamandrivorans* (*Bsal*), has been described (Martel et al. 2013). With no effective means to control spread of *Bsal* once it is established in wild host populations, *Bsal* invasion of North America could lead to rapid epizootic (wildlife epidemic) declines and extinctions in the world's richest and most diverse salamander fauna. We demonstrate the likelihood of *Bsal* introduction to North America via international trade, the likelihood of species being exposed to *Bsal*, and the potential impact of species exposure to *Bsal*. This presents a unique opportunity for wildlife management officials and the international amphibian trade community to prevent the spread of this deadly pathogen and to develop and implement rapid risk assessments and international responses to EIDs in wildlife.

This highly virulent *Bsal* pathogen was discovered in the Netherlands during a mass die-off in European fire salamanders (Martel et al. 2014; Martel et al. 2013). Martel et al. (2014) proposed that *Bsal* originated in Asia and spread to wild European salamanders via the

[1] This is a version of a previously published work:
Yap, TA, Koo, MS, Ambrose, RF, Wake DB, Vredenburg, VT (2015) Averting a North American biodiversity crisis. *Science* 349(6247):481–482. doi:10.1126/science.aab1052

international salamander pet trade. They warned that *Bsal* represents a substantial threat to salamanders in other regions that may also be naïve to the pathogen (e.g., North America). Furthermore, they identified three actively traded Asian salamander species as reservoirs for *Bsal*: *Cynops cyanurus*, *Cynops pyrrhogaster*, and *Paramesotriton deloustali*.

Bsal has already spread from the Netherlands to Belgium (Martel et al. 2014), and there is evidence of its spread in international trade (Cunningham et al. 2015). The introduction of *Bsal* to naïve areas could lead to major salamander declines, which would have severe ecosystem impacts. In woodland communities, salamanders represent a substantial portion of vertebrate biomass and play key roles in trophic dynamics and the carbon cycle (Best & Welsh, Jr. 2014).

North American Threat

North America is the world's salamander biodiversity hotspot with 48% of 676 recognized salamander species representing 9 of the 10 known families within the order Caudata (190 species in the United States, 137 in Mexico, and 21 in Canada) (AmphibiaWeb 2015). *Bsal* has not been reported in North America, although few studies have been published in the short time since *Bsal* was described (Muletz et al. 2014; Bales et al. 2015).

We combined projections from a *Bsal* habitat suitability model (HSM) (Figure 2.1A) with a host species richness map (Figure 2.1B) to create a predictive model of host vulnerability (Figure 2.1C). We assumed host risk to be higher in areas of greater salamander species richness. Because the true niche of *Bsal* is unknown, we estimated occurrences on the basis of native ranges of the three putative *Bsal* reservoir species in Asia (See Appendix 2.1). We identified three zones of high risk in North America: southeastern United States (the southern extent of the

Appalachian Mountains and neighboring southeast region), western United States (the Pacific Northwest and the Sierra Nevada), and the highlands of central Mexico (portions of the Sierra Madre Oriental and the Trans-Mexican volcanic belt) (Figure 2.1C).

The U.S. vulnerability zones contain numerous species from the two most *Bsal*-susceptible families, Plethodontidae and Salamandridae (Martel et al. 2014). North American newts (Family Salamandridae), which exhibited high levels of infection and 100% mortality (Martel et al. 2013), have large, vagile populations important in both terrestrial and freshwater ecosystems, and they may act as superspreaders of infectious disease by greatly increasing *Bsal* transmission in these regions (Lloyd-Smith et al. 2005). The Mexican vulnerability zone, located in an area of high beta diversity and endemism, has already been experiencing severe salamander declines (Lips et al. 2006; Cheng et al. 2011).

Risk in Trade

Risk of *Bsal* invasion is compounded by the magnitude of international salamander trade. We examined the most recent 5 years (2010–2014) of live salamander trade entering the United States and identified the most active ports of entry using total gross imports (779,002 salamanders). About 99% originated from Asia, and 98% were species native to Asia (Table 2.1). The major sources were Hong Kong, mainland China, Singapore, and Japan. Alarmingly, species in the genera Cynops and Paramesotriton, which included all three putative *Bsal* reservoirs (Martel et al. 2014), made up 91% of all salamander imports.

The five most active U.S. ports were located within or near the predicted salamander vulnerability zones (Figure 2.1C) and accounted for more than 98% of all U.S. salamander

imports (Table 2.1). Trade data from Canada and Mexico were not analyzed; however, Mexico City is a likely port of entry and is located within a predicted salamander high-vulnerability area.

Bsal is highly transmissible by direct contact (Martel et al. 2014); therefore, shipments containing cohoused animals and shared water increase the potential for pathogen spread. Given the magnitude of international salamander trade originating from Asia and containing potential *Bsal* reservoirs, the risk of *Bsal* introduction to North America is high.

Mitigation and Response

Species declines and extinctions due to wildlife EIDs and the lack of rapid responses (Voyles et al. 2014; Tompkins et al. 2015) warrant immediate action to mitigate the spread of *Bsal*. Preventive action is far more cost-effective than emergency responses to disease outbreaks due to pathogen spread (Langwig et al. 2015), and potentially irreversible environmental consequences could be avoided (Oye et al. 2014). The U.S. Fish and Wildlife Service can play a pivotal role in mitigating the threat of *Bsal* spread by placing an immediate ban on live salamander imports until effective EID prevention and management protocols are in place.

Immediate action in the United States, although critically important, is not sufficient. Because of globalization and human-mediated movements, an international infrastructure that facilitates rapid responses—similar to that of the World Health Organization (WHO) for human disease—is required to mitigate the spread of EIDs in wildlife (Voyles et al. 2014).

Although the World Organization for Animal Health (OIE) and the Convention on International Trade in Endangered Species of Wild Fauna and Flora (CITES) provide guidelines for animal disease and the trade of endangered species, respectively, membership is voluntary,

systematic record-keeping is limited, and wildlife EIDs are not prioritized. These institutions should work with government agencies and experts in disease ecology and animal trade to implement an international effort for surveillance, research, and management actions in an adaptive management framework for effective wildlife EID intervention (Langwig et al. 2015). To enhance global biosecurity and to help prevent the spread of *Bsal* and other wildlife EIDs, a mandatory international system that will track all traded species, identify potential wildlife EID threats, and develop and facilitate emergency protocols is needed (Chan et al. 2015).

Immediate efforts are required to monitor zones of salamander *Bsal* high vulnerability (Figure 2.1C). New studies on the basic biology of *Bsal* and on host-pathogen dynamics should also be a priority. Future studies should incorporate new data on transmission, susceptibility, and other potentially influential variables (e.g., species life-history traits, host microbiome, or co-occurring pathogens) to better understand the complex disease system. In the interim, the trade industry should take preventive measures from protocols that have been developed for the detection of *Bsal* (Blooi et al. 2013) and the treatment of infected individuals (Blooi et al. 2015a; Blooi et al. 2015b).

Acknowledgements

This work was supported by UCLA–Charles F. Scott Fellowship (T.A.Y.) and NSF IOS-1258133 (V.T.V.). We thank S. M. Rovito for Mexican species occurrence data and the Museum of Vertebrate Zoology at University of California, Berkeley for technical support. Original data are archived at AmphibiaWeb, VertNet, the International Union for Conservation of Nature,

WorldClim, and the U.S. Fish and Wildlife Service, and we thank these organizations and collections for sharing their data. We also thank the anonymous reviewers.

Figures

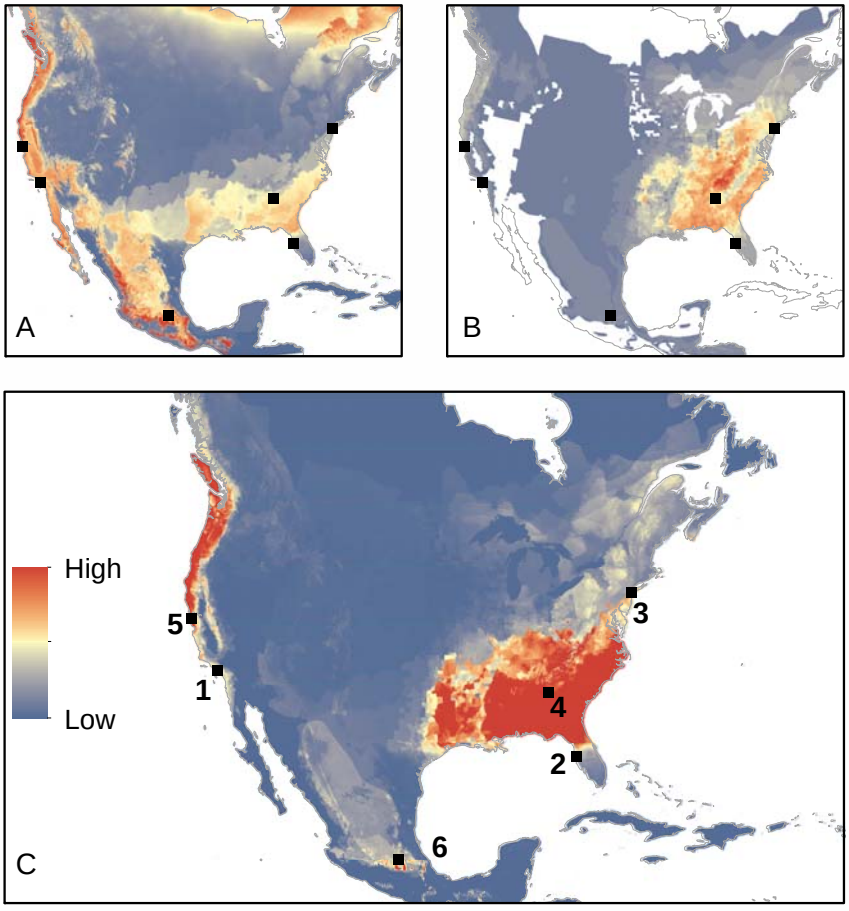

Figure 2.1 Mapping the threat of *Bsal* to North American salamanders. (A) *Bsal* habitat suitability model based on 133 carrier occurrences and six bioclimatic variables. (B) Salamander species-richness map. (C) Salamander *Bsal* vulnerability model. Major ports (black squares) for salamander imports follow Table 2.1.

Tables

Table 2.1 Major ports of salamander imports in North America (2010-2014). Imported salamanders were considered a *Bsal* threat if they have native ranges in Asia or were in shipments that passed through Asian ports before entering the United States. Those not considered a *Bsal* threat are not native to Asia and never passed through an Asian port before entering the United States. All values are number of salamanders (see Appendix 2.1).

Major ports of salamander imports in North America 2010-2014				
Port		***Bs* threat (Number of salamanders)**	**Non-*Bs* threat (Number of salamanders)**	**All shipments (Number of salamanders)**
1	Los Angeles, CA	418,692	1,198	419,890
2	Tampa, FL	272,338	1,140	273,478
3	New York, NY	55,441	70	55,511
4	Atlanta, GA	13,272	40	13,312
5	San Francisco, CA	3,164	6,459	9,623
6	Mexico City	No Data	No Data	No Data
	Total (Top 5 US Ports)	**762,907**	**8,907**	**771,814**
	All US Ports Combined	**768,572**	**10,430**	**779,002**

Appendix

Appendix 2.1 North America *Bsal* vulnerability model: Materials and Methods

Salamander vulnerability model

To estimate the potential biological impact and geographic scope of *Batrachochytrium salamandrivorans* (*Bsal*) in North America, we produced a salamander vulnerability model in which we considered climatic variables, species-richness/host-species densities, and locations of major ports of entry. We weighted our *Bsal* habitat suitability model (HSM) (Figure 2.1A) with

salamander richness (Figure 2.1B) and indicated the most likely ports of entry from U.S. salamander (Caudata) trade data (Figure 2.1C and Table 2.1).

Habitat suitability model

We created a climate-driven, presence-only HSM for *Bsal* in North America using maximum-entropy modeling software, Maxent version 3.3.3k (Phillips et al. 2004). We conducted an ensemble forecast to create a model trained on occurrences within the species ranges of the three putative *Bsal* reservoirs from Asia, C*ynops cyanurus*, *C. pyrrhogaster*, and *Paramesotriton deloustali* (Martel et al. 2014), and projected to North America. We ran 100 model simulations using cross-validation, which was then averaged by Maxent to produce a final probabilistic density function of potentially suitable *Bsal* habitat in North America (Figure 2.1A).

Training or initial input data included 133 occurrence points and the following six bioclimatic variables (Rödder et al. 2009) from the Worldclim database (http://www.worldclim.org/bioclim) at 30 arc second resolution (ca. 1 km per raster cell) (Hijmans et al. 2005): annual mean temperature, maximum temperature of the warmest month, minimum temperature of the coldest month, annual precipitation, precipitation of the wettest month, and precipitation of the driest month.

Because information regarding the distribution of *Bsal* is currently limited, we simulated the occurrence of *Bsal*-positive sites using georeferenced occurrence data for *C. cyanurus*, *C. pyrrhogaster*, and *P. deloustali* obtained from VertNet (http://vertnet.org/), a biodiversity database aggregator that currently provides access to occurrence records from over 200 biocollections around the world (see Table 2.2 for specimens used in modeling). We assumed the proposed reservoir species share an evolutionary history with *Bsal* [(as hypothesized by Martel *et*

al. (2014)], and, therefore, locations where these carrier species occur likely have suitable *Bsal* habitat. Thus, we treated sites in which the proposed *Bsal* reservoir species are recorded as proxy sites for where *Bsal* could occur.

From 344 verified georeferenced records, a total of 58 sites (55 for *C. pyrrhogaster*, 2 for *P. deloustali*, and 1 for *C. cyanurus*) fell within these species' ranges (Figure 2.2). We used species ranges from the IUCN Red List (version 2014.3 from http://www.iucnredlist.org/technical-documents/spatial-data). Due to the limited number of occurrences for *P. deloustali* and *C. cyanurus*, we randomly sampled 100 additional points from within each species' range. Because these species have locally restricted distributions in mountainous regions, we filtered these data further by restricting samples to those that only occurred within the species' elevational ranges according to IUCN. This resulted in 65 random sites within the *C. cyanurus* range and 10 within the *P. deloustali* range (Table 2.3). Random points were not generated for *C. pyrrhogaster* because 55 occurrences from VertNet were well-dispersed within its range. As a result, a total of 133 sample sites were used for the HSM (55, 66, and 12 sites for *C. pyrrhogaster*, *C. cyanurus*, and *P. deloustali,* respectively) (Figure 2.2).

Salamander species-richness and vulnerability models

We estimated salamander richness in North America (Canada, the United States, and Mexico) by overlaying 300 range maps from the IUCN Red List. Although the IUCN Red List range maps are sometimes limited, they are the global standard for conservation groups. In addition, we supplied six additional, expert-based range maps (*Batrachoseps altasierrae. Batrachoseps bramei, Bolitoglossa chinanteca, Pseudoeurycea cafetalera, Thorius adelos,* and *Thorius maxillabrochus*) and modified five ranges of species endemic to California (*Aneides*

lugubris, Aneides flavipunctatus, Hydromantes brunus, Hydromantes platycephalus, Hydromantes shastae). This resulted in a total of 306 unique species ranges for North America. We created a grid of the tally of intersecting ranges per cell (Figure 2.1B). Spatial data for produced or modified range maps are available at https://github.com/AmphibiaWeb. All range maps are viewable on AmphibiaWeb by species (http://amphibiaweb.org).

We created a salamander-vulnerability model by calculating the product of the *Bsal* HSM and the salamander-richness model. The vulnerability model emphasizes areas where *Bsal* has suitable bioclimatic conditions and high potential host biodiversity. We used ArcGIS 10.2.2 (ESRI) to produce all GIS layers and used R Statistical Program to calculate richness.

Salamander trade data

Because of the lack of systematic global trade data (e.g., from Canada and Mexico), we focused on the live amphibian trade within the United States. In a Freedom of Information Act request, we asked for live amphibian import and export data from the U.S. Fish and Wildlife Service (USFWS) on 14 January 2015 (FWS-2015-00396). The data included shipment records that each have a USFWS-assigned declaration control number; species identification (e.g., to genus or species level); whether the shipment was imported to or exported from the United States; the country of origin; the country of import or export; the quantity (e.g., number of individuals); the date of the shipment; the port of entry or exit; the source (e.g., wild, captive, ranched); the purpose (e.g., commercial, scientific, educational, zoos); and the U.S. business that was importing or exporting the shipment. Not all shipments were identified to Order; for example, several shipments were recorded as “amphibians” or “non-CITES,” and therefore were not included in the analyses. We report on the most recent 5 years (2010–2014).

Although only three salamander carriers were proposed for *Bsal* by Martel *et al*. (2014), not all Asian salamanders have been tested, and it is possible that other species in the international trade could harbor *Bsal* without showing clinical signs of chytridiomycosis. Therefore, to determine the salamanders' risk of being exposed to or infected with *Bsal*, we divided all records into two categories: *Bsal* threat and non-*Bsal* threat. We defined *Bsal* threat salamanders as those (i) with native ranges in Asia, or (ii) in shipments that passed through Asian ports before entering the United States. Non-*Bsal* threat salamanders were defined as those (i) nonnative to Asia and (ii) having never passed through an Asian port before arrival in the United States.

There are instances in which salamanders are imported to the United States to be exported elsewhere. Although these individuals are not being dispersed to local businesses within the United States, they still pose a threat of *Bsal* introduction. These salamanders could become infected during transport or even while being processed in shared facilities with other infected individuals. Therefore, to determine the numbers of salamanders entering or passing through the United States, we calculated gross imports at each port for the most recent 5 years (2010 to 2014) shown in Table 2.1 as *Bsal* threat and non-*Bsal* threat.

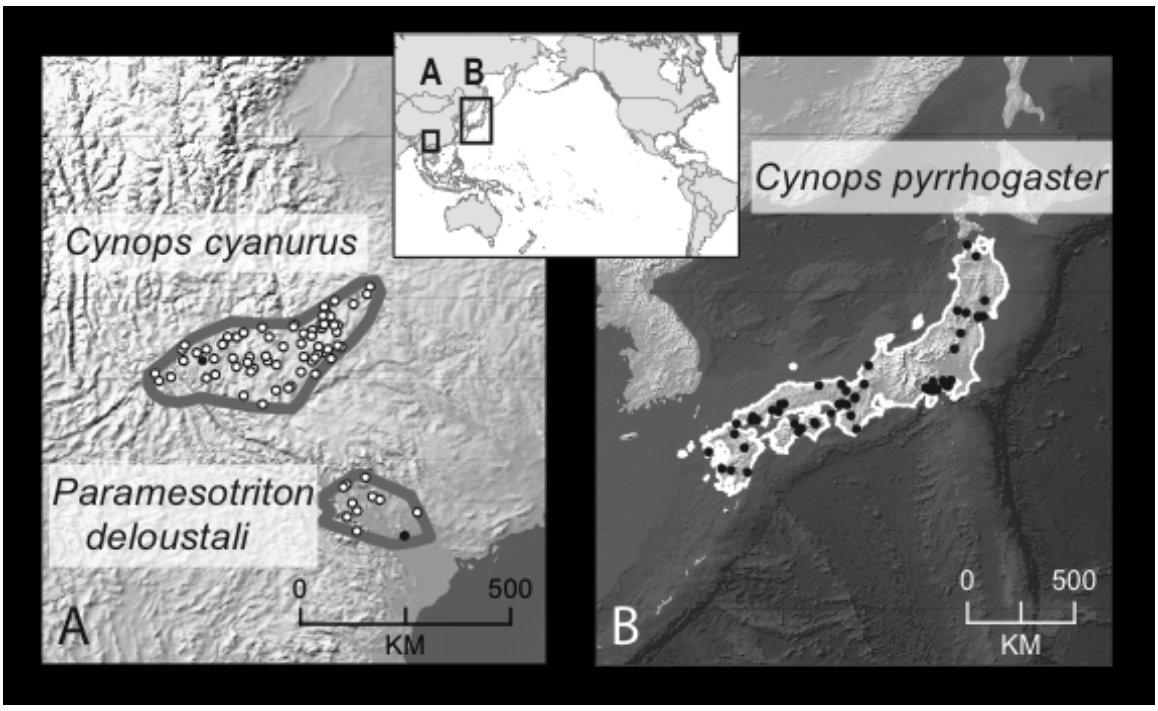

Figure 2.2 *Bsal* model training data. We selected 133 *Bsal*-positive sites within the geographical and elevational ranges of the putative reservoir species: (A) *Cynops cyanurus* and *Paramesotriton deloustali*, and (B) *Cynops pyrrhogaster*. Black circles represent voucher specimens. White circles represent randomly generated points.

Table 2.2 Voucher specimens used in modeling accessed from VertNet. Abbreviations follow: AM, Australian Museum; CAS, California Academy of Sciences; CM, Carnegie Museum; LACM, Natural History Museum of Los Angeles County; MCZ, Museum of Comparative Zoology (Harvard U.); MVZ, Museum of Vertebrate Zoology (UC Berkeley); OMNH, Sam Noble Oklahoma Museum of Natural History; PSM, Puget Sound Museum; ROM, Royal Ontario Museum; USNM, U.S. National Museum of Natural History.

State province/ island	**Country**	**Latitude**	**Longitude**	**Geodetic datum**	**Voucher specimens**
Cynops cyanurus					
Yunnan Province	China	25.01667	101.51667	WGS84	MVZ:Herp:219757;MVZ:Herp:219758;MVZ:Herp:219759;MVZ:Herp:219760
Cynops pyrrhogaster					
Awaji Island	Japan	34.33333	134.84819	Japanese geodetic datum 2000	CAS:HERP:16341; CAS:HERP:16345; CAS:HERP:16346; CAS:HERP:16342; CAS:HERP:16343; CAS:HERP:16344
Honshu Island	Japan	38.266	140.866	Not recorded (forced WGS84)	AM:Herpetology:R.101015
Honshu Island	Japan	38.533	140.016	Not recorded (forced WGS84)	AM:Herpetology:R.101017; AM:Herpetology:R.101018; AM:Herpetology:R.101323; AM:Herpetology:R.101016
Honshu Island	Japan	38.253	140.871	WGS84	AM:Herpetology:R.101021; AM:Herpetology:R.101019; AM:Herpetology:R.101020; AM:Herpetology:R.101022
Honshu Island	Japan	38.266	140.871	WGS84	AM:Herpetology:R.101022

Honshu Island	Japan	38.438	140.365	WGS84	AM:Herpetology:R.101287; AM:Herpetology:R.101288; AM:Herpetology:R.101289
Honshu Island	Japan	34.95181	135.81944	Japanese geodetic datum 2000	CAS:HERP:135894
Honshu Island	Japan	34.69986	135.16167	Japanese geodetic datum 2000	CAS:HERP:16024; CAS:HERP:16026; CAS:HERP:16027; CAS:HERP:16028; CAS:HERP:16029; CAS:HERP:16030; CAS:HERP:16031; CAS:HERP:16032; CAS:HERP:16034; CAS:HERP:16036; CAS:HERP:16037; CAS:HERP:16022; CAS:HERP:16023; CAS:HERP:16025; CAS:HERP:16033; CAS:HERP:16035
Honshu Island	Japan	35.51667	135.27056	Japanese geodetic datum 2000	CAS:HERP:16326; CAS:HERP:16324; CAS:HERP:16325; CAS:HERP:16327
Honshu Island	Japan	34.24278	135.65194	Japanese geodetic datum 2000	CAS:HERP:211008; CAS:HERP:211006; CAS:HERP:211007
Honshu Island	Japan	38.94542	141.12792	Japanese geodetic datum 2000	CAS:HERP:25116; CAS:HERP:25117; CAS:HERP:25119; CAS:HERP:25121; CAS:HERP:25122; CAS:HERP:25118; CAS:HERP:25120; CAS:HERP:25123
Honshu Island	Japan	36.28944	136.36333	Japanese geodetic datum	CAS:HERP:25126; CAS:HERP:25124; CAS:HERP:25125; CAS:HERP:25127

				2000	
Honshu Island	Japan	41.20667	140.39319	Japanese geodetic datum 2000	CAS:HERP:25129; CAS:HERP:25130; CAS:HERP:25131; CAS:HERP:25132; CAS:HERP:25128
Honshu Island	Japan	37.60264	140.14986	Japanese geodetic datum 2000	CAS:HERP:25137; CAS:HERP:25134; CAS:HERP:25135; CAS:HERP:25136
Honshu Island	Japan	40.752459	140.775375	WGS84	CAS:HERP:25958; CAS:HERP:25962; CAS:HERP:25963; CAS:HERP:25964; CAS:HERP:25965; CAS:HERP:25133; CAS:HERP:25959; CAS:HERP:25960; CAS:HERP:25961; CAS:HERP:25966
Honshu Island	Japan	36.96181	139.89194	Japanese geodetic datum 2000	CAS:HERP:26719; CAS:HERP:26722; CAS:HERP:26717; CAS:HERP:26718; CAS:HERP:26720; CAS:HERP:26721
Honshu Island	Japan	34.74375	135.29569	Japanese geodetic datum 2000	CAS:HERP:33044
Honshu Island	Japan	35.45292	139.62556	Japanese geodetic datum 2000	CAS:HERP:359; CAS:HERP:360
Honshu Island	Japan	35.66986	139.42181	Japanese geodetic datum 2000	CAS:SUA:1561

Honshu Island	Japan	35.52264	136.19458	Japanese geodetic datum 2000	CAS:SUA:1616; CAS:SUA:1617; CAS:SUA:1618; CAS:SUA:1619
Honshu Island	Japan	34.04444	131.57625	Japanese geodetic datum 2000	CAS:SUA:1757; CAS:SUA:1758
Honshu Island	Japan	34.19694	131.63347	Japanese geodetic datum 2000	CAS:SUA:2710; CAS:SUA:2711; CAS:SUA:2712
Honshu Island	Japan	34.073404	131.824328	WGS84	LACM:Herps:105538*; LACM:Herps:105540*; LACM:Herps:105539*
Honshu Island	Japan	35.28833	138.86236	Japanese geodetic datum 2000	LACM:Herps:141230; LACM:Herps:141232; LACM:Herps:141233; LACM:Herps:141234; LACM:Herps:141235; LACM:Herps:143265; LACM:Herps:143268; LACM:Herps:144333; LACM:Herps:141231; LACM:Herps:141236; LACM:Herps:141237; LACM:Herps:143266; LACM:Herps:143267; LACM:Herps:143269; LACM:Herps:144332; LACM:Herps:144335
Honshu Island	Japan	35.26028	139.00528	Japanese geodetic datum 2000	LACM:Herps:141238
Honshu Island	Japan	35.33542	139.16611	Japanese geodetic datum 2000	LACM:Herps:143235; LACM:Herps:143236; LACM:Herps:143237; LACM:Herps:144331; LACM:Herps:146590; LACM:Herps:144334;

					LACM:Herps:144336
Honshu Island	Japan	35.46194	134.34625	Japanese geodetic datum 2000	LACM:Herps:29076; LACM:Herps:29077; LACM:Herps:29078; LACM:Herps:29079; LACM:Herps:29080
Honshu Island	Japan	35.5	139.5	WGS84	MCZ:Herp:A-125121; MCZ:Herp:A-125122; MCZ:Herp:A-125124; MCZ:Herp:A-125126; MCZ:Herp:A-125127; MCZ:Herp:A-125133; MCZ:Herp:A-125138; MCZ:Herp:A-125123; MCZ:Herp:A-125125; MCZ:Herp:A-125128; MCZ:Herp:A-125129; MCZ:Herp:A-125130; MCZ:Herp:A-125131; MCZ:Herp:A-125132; MCZ:Herp:A-125134; MCZ:Herp:A-125135; MCZ:Herp:A-125136; MCZ:Herp:A-125137; MCZ:Herp:A-1607; MCZ:Herp:A-1915
Honshu Island	Japan	35.367	138.733	WGS84	MCZ:Herp:A-125141; MCZ:Herp:A-125139; MCZ:Herp:A-125140; MCZ:Herp:A-2587
Honshu Island	Japan	35.685	139.751	WGS84	MCZ:Herp:A-1865; MCZ:Herp:A-125120
Honshu Island	Japan	38.29694	141.07333	Unknown	MVZ Herps:22507
Honshu Island	Japan	35.60806	139.00333	Unknown	MVZ Herps:42128; MVZ Herps:42129; MVZ Herps:42126; MVZ Herps:42127; MVZ Herps:42130
Honshu Island	Japan	34.98554	135.81722	Unknown	MVZ Herps:66740; MVZ Herps:66741; MVZ Herps:66742; MVZ Herps:66745; MVZ Herps:66743; MVZ Herps:66744

Honshu Island	Japan	34.6772	135.486	Japanese geodetic datum 2000	USNM:Amphibians & Reptiles:14865.626262
Honshu Island	Japan	34.4557	132.437	Japanese geodetic datum 2000	USNM:Amphibians & Reptiles:245074.6098935; USNM:Amphibians & Reptiles:245076.6098937; USNM:Amphibians & Reptiles:245077.6098938; USNM:Amphibians & Reptiles:245079.609894; USNM:Amphibians & Reptiles:245080.6098941; USNM:Amphibians & Reptiles:245085.6098946; USNM:Amphibians & Reptiles:245087.6098948; USNM:Amphibians & Reptiles:245088.6098949; USNM:Amphibians & Reptiles:245090.6098951; USNM:Amphibians & Reptiles:245091.6098952; USNM:Amphibians & Reptiles:245093.6098954; USNM:Amphibians & Reptiles:245095.6098956; USNM:Amphibians & Reptiles:245075.6098936; USNM:Amphibians & Reptiles:245078.6098939; USNM:Amphibians & Reptiles:245081.6098942; USNM:Amphibians & Reptiles:245082.6098943; USNM:Amphibians & Reptiles:245083.6098944; USNM:Amphibians & Reptiles:245084.6098945; USNM:Amphibians & Reptiles:245086.6098947; USNM:Amphibians & Reptiles:245089.609895; USNM:Amphibians & Reptiles:245092.6098953; USNM:Amphibians & Reptiles:245094.6098955
Honshu Island	Japan	34.6972	132.754	Japanese geodetic datum 2000	USNM:Amphibians & Reptiles:245096.6098957; USNM:Amphibians & Reptiles:245097.6098958; USNM:Amphibians & Reptiles:245102.6098963;

					USNM:Amphibians & Reptiles:245103.6098964; USNM:Amphibians & Reptiles:245104.6098965
Honshu Island	Japan	34.3983	132.691	Japanese geodetic datum 2000	USNM:Amphibians & Reptiles:245098.6098959; USNM:Amphibians & Reptiles:245099.609896
Honshu Island	Japan	34.7214	132.91	Japanese geodetic datum 2000	USNM:Amphibians & Reptiles:245100.6098961; USNM:Amphibians & Reptiles:245101.6098962
Honshu Island	Japan	35.4529	139.626	Japanese geodetic datum 2000	USNM:Amphibians & Reptiles:277399.6127726; USNM:Amphibians & Reptiles:277398.6127725; USNM:Amphibians & Reptiles:277400.6127727; USNM:Amphibians & Reptiles:277401.6127728; USNM:Amphibians & Reptiles:8851.6003973; USNM:Amphibians & Reptiles:57211.6033454
Honshu Island	Japan	35.2424	135.46	Japanese geodetic datum 2000	USNM:Amphibians & Reptiles:31794.6009817; USNM:Amphibians & Reptiles:31795.6009818; USNM:Amphibians & Reptiles:31796.6009819
Honshu Island	Japan	35.3692	138.716	Japanese geodetic datum 2000	USNM:Amphibians & Reptiles:34288.601214; USNM:Amphibians & Reptiles:34289.6012141; USNM:Amphibians & Reptiles:34290.6012142; USNM:Amphibians & Reptiles:34291.6012143; USNM:Amphibians & Reptiles:34293.6012145; USNM:Amphibians & Reptiles:34297.6012149; USNM:Amphibians & Reptiles:34298.601215; USNM:Amphibians & Reptiles:34299.6012151; USNM:Amphibians & Reptiles:34300.6012152;

					USNM:Amphibians & Reptiles:34301.6012153; USNM:Amphibians & Reptiles:34303.6012155; USNM:Amphibians & Reptiles:34304.6012156; USNM:Amphibians & Reptiles:34306.6012158; USNM:Amphibians & Reptiles:34308.601216; USNM:Amphibians & Reptiles:34292.6012144; USNM:Amphibians & Reptiles:34294.6012146; USNM:Amphibians & Reptiles:34295.6012147; USNM:Amphibians & Reptiles:34296.6012148; USNM:Amphibians & Reptiles:34302.6012154; USNM:Amphibians & Reptiles:34305.6012157; USNM:Amphibians & Reptiles:34307.6012159
Honshu Island	Japan	35.2861	139.159	Japanese geodetic datum 2000	USNM:Amphibians & Reptiles:39000.6016474
Kyushu Island	Japan	32.06875	130.37056	Japanese geodetic datum 2000	CAS:HERP:135776; CAS:HERP:135773; CAS:HERP:135774; CAS:HERP:135775
Kyushu Island	Japan	32.0125	130.74167	Japanese geodetic datum 2000	CAS:HERP:24284; CAS:HERP:24285; CAS:HERP:24286; CAS:HERP:24283; CAS:HERP:24287
Kyushu Island	Japan	32.75847219	129.8311111	Japanese geodetic datum 2000	CAS:HERP:74500; CAS:HERP:74501
Kyushu Island	Japan	33.90722	130.96944	Unknown	MVZ:Herps:22509

Kyushu Island	Japan	33.4876 1368	130.892532 4	Japanese geodetic datum 2000	PSM:Herp:Herp-09786
Kyushu Island	Japan	31.92	131.42	Unknown	USNM:Amphibians & Reptiles:30735.6009007; USNM:Amphibians & Reptiles:30737.6009009; USNM:Amphibians & Reptiles:30738.600901; USNM:Amphibians & Reptiles:30736.6009008
Shikoku Island	Japan	33.8956 9	134.20542	Japanese geodetic datum 2000	CAS:HERP:16454
Shikoku Island	Japan	33.9524 2	134.14139	Japanese geodetic datum 2000	CAS:HERP:211037; CAS:HERP:211038; CAS:HERP:211039; CAS:HERP:211040; CAS:HERP:211041
Shikoku Island	Japan	33.7147 2	133.62128	Japanese geodetic datum 2000	CAS:HERP:211062; CAS:HERP:211064; CAS:HERP:211063
Shikoku Island	Japan	33.9076 1566	133.341705 3	WGS84	OMNH:Amphibians:27520; OMNH:Amphibians:27521; OMNH:Amphibians:27519
Shikoku Island	Japan	33.5828	133.51	Japanese geodetic datum 2000	USNM:Amphibians & Reptiles:31894.6009917; USNM:Amphibians & Reptiles:31897.600992; USNM:Amphibians & Reptiles:31899.6009922; USNM:Amphibians & Reptiles:31900.6009923; USNM:Amphibians & Reptiles:31901.6009924; USNM:Amphibians & Reptiles:31898.6009921
Honshu Island	Japan	33.6753	135.887618	WGS84	PSM:Herp-08005*; PSM:Herp-08006*

		31			
Kyushu Island	Japan	32.927648	131.290129	WGS84	CM:Herps:62290*
Paramesotriton deloustali					
Vinh Phu	Vietnam	21.45361	105.64361	Unknown	MVZ:Herps:222123; MVZ:Herps:223629; MVZ:Herps:226269; MVZ:Herps:222122; MVZ:Herps:223627; MVZ:Herps:223628; MVZ:Herps:226270; MVZ:Herps:206310; MVZ:Herps:206311; MVZ:Herps:206312; MVZ:Herps:225135
Vinh Phu	Vietnam	21.4541667	105.6413889	Unknown	ROM:25690; ROM:25692; ROM:25689; ROM:25691; ROM:25693; ROM:25694; ROM:29771; ROM:30635; ROM:30636; ROM:30637; ROM:30638; ROM:30634; ROM:30639

*Coordinates were corrected

Table 2.3 The random points used as carrier proxy sites for *Cynops cyanurus* range and *Paramesotriton deloustali*.

Carrier Species	Latitude	Longitude
Cynops cyanurus	25.1849	103.986
Cynops cyanurus	25.9662	104.075
Cynops cyanurus	24.6042	100.627
Cynops cyanurus	25.3648	103.532
Cynops cyanurus	25.0161	101.127
Cynops cyanurus	25.1611	103.873
Cynops cyanurus	25.0909	102.475
Cynops cyanurus	24.9331	103.032
Cynops cyanurus	25.6426	103.762
Cynops cyanurus	25.5028	102.032
Cynops cyanurus	26.528	104.939
Cynops cyanurus	25.2503	104.074
Cynops cyanurus	26.117	104.003
Cynops cyanurus	24.4988	103.317
Cynops cyanurus	25.6902	102.737
Cynops cyanurus	24.6789	100.872
Cynops cyanurus	25.5707	103.579
Cynops cyanurus	24.7455	103.817
Cynops cyanurus	24.8571	102.56
Cynops cyanurus	25.7552	103.398
Cynops cyanurus	25.2516	101.591
Cynops cyanurus	25.526	103.746
Cynops cyanurus	25.3622	101.934
Cynops cyanurus	24.9806	102.438
Cynops cyanurus	24.7523	100.546
Cynops cyanurus	25.6805	103.952
Cynops cyanurus	25.7429	104.282
Cynops cyanurus	25.3032	103.161
Cynops cyanurus	24.6655	101.596
Cynops cyanurus	25.2965	104.349
Cynops cyanurus	25.0098	102.847
Cynops cyanurus	25.3024	103.886
Cynops cyanurus	26.3739	104.883
Cynops cyanurus	25.0688	102.131
Cynops cyanurus	25.6082	104.258
Cynops cyanurus	25.0972	103.587

Cynops cyanurus	25.1078	102.811
Cynops cyanurus	25.0566	104.143
Cynops cyanurus	24.9984	103.757
Cynops cyanurus	24.1269	102.744
Cynops cyanurus	25.7666	103.944
Cynops cyanurus	25.2393	101.1
Cynops cyanurus	26.1739	104.6
Cynops cyanurus	25.7412	104.209
Cynops cyanurus	25.0806	103.812
Cynops cyanurus	25.7113	103.372
Cynops cyanurus	25.7574	104.004
Cynops cyanurus	25.3492	101.92
Cynops cyanurus	24.7947	102.507
Cynops cyanurus	26.2421	104.216
Cynops cyanurus	25.4952	102.877
Cynops cyanurus	25.9205	104.135
Cynops cyanurus	25.176	101.397
Cynops cyanurus	25.9348	103.972
Cynops cyanurus	25.3268	104.276
Cynops cyanurus	25.3301	101.147
Cynops cyanurus	24.8897	102.209
Cynops cyanurus	25.4986	102.217
Cynops cyanurus	24.732	101.774
Cynops cyanurus	25.5894	102.359
Cynops cyanurus	24.4143	103.017
Cynops cyanurus	24.7917	103.528
Cynops cyanurus	24.3029	102.355
Cynops cyanurus	24.4587	103.272
Cynops cyanurus	25.0551	101.749
Paramesotriton deloustali	22.2465	104.992
Paramesotriton deloustali	21.9261	105.902
Paramesotriton deloustali	22.4852	104.463
Paramesotriton deloustali	22.4347	104.395
Paramesotriton deloustali	22.1846	105.136
Paramesotriton deloustali	21.8379	104.472
Paramesotriton deloustali	22.6329	104.845
Paramesotriton deloustali	22.115	104.578
Paramesotriton deloustali	21.9587	104.673
Paramesotriton deloustali	21.5473	104.672

3. CHAPTER 3: Estimating compounded risk of two fungal pathogens, *Batrachochytrium dendrobatidis* and *Batrachochytrium salamandrivorans,* to North American amphibians and investigating the influence of an invasive carrier species and pathogen invasion history

Abstract

Over the past few decades *Batrachochytrium dendrobatidis* (*Bd*), one of the causal agents of the amphibian fungal skin disease chytridiomycosis, has been implicated in the declines and extinctions of over 200 species worldwide. Recently a second, closely related pathogen that also causes chytridiomycosis, *Batrachochytrium salamandrivorans* (*Bsal*), was discovered in the Netherlands, and its presence in the international amphibian trade increases the threat of pathogen invasion. To guide conservation efforts, we predict the risk of chytridiomycosis to amphibians from *Bd* and/or *Bsal* in North America by creating models that incorporate habitat suitability, host availability, and pathogen invasion history. We hypothesize that the Global Panzootic Lineage of *Bd* (*Bd*-GPL), which is the strain associated with all *Bd* epizootics, originated in the eastern US, where the American bullfrog (*Rana catesbeiana*), a known *Bd* carrier, is native and no chytridiomycosis-caused declines have been observed. When we incorporated historical context into our model and treated the eastern US as the native range of *Bd*, we found invasive *Bd* risk to be highest in the mountain ranges of the western US and Mexico, and we uncovered a pattern that suggests the translocation of *R. catesbeiana* to western North America may have facilitated *Bd* spread. Areas with the highest relative risk of exposure to both *Bd* and *Bsal* include the Southeast US, the West Coast, the Sierra Nevada Mountains, the northern Rocky Mountains, and the highlands of central Mexico. All but one of 263 threatened amphibian species had at least 25% overlap with areas identified as vulnerable to *Bd* and/or *Bsal*.

These findings may guide future surveillance and species susceptibility studies needed to enhance our understanding of the pathogen invasion history, disease dynamics, and potential interactions of *Bd* and *Bsal*.

Keywords: Chytridiomycosis, *Batrachochytrium dendrobatidis*, *Batrachochytrium salamandrivorans*, *Rana catesbeiana*, habitat suitability, pathogen invasion history

Introduction

Chytridiomycosis, an emerging infectious disease (EID) caused by the fungal pathogen *Batrachochytrium dendrobatidis* (*Bd*), has significantly affected global amphibian biodiversity, infecting over 500 species (Olson et al. 2013) and causing declines and extinctions in at least 200 species (Alroy 2015; Fisher et al. 2009; Skerratt et al. 2007). *Bd* has been recorded in all three Orders of Amphibia (Anura, Caudata, Gymnophiona), though the majority of declines and extinctions due to *Bd* have occurred in frogs (Anura). There is a variety of strains of *Bd* with ranging virulence and pathogenicity, and the strain associated with epizootics (i.e. epidemics in wildlife) is the Global Panzootic Lineage of *Bd* (*Bd*-GPL) (Farrer et al. 2011). Recently, a new infectious chytrid fungal pathogen related to *Bd*, *Batrachochytrium salamandrivorans* (*Bsal*), was discovered (Martel et al. 2013) and has been found to only infect salamanders (Martel et al. 2014). *Bsal* is hypothesized to have evolved in Asia and spread to Europe via the international pet trade (Martel et al. 2014; Sabino-Pinto et al. 2015; Spitzen-van der Sluijs et al. 2016). Global trade likely also played a role in the current *Bd* pandemic by spreading non-native, infected animals worldwide and exposing naïve populations to them (Fisher & Garner 2007; Schloegel et al. 2012; Liu et al. 2013). Early evidence indicates that *Bsal* is behaving similarly, first invading

the Netherlands and spreading rapidly (Martel et al. 2013; Martel et al. 2014; Spitzen-van der Sluijs et al. 2016).

Historical surveys made possible by a technique that enables the identification of *Bd* zoospores on museum specimens (Cheng et al. 2011) has helped unfold some of the history of chytridiomycosis. The presence of *Bd* in North America dates back to the 1880s (Ouellet et al. 2005; Talley et al. 2015), and James et al. (James et al. 2015) hypothesize that *Bd*-GPL, or its preceding strain, originated in the temperate zone of North America. However, disease dynamics are not uniform across geographic space. While pathogen host dynamics east of the Rocky Mountains reflect an enzootic state with no known declines due to *Bd* (Muletz et al. 2014; Talley et al. 2015; Bales et al. 2015), *Bd* epizootics have been documented in the western part of North America (in California (Padgett-Flohr & Hopkins 2009; Vredenburg et al. 2010; Vredenburg et al. 2013; Huss et al. 2013) and Colorado (Muths et al. 2003)) and in Mexico (Cheng et al. 2011). Based on this and evidence from several studies showing *Bd* invasion in California (Padgett-Flohr & Hopkins 2009; Vredenburg et al. 2010; Sette et al. 2015; Yap et al. 2016), we hypothesize that *Bd*-GPL (or its preceding strain) most likely originated more specifically in the eastern US. This region is the native range of *Rana catesbeiana*, a known *Bd* reservoir (Daszak et al. 2000; Hanselmann et al. 2004) that is popular in international commercial trade and implicated in disease spread (Hanselmann et al. 2004; Garner, Perkins, Govindarajulu, Seglie, Walker, a. a Cunningham, et al. 2006; Fisher & Garner 2007; Huss et al. 2013; Liu et al. 2013). Further, Rödder et al. (2013) showed that *Bd* and *R. catesbeiana* have high niche overlap, and *Bd*-GPL being native to the eastern US could explain *R. catesbeiana*'s ability to tolerate its infection and the lack of *Bd*-related declines in the eastern US. If *Bd*-GPL originated in the

eastern US, the threat of disease may be greater in areas outside of this region, where amphibian populations do not have a history of pathogen exposure, and the translocation of *R. catesbeiana* to these non-native regions could be one of the main drivers of *Bd* spread in North America. *Bsal* has not yet been documented in North America, though few studies have been conducted since its discovery (Muletz et al. 2014; Bales et al. 2015), and there is a high threat of it being introduced through either regulated or non-regulated pet trade of potential reservoir species (Yap et al. 2015; Richgels et al. 2016).

An area's pathogen invasion history may help explain the varied disease dynamics in different communities, as populations never exposed to a given pathogen (or a related pathogen) are at greater risk of experiencing an epizootic (Rachowicz et al. 2005; Lips et al. 2006; Vredenburg et al. 2010) compared to those that have existed with the pathogen in an enzootic state (Briggs et al. 2010; Rodriguez et al. 2014; Talley et al. 2015). However, while exposure to a single pathogen may pose a significant threat, it is unclear how interactions between two closely related pathogens may influence species susceptibility and disease risk. The most disruptive effect of a single pathogen infection is death, but surviving species could incur sub-lethal effects from infection (or from fighting off infection) that could suppress immune defenses against other stressors (Parris & Cornelius 2004; Parris & Beaudoin 2004; Davidson et al. 2007; Bielby et al. 2015; Fites et al. 2013), such as a second deadly pathogen. This could at least partially explain the *Bsal*-induced mass mortalities of *S. salamandra* where *Bd* was co-existing with local amphibian populations (Martel et al. 2013; Spitzen-van der Sluijs et al. 2014). Thus, species in areas where *Bd* is already present could be more vulnerable to *Bsal* exposure, and the introduction of *Bsal* to the area could result in disease outbreaks.

Alternatively, species or populations previously exposed to a similar pathogen may benefit from cross immunity, in which a host acquires immunity or partial immunity to one pathogen because of previous infection from a closely related pathogen (McMahon et al. 2014). This could potentially explain the lack of *Bd*-related declines in areas where both an endemic strain of *Bd* and *Bd*-GPL are present, such as in Brazil, South Africa, and Switzerland (Rodriguez et al. 2014; Martel et al. 2014). Perhaps the evolutionary history and co-existence with local, endemic *Bd* lineages has primed local amphibian populations to be able to resist or tolerate infection from *Bd*-GPL. If immunity to *Bd* translates to cross immunity to *Bsal*, then persisting populations in areas where *Bd* is in an enzootic state may be safeguarded against *Bsal* infections, and amphibians in areas where *Bd* is more recently established or where neither *Bd* nor *Bsal* currently occur may have the highest disease risk.

In addition to pathogen invasion history providing insight into the disease dynamics of these pathogens, host availability is a critical factor in disease maintenance and spread (Lloyd-Smith et al. 2005). A pathogen cannot persist without sufficient abundance of susceptible hosts; therefore, the establishment of *Bd* and/or *Bsal* in an area with suitable habitat depends on the presence and abundance of amphibian hosts. Information on host abundance at the community level for a continental assessment is presently not available; however, species richness can serve as an approximation of host abundance to determine areas where more hosts might be available to increase the chances of pathogen invasion and spread. That is, higher species richness might increase the number and diversity of potentially available hosts as well as the probability that at least one species might be a highly susceptible species, a reservoir species, or a super-spreader (DiRenzo et al. 2014), which could lead to increased disease risk (Power & Mitchell 2004;

Keesing et al. 2006). Therefore, species richness may be an important component to consider when assessing the threat of *Bd* and/or *Bsal* to North American amphibians.

With the threat of two deadly pathogens spreading in North America, it is important to determine the areas and species most at risk of disease from one or both pathogens. To do this, we estimate and compare the potential distributions of *Bd* and *Bsal* by creating high-resolution (30 arc-seconds or ~1 km) habitat suitability models (HSMs) using presence-only data as well as climate and land use variables. We then include potential biotic interactions and disease dynamics by weighting the HSMs with species richness. We identify areas most vulnerable to *Bd* and/or *Bsal* in North America and investigate the potential influence of an area's pathogen invasion history and the translocation of *R. catesbeiana* outside of its native range. We also show the potential threat of *Bd* and/or *Bsal* to all 263 threatened amphibian species in North America (IUCN 2016).

Materials and Methods

Habitat suitability models for Bd and Bsal

We created presence-only HSMs driven by climate and land use factors using Maxent version 3.3.3k (Phillips et al. 2004). Initial HSMs were trained on pathogen occurrence data and 23 environmental factors relevant to the establishment of *Bd* and *Bsal*. We then used a subset of the most important parameters to create pruned models for analysis.

We obtained 19 bioclimatic variables from the Worldclim database (http://www.worldclim.org/bioclim), which are a set of interpolated temperature and precipitation conditions based on monthly averages measured at weather stations across the

globe from the years 1950 to 2000, latitude, longitude, and elevation (Hijmans et al. 2005). In addition, we used mean potential evapotranspiration (PET), mean aridity (AI), and mean actual evapotranspiration (AET, or soil-water balance, from the CGIAR-CSI Consortium for Spatial Information (http://www.cgiar-csi.org/data/undefined/), all of which use climate data from WorldClim as primary input. PET is a measure of the ability of the atmosphere to remove water from the surface through evapotranspiration, and it was calculated using mean monthly temperature, temperature range, and radiation from above the atmosphere (Zomer et al. 2007). AI is a function of precipitation, temperature, and PET, and it quantifies the level of dryness at a given location (Zomer et al. 2008). AET is the effective quantity of water that is removed from the surface by evapotranspiration based on climatic conditions, and it was calculated using PET and soil moisture content (Trabucco & Zomer 2010). To incorporate land use patterns, we used the global human footprint (HF) from the Wildlife Conservation Society (http://sedac.ciesin.columbia.edu), which quantifies anthropogenic influences on land cover based on accessibility, land transformation, human population density, and electrical power infrastructure between the years 1995 to 2004 (Sanderson et al. 2011).

Modeling invasive species is challenging because it requires the extrapolation of information from a known environmental range to unknown, non-native geographic regions. It is important to consider biases that may over-influence model outcomes, such as sampling bias, which can lead to increased spatial autocorrelation and pseudoreplication. This can cause the model to overfit to environmental biases associated with the occurrence data. Boria et al. (2014) showed that applying a spatial filter to presence data reduces overfitting; therefore, we applied a spatial filter by randomly choosing one pathogen occurrence site from every 10 arc-minute (~12

km) area using R (dismo (Hijmans et al. 2013) and maptools (Bivand & Lewin-Koh 2014) packages). We further minimized sampling bias by restricting background sampling areas to a minimum convex hull polygon around the occurrence points (Rödder et al. 2009; Phillips & Elith 2013; Thorne et al. 2012; Mainali et al. 2015). Another concern is that these types of models assume the species is in an equilibrium state of distribution, which may not be the case when dealing with invasive species (Mainali et al. 2015; Thuiller et al. 2005). The lack of a presence point in a given locality does not necessarily indicate unsuitable habitat; it may be that the species was not yet there or it was missed at the time of surveillance. In addition, by default, Maxent randomly chooses 10,000 background points from the designated training area, which could potentially inflate the chances of false absences. To address these issues and further minimize the chances of the model misidentifying unsuitable habitat, we limited the number of background points to be equal to the number of presence points (Mainali et al. 2015; Liu et al. 2005).

Some of the bioclimatic variables are highly correlated with each other; therefore, to reduce the chances of overfitting the model due to multicollinearity of the model predictors, we ran an initial model for each pathogen with all 23 continuous variables. We conducted jack-knife tests to determine the relative importance of each predictor to the model. We also calculated Spearman's rank correlations (r) among all the variables to determine which variables were highly correlated with each other. Similar to previous studies (James et al. 2015; Liu et al. 2013), we used the results of the jackknife tests to choose the top-ranking model parameters that together contributed to approximately 90% of the full model for each pathogen. When variable

pairs had an $r^2 > 0.75$, we chose the higher ranking factor (Table 3.1). We then used the resulting subsets of environmental variables to create pruned HSMs for *Bd* and *Bsal*.

To evaluate model performance, we wanted to use existing presence data in North America that were collected independently from the data used to train our models. Because *Bd* is highly documented throughout North America and *Bsal* is not yet known to occur in North America, we focused on our *Bd* HSM to validate our HSM methodology. We obtained 889 *Bd*-positive records in North America from *Bd*-Maps (*Bd*-maps.net) that consisted of 659 unique localities. These data come from published literature prior to November 2014 and some have been used as training data in previous *Bd* modeling studies (Xie et al. 2016; James et al. 2015; Liu et al. 2013; Rödder et al. 2009). To avoid pseudoreplication with our test data, we applied a 10 arc-minute spatial filter on these sites, resulting in 432 test sites (131 within the *R. catesbeiana* native range and 301 outside of its range.

To account for variability and other uncertainties inherent in modeling, we ran 20 replicates for each species using crossvalidation: occurrence data were divided into 20 equal-sized folds, or groups, and for each replicate 19 folds were used for model training and 1 fold was used for model testing. We used 20 replicates because ensemble forecasts have been shown to make models more reliable and robust than single model outputs by accounting for variability (Araújo & New 2007), and the area under the receiver operating characteristic (AUC), a commonly used metric of model performance, had minimal differences when the model was run with more than 20 replicates (Vredenburg et al. unpublished data). The results were then averaged by Maxent to produce a final probabilistic density function of potentially suitable habitat.

Maxent calculates multiple threshold values for each model run to aid in model interpretation. Areas with values above these thresholds can be interpreted as a reasonable estimate of a species' distribution or suitable habitat, depending on the quality of the data. For our analyses, we used the minimum training presence logistic threshold, which is the mean of the lowest probability that the training points (i.e., true positives) fall on for each of the 20 replicates.

Bd Habitat Suitability Model

For the *Bd* HSM, we used 299 *Bd*-positive sites within North America. Data were from previous studies (Cheng et al. 2011; Sette et al. 2015; Talley et al. 2015; Yap et al. 2015) and unpublished data (Vredenburg et al. unpublished). Applying a 10 arc-minute spatial filter resulted in 184 *Bd*-positive sites for model training (Appendix 3.1A). Though these sites are not evenly distributed geographically across North America, the areas sampled represent areas with different *Bd* histories. We used sites in Illinois, where *Bd* has had a relatively constant prevalence for over 120 years (Talley et al. 2015), and, in contrast, we also used sites in California and Mexico, where there is evidence of more recent *Bd* invasions and declines (Cheng et al. 2011; Sette et al. 2015; Yap et al. 2016; Vredenburg et al. unpublished). The environmental variables used in the pruned *Bd* HSM included four variables for each of temperature and precipitation and one land use variable (Table 3.1).

Bsal Habitat Suitability Model

There are no published records of *Bsal* in Asia, its proposed place of origin (Martel et al. 2014); therefore, we used 133 *Bsal* proxy sites from Yap et al. (2015) to train our *Bsal* HSM. After we applied the 10 arc-minute spatial filter, we had 95 *Bsal* proxy sites for model training

(Appendix 3.1B): 29 known and 66 estimated occurrence points of the three putative host species identified by Martel et al. (Martel et al. 2014), *Cynops cyanurus*, *Cynops pyrrhogaster*, and *Paramesotriton deloustali*. As shown by Larson and Olden (Larson & Olden 2012), multiple proxy or 'avatar' species can be used to predict the distribution of data-poor species. Following Yap et al. (2015) we followed the hypothesis that the proposed reservoir species share an evolutionary history with *Bsal* (Martel et al. 2014), and, therefore, locations where these carrier species occur likely have suitable *Bsal* habitat. The environmental variables used in the pruned *Bsal* HSM included four temperature variables, three precipitation/moisture variables, and one land use variable (Table 3.1).

Amphibian species richness

We estimated amphibian richness in mainland North America by overlaying 597 unique species ranges (AmphibiaWeb 2015). We obtained 586 original range maps from the IUCN Red List (http://www.iucnredlist.org), which are based on expert knowledge and are the best estimated representations of species distributions in their native ranges globally. We created 11 new range maps for species with no IUCN range and updated 8 of the IUCN range maps. New and updated ranges were based on primary and secondary literature, georeferenced occurrence data available from VertNet (http://vertnet.org/), and expert opinion. We created a raster file in which we tallied the intersecting ranges per grid cell using R (dplyr (Wickham & Francois 2014) and raster (Hijmans 2014) packages) for total amphibians and for only salamanders. We normalized the richness models so that values were between 0 and 1. Spatial data for created or

updated range maps are available at https://github.com/AmphibiaWeb. All range maps are viewable on AmphibiaWeb by species (http://amphibiaweb.org).

Vulnerability models for Bd and/or Bsal

To identify regions of North America most vulnerable to chytridiomycosis, we used several approaches. First we looked at vulnerability to disease from the individual pathogens, weighting the *Bd* HSM with total amphibian richness (AR) and the *Bsal* HSM with salamander richness (SR). To ensure that areas with high pathogen suitability and low richness held more weight in disease risk compared to areas with high richness and low pathogen suitability, we calculated the product of the pathogen HSM and the square root of the richness model. To determine areas where amphibians may be exposed to at least one pathogen (cumulative disease risk), we added the pathogens' vulnerability models. To identify areas where amphibians could be exposed to both *Bd* and *Bsal* (combined disease risk), we multiplied the pathogens' vulnerability models. We calculated the following scenarios:

1. *Bd* vulnerability = *Bd* HSM * AR
2. *Bsal* vulnerability = *Bsal* HSM * SR
3. Cumulative Disease Risk = (*Bd* HSM * AR) + (*Bsal* HSM * SR)
4. Combined Disease Risk = (*Bd* HSM * AR) * (*Bsal* HSM * SR)

Pathogen invasion history and the translocation of R. catesbeiana

To investigate the potential influence of pathogen invasion history, we created an invasive risk model by excluding the potential native range of *Bd* from our overall risk models. To do this we used the native range of *R. catesbeiana* to represent the potential native range of

Bd-GPL, and we recalibrated our relative risk models within just the non-native region. We obtained the native range of *R. catesbeiana* by combining the areas designated by the US Geological Survey (USGS) and IUCN.

We assessed the predictive performance of the *Bd* risk models by calculating the percentage of the *Bd* test sites (432 in overall region, 301 in invasive region) that fell within high relative risk areas for the overall *Bd* risk model and the invasive *Bd* risk model. To do this, we applied the Jenks natural breaks classification (Jenks 1967) to our model data, which clusters values into classes in such a way that most similar values are grouped together, reducing the variance within each class while maximizing the variance between classes. We created four relative risk classes and calculated the percentage of points that fell within each relative risk class for each model. We define high relative risk as areas that include the top two relative risk classes.

We then compared the percentage of *Bd* sites that fell within high relative risk areas when using the overall *Bd* risk model versus the invasive *Bd* risk model. We also did this with 19 sites where known epizootic declines have occurred, three of which were from *Bd*-Maps test data located in the Sierra Nevada Mountains (Vredenburg et al. 2010) and 16 of which were from the training data located in Mexico (Cheng et al. 2011). Although these are not statistical tests, they provide insight as a general evaluation of our models.

To investigate the potential influence of invasive *R. catesbeiana* on *Bd* spread, we overlaid the invasive range of *R. catesbeiana* on our *Bd* risk models. These data, which were obtained from the USGS, indicate areas in the US where established populations of *R. catesbeiana* have been confirmed. We compared the overall and invasive risk models with where

Bd occurrences have been recorded, the invasive range of *R. catesbeiana*, and areas predicted as having high relative risk.

Identifying risk to special status species

The IUCN has designated 263 species in North America as threatened (Appendix 3.2). Many of these species are highly localized with small ranges, which makes them extremely vulnerable to environmental threats. To determine the risk of exposure to both *Bd* and *Bsal* to threatened species in North America, we calculated the area and percent overlap of each threatened species' range with cumulative risk and combined risk.

Results

Bd habitat suitability and vulnerability, and the potential influence of R. catesbeiana and historical context

Areas predicted to have high habitat suitability for *Bd* encompass almost the entire eastern half of the US, the Pacific Northwest, and mountain ranges in the western US and Mexico, including the Rocky Mountains, the Sierra Nevada, the Sierra Madre Oriental, and the Trans-Mexican volcanic belt (Figure 3.1A). The areas that are deemed unsuitable or as having low suitability include the lowland tropical forests of Mexico and the Southeast US as well as the arid regions in the great plains and the desert. The predicted unsuitability in the Yucatan Peninsula is surprising, though this may be due to not having any *Bd* training sites within an environmental context similar enough to that region. The Southeast US has the highest number (up to 46) of overlapping amphibian species ranges (Figure 3.1B). General *Bd* vulnerability is

highest in the eastern US (Figure 3.1C), while the highest invasive *Bd* vulnerability is in the Pacific Northwest, the Sierra Nevada, and portions of the Rocky Mountains down through the Sierra Madre Oriental and the Trans-Mexican volcanic belt of Mexico (Figure 3.1D). Approximately 94% (405/432) of the *Bd* test sites fell in areas predicted to have overall *Bd* risk and 93% (281/301) fell in areas predicted to have invasive *Bd* risk. The percentage of sites that fell within high relative risk areas almost doubles from 31% (133/432) in the overall *Bd* risk model to 61% (184/301) in the invasive *Bd* risk model. For the sites with known declines, only 37% (7/19) were in areas predicted to have high relative risk in the overall *Bd* risk model while the invasive *Bd* risk model had 95% (18/19) in high relative risk areas.

When we compare overall *Bd* risk to the invasive range of *R. catesbeiana*, there is some overlap with high relative risk areas along the northwest coast, but a majority of *R. catesbeiana*'s invasive range seems to occur in low relative risk areas (Figure 3.2A). However, when we compare invasive *Bd* risk to the invasive range of *R. catesbeiana*, we find that there is a high amount of overlap throughout most of the western US, and *Bd* occurrences generally align with established invasive populations of *R. catesbeiana* (Figure 3.2B).

Bsal habitat suitability and vulnerability

Areas highlighted as suitable *Bsal* habitat include the west coast, the Sierra Nevada mountain range, the northern Rocky Mountains, the highlands of Mexico, and the Southeast US (Figure 3.3A). Salamander richness is greatest in Appalachia and the Southeast US, with some areas having up to 29 overlapping ranges (Figure 3.3B). When we weight the *Bsal* HSM with salamander richness the Southeast US, the West Coast, and the highlands of central Mexico are

predicted to be the most vulnerable to *Bsal* (Figure 3.3C). And when we exclude the potential native range of *Bd*, the relative *Bsal* threat is more pronounced in the Pacific Northwest, northern Rocky Mountains, the Sierra Madre Oriental and the Trans-Mexican volcanic belt of Mexico (Figure 3.3D).

Cumulative and combined vulnerability

The highest cumulative suitability (*Bd* + *Bsal*) occurs in the Southeast US and the Pacific Northwest (Appendix 3.3A), and when weighted with species richness, the resulting cumulative risk has a similar pattern (Figure 3.4A). When we account for *Bd*'s potential native range in the eastern US, the highest cumulative disease risk occurs in the west coast and mountain ranges in the western US and throughout Mexico (Figure 3.4B). The combined (*Bd* * *Bsal*) HSM shows the highest habitat suitability in the Pacific Northwest, mountain ranges in the western US and throughout Mexico, and the southeastern US (Appendix 3.3B). When weighted with species richness, the resulting combined risk model is similar to the *Bsal* risk model (Figure 3.4C), showing the highest relative risk in Appalachia and the Southeast US, followed by the West Coast including the northern Rocky Mountains and the Sierra Nevada, and the lowest relative risk in the mountains of Mexico (Figure 3.4C). When we exclude the potential native range of *Bd*, the West Coast, including the Sierra Nevada, and the Sierra Madre Oriental and the Trans-Mexican volcanic belt of Mexico have the highest combined disease risk (Figure 3.4D).

Identifying risk to special status species

Of the 263 threatened amphibians in North America, all but one have ranges with at least 25% overlap with areas with the cumulative *Bd*/*Bsal* risk (predicted suitable areas identified in

Figure 3.4A), and 74% of threatened species (66 anurans and 129 caudates) have their entire range overlapping with areas of cumulative risk (Figure 3.5). When considering areas with combined *Bd*/*Bsal* risk (predicted suitable areas identified in Figure 3.4C), 241 species have ranges with at least partial overlap, of which 99 species (21 anurans and 78 caudates) have 100% overlap (Figure 3.5).

Of particular concern are species that are highly localized with small ranges, the majority of which are located in Mexico. Due to their limited ranges, these species are already vulnerable to other common stressors, such as habitat loss or climate change. The invasion and establishment of one or both pathogens could add more pressure to species survival. For the 149 threatened species with range areas less than 500 km^2, 139 species (43 anurans and 96 caudates) had 100% range overlap with cumulative risk areas and 74 species (16 anurans and 58 caudates) had 100% range overlap with combined risk areas.

Discussion

The global impact of chytridiomycosis on amphibians is the worst known example of a global epizootic, with hundreds of species affected. Despite almost two decades of research since *Bd* was described, our understanding of the basic biology in this host/pathogen system is still limited. Using HSMs and vulnerability models as exploratory and predictive tools helps us understand present impacts and allows us to predict future impacts at a scale not possible using traditional field or laboratory-based studies.

The *Bd* HSM we constructed (Figure 3.1A) has outputs similar to HSMs from previous studies (Rödder et al. 2009; James et al. 2015; Liu et al. 2013; Xie et al. 2016), though areas

identified as suitable *Bd* habitat in our HSM extend more towards the interior US and Mexico. Our overall *Bd* risk model (Figure 3.1C) substantially differs from that of Grant et al. (2016), which highlights only the northeastern US and central Rocky Mountains as having high *Bd* risk and poorly reflects where *Bd* has been documented in the western and southeastern US. We believe we improved model performance and reduced overfitting by restricting our training points to only North America, implementing a spatial filter on the *Bd* data, using limited background areas and points, and using a higher resolution of 30 arc-seconds (~1km^2) compared to 2.5 arc-minutes (~4km^2).

In our results, the eastern/southeastern US is consistently highlighted as having high *Bd* suitability and high disease risk. This pattern supports our hypothesis that *Bd*-GPL (or its preceding strain) may be native to this region and the hypothesis of Huss et al. (2013) that *R. catesbeiana* may have acted as a significant spreader of disease to the western US and Mexico. Thus we believe that our overall *Bd* risk model (Figure 3.1C) may merely reflect the high suitability for *Bd* in its region of origin rather than the threat of *Bd* to naïve amphibian populations. When we account for *Bd*'s potential native range, there are many areas highlighted as having high disease risk in the western US and in Mexico that were not previously emphasized (Figure 3.1D), which includes areas where declines have been documented (Padgett-Flohr & Hopkins 2009; Vredenburg et al. 2010; Vredenburg et al. 2013; Cheng et al. 2011; Sette et al. 2015). These areas also coincide with established invasive populations of *R. catesbeiana* (Figure 3.2B), which reiterates the major role invasive species like *R. catesbeiana* may have had (and may continue to have) in *Bd* spread and the importance of considering pathogen invasion history when estimating disease risk. Additional historical and present-day surveys are needed to

investigate our hypothesis and enhance our knowledge of *Bd*'s history, species susceptibility, and potential defenses against *Bd*.

More studies are also needed to determine the distribution and threat of *Bsal*. Our *Bsal* HSM (Figure 3.3A) is quite different from Richgels et al. (Richgels et al. 2016), likely because they used only temperature thresholds to estimate habitat suitability. Their approach neglects biotic interactions, precipitation/moisture, and land use patterns that may influence not only the pathogen, but also the species that could host the pathogen. Salamander hosts likely seek refuge from warm air temperatures in cooler, moist microclimates where *Bsal* is more likely to survive. Thus, our use of presence points of putative reservoir species may improve our estimation of where *Bsal* could survive. In addition, in a laboratory experiment by Blooi et al. (Blooi et al. 2015), *Bsal* zoospores on salamander hosts were able to withstand high temperatures for longer time periods than in vitro *Bsal* zoospores, further indicating the importance of host-pathogen dynamics. Our *Bsal* HSM is similar to that of Yap et al. (2015), though there are a few differences. *Bsal* suitability along the west coast extends to the northern Rocky Mountains, and in the Southeast US suitability encompasses more of the Appalachian Mountains up to the New England area than in the previous study. In addition, the northern areas of North America, including most of Canada and many midwestern and northeastern US states, are predicted to be unsuitable for *Bsal*.

Our *Bsal* vulnerability model is generally similar to previous risk models (Yap et al. 2015; Richgels et al. 2016), highlighting the Southeast US, Pacific Northwest, and the highlands of Mexico as having the highest relative risk. However, there are some key differences with the Richgels et al. (2016) model, which emphasizes more of the eastern and northeastern US as

having increased risk. Our model indicates much of this area to be unsuitable for *Bsal*, and therefore species that occur there have less relative risk of *Bsal* exposure. This difference is likely due to the differences in our HSM approach since the methods they used to incorporate salamander richness are similar to ours.

Our vulnerability models demonstrate that most of the amphibians of North America are at risk of being exposed to one or both pathogens responsible for chytridiomycosis (Figure 3.4A and Figure 3.4C). When we look at relative disease risk from *Bd* exposure alone, taking its potential native range in the eastern US into account (Figure 3.1D), we assume amphibians in the eastern US are less vulnerable to disease because of their hypothesized co-evolution with *Bd*. However, when we incorporate the possibility of *Bsal* exposure, that vulnerability must be revisited, particularly considering that *Bsal* has caused mass mortalities of *Salamandra salamandra* in the same region of the Netherlands where *Bd* was found to be in an enzootic state (Martel et al. 2013; Spitzen-van der Sluijs et al. 2014). It is still unknown if exposure to *Bd* will exacerbate or diminish the effects of *Bsal*, and future studies should focus on this key question. The Southeast US is the world's salamander biodiversity hotspot, and with suitable habitat for both *Bd* and *Bsal* as well as ample potential hosts, the threat of disease spread may be high.

Bsal has only been shown to infect salamanders (Martel et al. 2014), which would suggest that only salamanders are at increased risk of disease; however, only 10 of over 6,500 known species of frogs and one out of over 200 known species of caecelians have been tested since *Bsal*'s description in 2013 (Martel et al. 2013). In addition, only one of the frog species that was tested, *R. catesbeiana*, occurs in North America. With the devastation *Bd* has caused to amphibian populations globally in the past few decades, it is important to consider the possibility

that *Bsal* could infect other species that have not yet been tested. Furthermore, while *Bd* has impacted frogs the most out of the three amphibian Orders, salamanders have also experienced declines due to *Bd* (Cheng et al. 2011; Sette et al. 2015), and they could act as *Bd* reservoirs (Chatfield et al. 2012; Davidson et al. 2013). Analogous relationships between frogs and *Bsal* may exist; therefore, it is important to consider the potential threat of *Bsal* to all amphibians.

The uncertainty of how these two closely related pathogens may interact with each other limits our ability to predict cumulative or combined disease risk. We assessed relative risk based on previous exposure to *Bd* in an endemic region as being either neutral (Figure 3.4A and Figure 3.4C) or protective (Figure 3.4B and Figure 3.4D), though there are other potential scenarios of how these pathogens may interact with each other. For example, there is a possibility that amphibian populations in areas where *Bd* seems to be in an enzootic state may be more susceptible to *Bsal*, as may be the case in the declines seen in wild *S. salamandra* where *Bd* was co-existing with local amphibian populations (Martel et al. 2013; Spitzen-van der Sluijs et al. 2014). Another possibility is that an area may be exposed to *Bsal* before being exposed to *Bd*, and it is unclear how that may affect how a species is impacted. Species susceptibility studies are needed to further our understanding of these multi-host, multi-pathogen dynamics.

Of the 263 threatened amphibian species in North America, 211 occur in Mexico (AmphibiaWeb 2015). This comprises more than 50% of Mexico's 377 species, most of which are highly localized, endemic species nestled in the central and southern mountain ranges. Many of these species' ranges occur entirely within cumulative and/or combined disease risk areas. Because many of their ranges do not overlap with each other, even relatively low to moderate disease risk in Mexico could be a significant threat to biodiversity. For our models we only

considered local species richness (alpha diversity), depicting where species ranges overlap but not distinguishing between which species are overlapping. This neglects the beta diversity of amphibians, which accounts for the differentiation of species assemblages among habitats, considering both alpha diversity and regional species richness (gamma diversity) (Whittaker 1960). Thus, when we look only at alpha diversity of North America (Figure 3.1B), Mexico's high amphibian richness and endemism is overshadowed by the high alpha diversity in the eastern US, which leads to risk models potentially minimizing the threat of disease to amphibian biodiversity in Mexico. Therefore, when interpreting these models, it is important to understand the parameters used and limitations of our analyses.

Conclusion

By integrating environmental suitability, host availability, and pathogen invasion history, we created models that reflect key risk factors and highlight significant threats of *Bd* and/or *Bsal* on amphibian populations in North America. The continuous spread of *Bd* threatens remaining uninfected populations, and the introduction of *Bsal* could compound the chances of more amphibian epizootics. By considering local pathogen invasion history, we were able to uncover a new pattern in *Bd* dynamics that suggests that *Bd*-GPL (or its preceding strain) may have originated in the eastern US and the translocation of *R. catesbeiana* to western North America by humans may have played a major role in *Bd* spread. More studies are needed to test these predictions and hypotheses.

Our models provide guidance for conservation and management efforts to focus on areas and species where we found relative disease threat to be highest. Targeted historical and present

day surveys could help test our hypotheses and further our understanding of the spatiotemporal distribution of *Bd* and *Bsal*. More localized, community-level studies, monitoring, and surveillance are needed to further our understanding of the disease ecology and host-pathogen dynamics of *Bd* and *Bsal*. Finally, species susceptibility studies could lead to the identification of the potential interactions between these pathogens and the discovery of potential defenses against disease.

Acknowledgements

This work was supported by NSF IOS-1258133 (V.T.V.). We thank Vredenburg lab collaborators and *Bd*-Maps for georeferenced occurrence data. We thank the US Geological Survey and IUCN for range map data. We thank Thomas Gillespie, James Lloyd-Smith, and Richard Vance for valuable feedback and suggestions. We also thank University of California, Berkeley and San Francisco State University GIS and informatics undergraduate apprentices for their species range work. And we thank the Museum of Vertebrate Zoology at University of California, Berkeley for technical support.

Figures

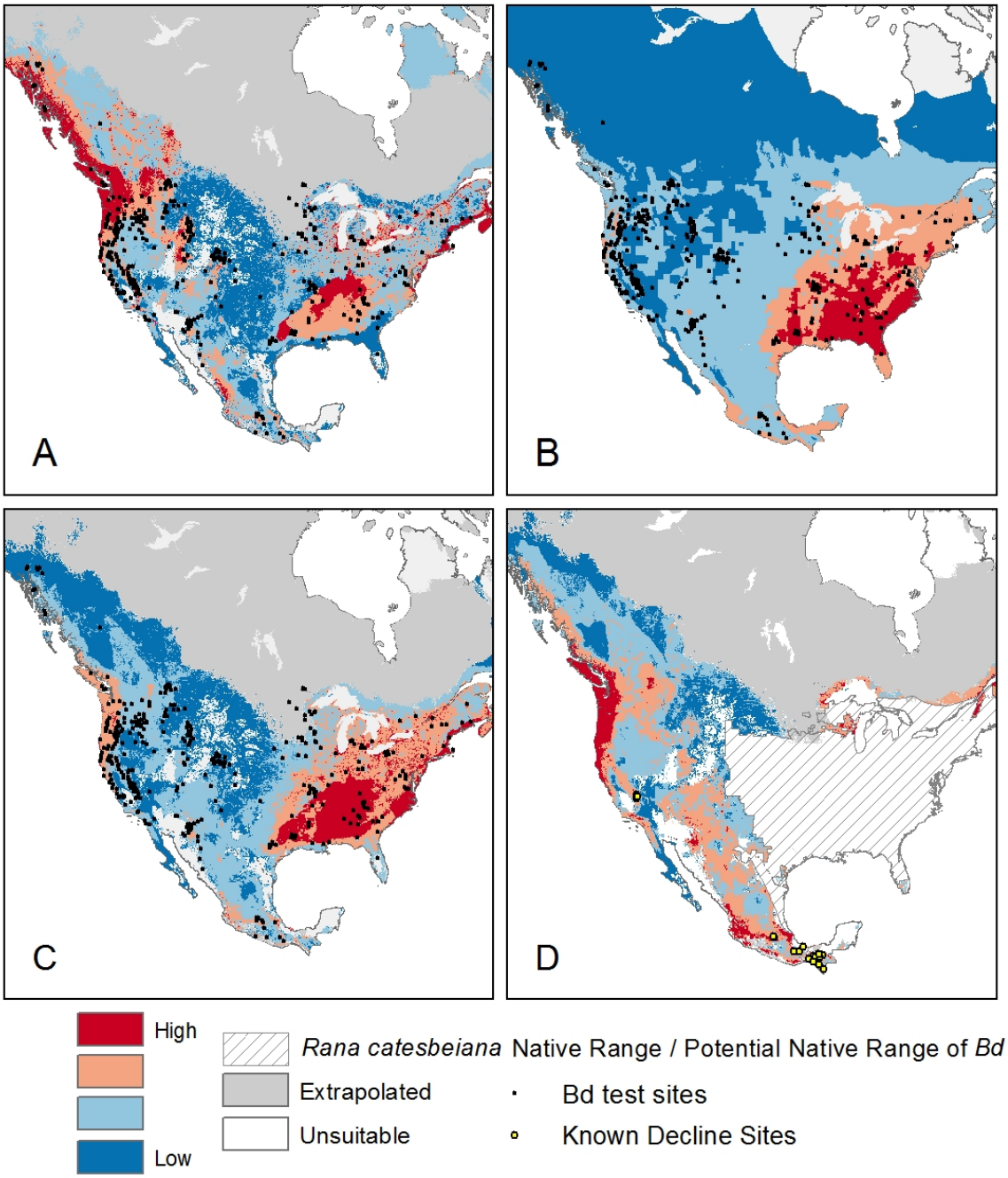

Figure 3.1 North America *Bd* models. A) *Bd* HSM, B) amphibian richness, C) overall *Bd* vulnerability, and D) invasive *Bd* vulnerability.

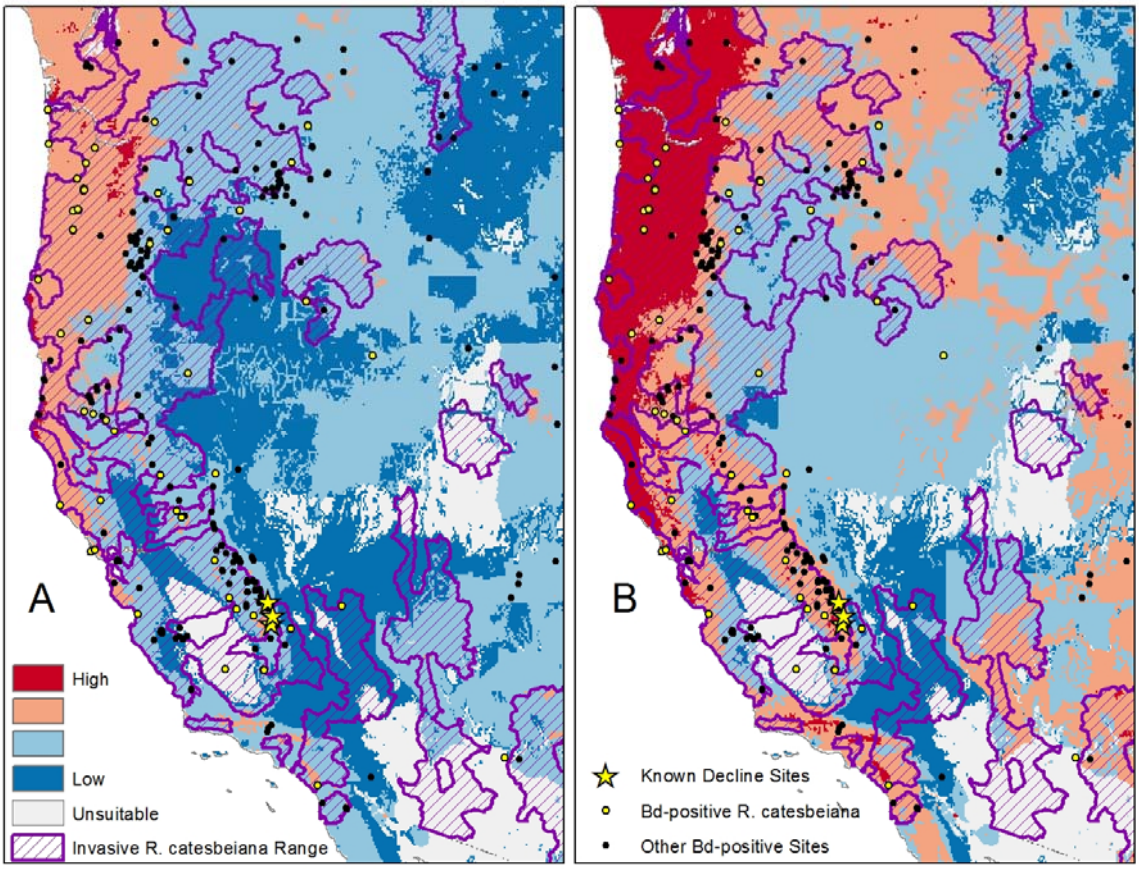

Figure 3.2 The potential influence of *R. catesbeiana* on *Bd* spread and the importance of considering historical context. *Bd* invasion patterns of A) overall risk, with no consideration of historical context, and B) invasive risk, where the potential native range of *Bd* is excluded.

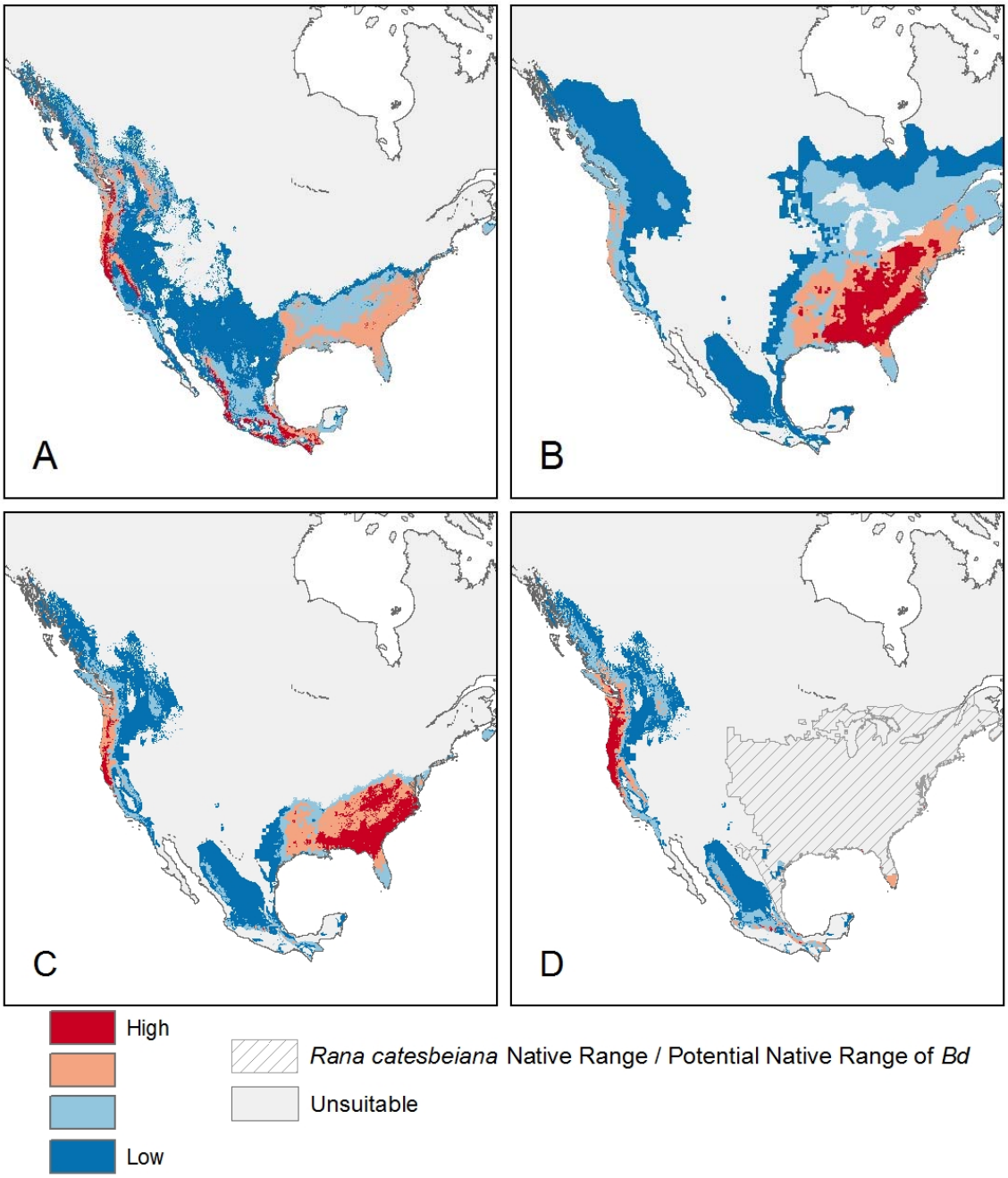

Figure 3.3 North America *Bsal* models. A) *Bsal* HSM, B) salamander richness, C) overall *Bsal* vulnerability, and D) invasive *Bsal* vulnerability.

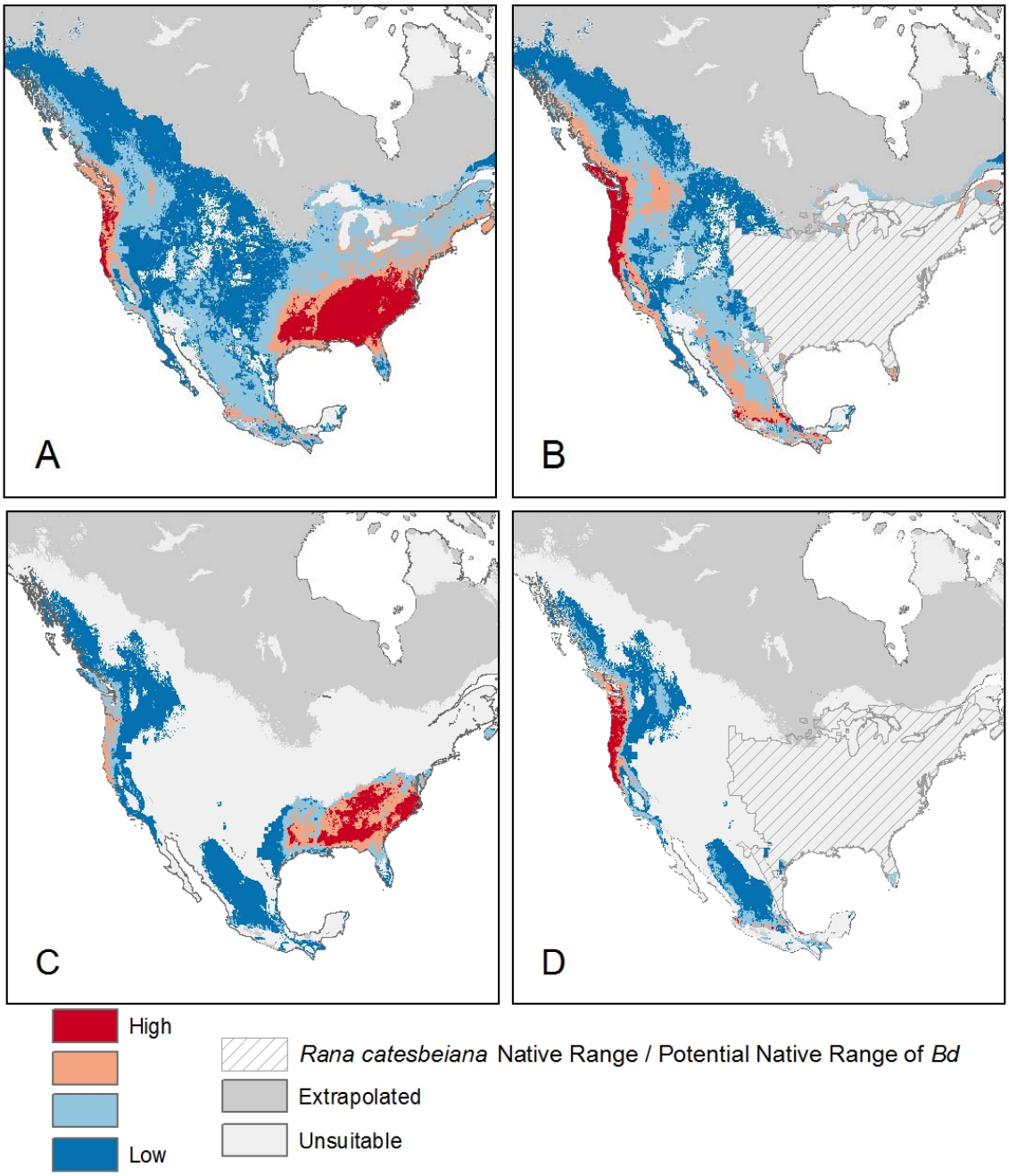

Figure 3.4 North America disease risk models. A) Overall cumulative disease risk (*Bd* vulnerability + *Bsal* vulnerability), B) Invasive cumulative disease risk, C) Overall combined disease risk (*Bd* vulnerability * *Bsal* vulnerability), and D) Invasive combined disease risk.

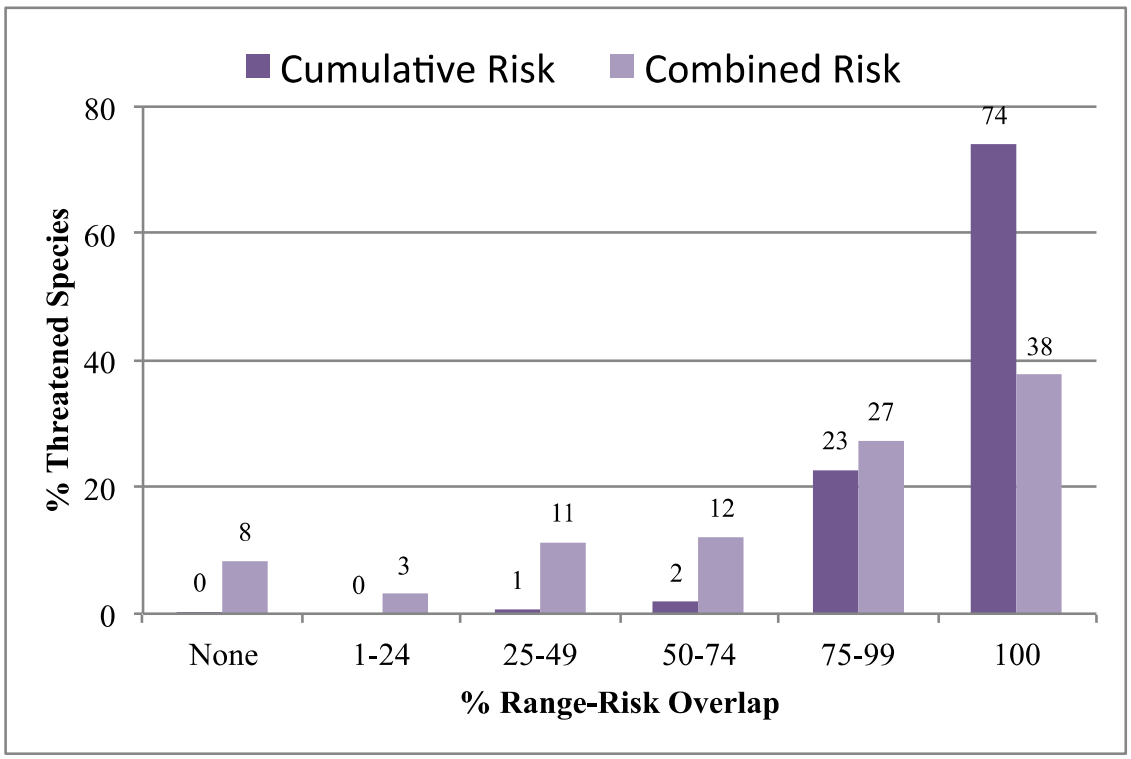

Figure 3.5 The number of threatened species and the portion of their ranges that overlap with overall disease risk.

Tables

Table 3.1 Environmental predictors for pruned habitat suitability models for *Bd* and *Bsal* in North America

Environmental Predictor	***Bd***	***Bsal***
Mean Diurnal Temperature Range (Bio2)		x
Isothermality (Bio3)	x	
Temperature Seasonality (Bio4)	x	x
Maximum Temperature of the Warmest Month (Bio5)	x	
Minimum Temperature of the Coldest Month (Bio6)	x	x
Temperature Annual Range (Bio7)		x
Mean Temperature of the Wettest Quarter (Bio8)	x	
Mean Temperature of the Driest Quarter (Bio9)	x	
Mean Temperature of the Warmest Month (Bio10)		x
Precipitation of the Wettest Month (Bio13)		x
Precipitation Seasonality (Bio15)	x	
Precipitation of Warmest Quarter (Bio18)	x	
Aridity (AI)		x
Human Footprint (HF)	x	x

Appendices

We used ArcGIS to produce additional figures that visualize the data we used to create our models and some of our model predictions. Appendix 3-1A shows the *Bd* occurrence points and the restricted background areas used to train our model. Data are clustered in the Midwest US, where *Bd* appears to be in an enzootic state (Talley et al. 2015), and in California and Mexico, where declines due to *Bd* have been observed (Vredenburg et al. 2010; Cheng et al. 2011). In Appendix 3-1B we show the *Bsal* proxy sites and background areas used for the *Bsal* HSM. In Appendix 3-2 we show the threatened species included in our analyses. In Appendix 3-3 we show the cumulative and combined *Bd* and *Bsal* HSMs. For Appendix 3-3A, we calculated the sum of the *Bd* and *Bsal* HSMs to get the cumulative disease risk HSM where *Bd* and/or *Bsal* could occur, based on only climate and land use data. For Appendix 3-3B, we calculated the product of the *Bd* and *Bsal* HSMs to get is the combined disease risk HSM where both *Bd* and *Bsal* could occur, based on only climate and land use data.

Appendix 3.1 Training points and background sampling areas for the habitat suitability models in North America of A) *Bd* and B) *Bsal*.

Appendix 3.2 List of threatened species in North America according to the IUCN (2016).

Order	**Species Name**
Anura	Anaxyrus californicus
Anura	Anaxyrus canorus
Anura	Anaxyrus exsul
Anura	Anaxyrus houstonensis
Anura	Anaxyrus nelsoni
Anura	Charadrahyla altipotens
Anura	Charadrahyla chaneque
Anura	Charadrahyla nephila
Anura	Charadrahyla taeniopus
Anura	Charadrahyla trux
Anura	Craugastor alfredi
Anura	Craugastor brocchi
Anura	Craugastor decoratus
Anura	Craugastor glaucus
Anura	Craugastor greggi
Anura	Craugastor guerreroensis
Anura	Craugastor hobartsmithi
Anura	Craugastor lineatus
Anura	Craugastor matudai
Anura	Craugastor megalotympanum
Anura	Craugastor montanus
Anura	Craugastor omiltemanus
Anura	Craugastor polymniae
Anura	Craugastor pozo
Anura	Craugastor pygmaeus
Anura	Craugastor rhodopis
Anura	Craugastor silvicola
Anura	Craugastor spatulatus
Anura	Craugastor stuarti
Anura	Craugastor tarahumaraensis
Anura	Craugastor uno
Anura	Craugastor vulcani
Anura	Duellmanohyla chamulae
Anura	Duellmanohyla ignicolor
Anura	Duellmanohyla schmidtorum
Anura	Ecnomiohyla echinata

Anura	Ecnomiohyla valancifer
Anura	Exerodonta chimalapa
Anura	Exerodonta juanitae
Anura	Exerodonta melanomma
Anura	Exerodonta pinorum
Anura	Exerodonta xera
Anura	Hyla walkeri
Anura	Hypopachus barberi
Anura	Incilius cavifrons
Anura	Incilius cristatus
Anura	Incilius cycladen
Anura	Incilius gemmifer
Anura	Incilius macrocristatus
Anura	Incilius perplexus
Anura	Incilius spiculatus
Anura	Incilius tacanensis
Anura	Incilius tutelarius
Anura	Lithobates chichicuahutla
Anura	Lithobates chiricahuensis
Anura	Lithobates dunni
Anura	Lithobates johni
Anura	Lithobates megapoda
Anura	Lithobates okaloosae
Anura	Lithobates omiltemanus
Anura	Lithobates onca
Anura	Lithobates pueblae
Anura	Lithobates sevosus
Anura	Lithobates sierramadrensis
Anura	Lithobates subaquavocalis
Anura	Lithobates tarahumarae
Anura	Lithobates tlaloci
Anura	Megastomatohyla mixe
Anura	Megastomatohyla mixomaculata
Anura	Megastomatohyla nubicola
Anura	Megastomatohyla pellita
Anura	Plectrohyla acanthodes
Anura	Plectrohyla arborescandens
Anura	Plectrohyla avia
Anura	Plectrohyla calthula

Anura	Plectrohyla calvicollina
Anura	Plectrohyla celata
Anura	Plectrohyla cembra
Anura	Plectrohyla charadricola
Anura	Plectrohyla chryses
Anura	Plectrohyla crassa
Anura	Plectrohyla cyanomma
Anura	Plectrohyla cyclada
Anura	Plectrohyla ephemera
Anura	Plectrohyla guatemalensis
Anura	Plectrohyla hartwegi
Anura	Plectrohyla hazelae
Anura	Plectrohyla ixil
Anura	Plectrohyla lacertosa
Anura	Plectrohyla matudai
Anura	Plectrohyla mykter
Anura	Plectrohyla pachyderma
Anura	Plectrohyla pentheter
Anura	Plectrohyla psarosema
Anura	Plectrohyla pycnochila
Anura	Plectrohyla robertsorum
Anura	Plectrohyla sabrina
Anura	Plectrohyla sagorum
Anura	Plectrohyla siopela
Anura	Plectrohyla thorectes
Anura	Rana draytonii
Anura	Rana muscosa
Anura	Rana pretiosa
Anura	Rana sierrae
Anura	Smilisca dentata
Anura	Tlalocohyla godmani
Caudata	Ambystoma altamirani
Caudata	Ambystoma amblycephalum
Caudata	Ambystoma andersoni
Caudata	Ambystoma bishopi
Caudata	Ambystoma bombypellum
Caudata	Ambystoma californiense
Caudata	Ambystoma cingulatum
Caudata	Ambystoma dumerilii

Caudata	Ambystoma granulosum
Caudata	Ambystoma leorae
Caudata	Ambystoma lermaense
Caudata	Ambystoma mexicanum
Caudata	Ambystoma ordinarium
Caudata	Ambystoma taylori
Caudata	Batrachoseps campi
Caudata	Batrachoseps regius
Caudata	Batrachoseps simatus
Caudata	Batrachoseps stebbinsi
Caudata	Batrachoseps wrighti
Caudata	Bolitoglossa engelhardti
Caudata	Bolitoglossa flavimembris
Caudata	Bolitoglossa flaviventris
Caudata	Bolitoglossa franklini
Caudata	Bolitoglossa mulleri
Caudata	Bolitoglossa riletti
Caudata	Bolitoglossa rostrata
Caudata	Bolitoglossa veracrucis
Caudata	Bolitoglossa zapoteca
Caudata	Bromeliohyla dendroscarta
Caudata	Chiropterotriton arboreus
Caudata	Chiropterotriton chiropterus
Caudata	Chiropterotriton chondrostega
Caudata	Chiropterotriton cracens
Caudata	Chiropterotriton dimidiatus
Caudata	Chiropterotriton lavae
Caudata	Chiropterotriton magnipes
Caudata	Chiropterotriton multidentatus
Caudata	Chiropterotriton orculus
Caudata	Chiropterotriton terrestris
Caudata	Cryptotriton adelos
Caudata	Cryptotriton alvarezdeltoroi
Caudata	Dendrotriton megarhinus
Caudata	Dendrotriton xolocalcae
Caudata	Eleutherodactylus angustidigitorum
Caudata	Eleutherodactylus dennisi
Caudata	Eleutherodactylus dilatus
Caudata	Eleutherodactylus dixoni

Caudata	Eleutherodactylus grandis
Caudata	Eleutherodactylus leprus
Caudata	Eleutherodactylus longipes
Caudata	Eleutherodactylus modestus
Caudata	Eleutherodactylus nivicolimae
Caudata	Eleutherodactylus rubrimaculatus
Caudata	Eleutherodactylus rufescens
Caudata	Eleutherodactylus saxatilis
Caudata	Eleutherodactylus syristes
Caudata	Eleutherodactylus verrucipes
Caudata	Eurycea chisholmensis
Caudata	Eurycea junaluska
Caudata	Eurycea latitans
Caudata	Eurycea nana
Caudata	Eurycea naufragia
Caudata	Eurycea neotenes
Caudata	Eurycea rathbuni
Caudata	Eurycea sosorum
Caudata	Eurycea tonkawae
Caudata	Eurycea tridentifera
Caudata	Eurycea wallacei
Caudata	Eurycea waterlooensis
Caudata	Gyrinophilus gulolineatus
Caudata	Gyrinophilus palleucus
Caudata	Gyrinophilus subterraneus
Caudata	Hydromantes brunus
Caudata	Hydromantes shastae
Caudata	Necturus alabamensis
Caudata	Notophthalmus meridionalis
Caudata	Nyctanolis pernix
Caudata	Parvimolge townsendi
Caudata	Phaeognathus hubrichti
Caudata	Plethodon amplus
Caudata	Plethodon asupak
Caudata	Plethodon cheoah
Caudata	Plethodon fourchensis
Caudata	Plethodon hubrichti
Caudata	Plethodon meridianus
Caudata	Plethodon petraeus

Caudata	Plethodon shenandoah
Caudata	Plethodon sherando
Caudata	Plethodon shermani
Caudata	Plethodon stormi
Caudata	Plethodon welleri
Caudata	Pseudoerurycea ahuitzotl
Caudata	Pseudoerurycea altamontana
Caudata	Pseudoerurycea anitae
Caudata	Pseudoerurycea aquatica
Caudata	Pseudoerurycea aurantia
Caudata	Pseudoerurycea bellii
Caudata	Pseudoerurycea boneti
Caudata	Pseudoerurycea brunnata
Caudata	Pseudoerurycea cochranae
Caudata	Pseudoerurycea conanti
Caudata	Pseudoerurycea firscheini
Caudata	Pseudoerurycea gadovii
Caudata	Pseudoerurycea gigantea
Caudata	Pseudoerurycea goebeli
Caudata	Pseudoerurycea juarezi
Caudata	Pseudoerurycea leprosa
Caudata	Pseudoerurycea lineola
Caudata	Pseudoerurycea longicauda
Caudata	Pseudoerurycea lynchi
Caudata	Pseudoerurycea melanomolga
Caudata	Pseudoerurycea mystax
Caudata	Pseudoerurycea naucampatepetl
Caudata	Pseudoerurycea nigra
Caudata	Pseudoerurycea nigromaculata
Caudata	Pseudoerurycea orchileucos
Caudata	Pseudoerurycea orchimelas
Caudata	Pseudoerurycea parva
Caudata	Pseudoerurycea praecellens
Caudata	Pseudoerurycea rex
Caudata	Pseudoerurycea robertsi
Caudata	Pseudoerurycea saltator
Caudata	Pseudoerurycea scandens
Caudata	Pseudoerurycea smithi
Caudata	Pseudoerurycea tenchalli

Caudata	Pseudoeurycea teotepec
Caudata	Pseudoeurycea tlahcuiloh
Caudata	Pseudoeurycea unguidentis
Caudata	Pseudoeurycea werleri
Caudata	Ptychohyla erythromma
Caudata	Ptychohyla leonhardschultzei
Caudata	Rhyacotriton olympicus
Caudata	Thorius adelos
Caudata	Thorius arboreus
Caudata	Thorius aureus
Caudata	Thorius boreas
Caudata	Thorius dubitus
Caudata	Thorius grandis
Caudata	Thorius infernalis
Caudata	Thorius lunaris
Caudata	Thorius macdougalli
Caudata	Thorius magnipes
Caudata	Thorius minutissimus
Caudata	Thorius minydemus
Caudata	Thorius munificus
Caudata	Thorius narismagnus
Caudata	Thorius narisovalis
Caudata	Thorius omiltemi
Caudata	Thorius papaloae
Caudata	Thorius pennatulus
Caudata	Thorius pulmonaris
Caudata	Thorius schmidti
Caudata	Thorius smithi
Caudata	Thorius spilogaster
Caudata	Thorius troglodytes
Gymnophiona	Agalychnis moreletii
Gymnophiona	Dermophis mexicanus

Appendix 3.3 Cumulative and combined habitat suitability models for *Bd* and *Bsal*. A) Cumulative HSMs (*Bd* HSM + *Bsal* HSM) and B) Combined HSMs (*Bd* HSM * *Bsal* HSM).

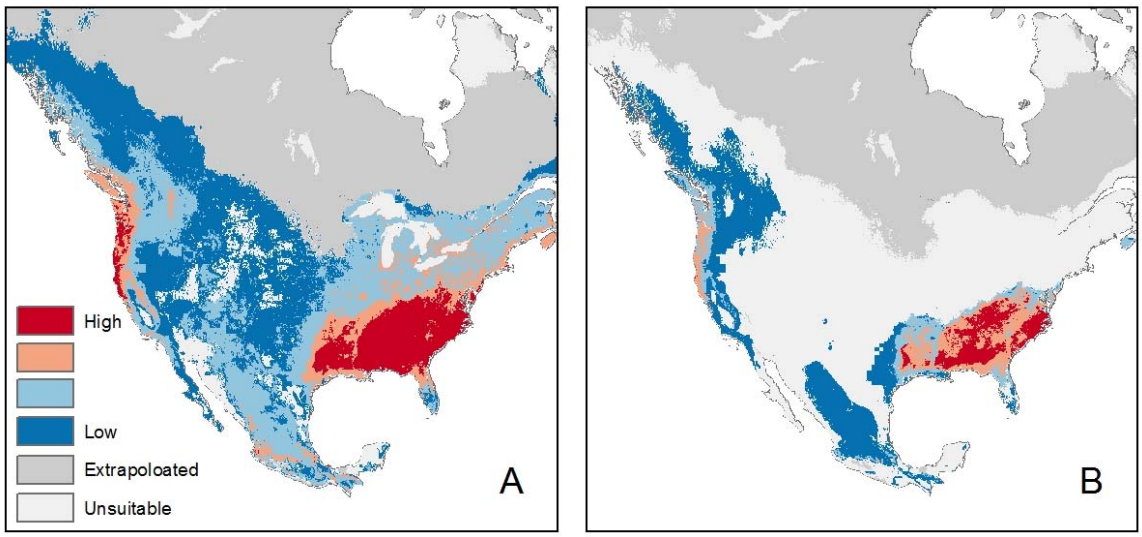

4. CHAPTER 4: Assessing the threat of the chytrid fungal pathogen, *Batrachochytrium dendrobatidis*, to amphibians in Asia and the potential effects of an invasive carrier species, amphibian richness, and climate change

Abstract

Since the 1970's chytridiomycosis, an emerging infectious disease caused by the fungal pathogen *Batrachochytrium dendrobatidis* (*Bd*), has devastated amphibian biodiversity globally, infecting over 500 species and causing declines and extinctions in at least 200 species. Humans may have facilitated the rapid spread of *Bd* by translocating an invasive carrier species like the American bullfrog (*Rana catesbeiana*) through international trade. We created a *Bd* vulnerability model combining habitat suitability models for *Bd* and *R. catesbeiana* and incorporating native host availability (i.e., amphibian richness) to predict the areas and species most at risk of *Bd* exposure in Asia, where one quarter of the world's amphibians occur and frog trade is popular, yet *Bd* epizootics have not yet been documented. We found that the potential presence of *R. catesbeiana* and amphibian richness may have a strong influence on *Bd* risk. Integrating these drivers with potential *Bd* suitability improved model performance, as 82% of all known *Bd* occurrences in Asia were found to occur in areas predicted to have high relative risk. We show that montane regions in China, Southeast Asia, and the Pacific Islands have the highest relative *Bd* risk, and most threatened species have at least some part of their range overlapping with these areas. We predict that climate change will lead to a 3-23% decrease in total area of *Bd* risk in Asia by 2070. Because of recent increases in *Bd* prevalence and *Bd*'s association with the potential presence of *R. catesbeiana* and amphibian richness, we hypothesize that *Bd* may be newly emerging in Asia, with human influences and globalization being the main drivers of

emergence. Our models provide helpful guidance for conservation planning and management by highlighting the threat of *R. catesbeiana* in *Bd* spread and identifying areas at highest risk to prioritize for surveillance and monitoring.

Introduction

Emerging infectious diseases (EIDs) are increasingly affecting wildlife and causing drastic declines across multiple taxa around the world (Daszak et al. 2000; Fisher et al. 2012). Since the 1970's chytridiomycosis, an EID caused by the fungal pathogen *Batrachochytrium dendrobatidis* (*Bd*), has devastated amphibian biodiversity globally (Wake & Vredenburg 2008), infecting over 500 species (Olson et al. 2013) and causing declines and extinctions in at least 200 species (Alroy 2015; Fisher et al. 2009; Skerratt et al. 2007). Surprisingly, there have been no documented declines or die-offs due to *Bd* (i.e., epizootics) in Asia, and the global panzootic lineage of *Bd* (*Bd*-GPL), the strain associated with amphibian epizootic declines, is most likely newly emerging there. Unlike in areas where *Bd* appears to be endemic with a prevalence ~20% (Talley et al. 2015; Rodriguez et al. 2014), the prevalence of *Bd* across most of Asia is relatively low at < 6% (Goka et al. 2009; Swei et al. 2011; Bai et al. 2012; Zhu et al. 2014; Zhu et al. 2016), and there are areas in northern China that are reported to lack *Bd* (Zhu et al. 2016). In addition, areas in South Korea and the Philippines have been experiencing a recent increase in *Bd* prevalence (Bataille et al. 2013, Vredenburg et al. unpublished).

Continued opportunities for the introduction of *Bd* through trade could lead to major amphibian declines in Asia. If *Bd* follows patterns seen with other invading pathogens, it likely takes time and multiple introductions before successful establishment and spread through host

populations. This pattern is evident in California, where the earliest record of *Bd* was found on an invasive American bullfrog (*Rana catesbeiana*) in 1928 (Huss et al. 2013), yet emergence and epizootics did not occur until the 1960s and 1970s (Bradford 1991; Wake & Vredenburg 2008; Padgett-Flohr & Hopkins 2009; Sette et al. 2015).

There are other potential explanations for the lack of *Bd* epizootics in Asia. It could be that *Bd* is endemic to the region (Goka et al. 2009), and local strains may be preventing epizootics by outcompeting *Bd*-GPL (Schloegel et al. 2012; Bataille et al. 2013). Alternatively, Asian amphibians may be protected by cross immunity from either endemic strains of *Bd* (McMahon et al. 2014) or from the more recently discovered *Batrachochytrium salamandrivorans* (*Bsal*), a pathogenic chytrid specific to salamanders that also causes chytridiomycosis and is hypothesized to have originated in Asia (Martel et al. 2014). However, if endemic strains of *Bd* or *Bsal* are able to deactivate the immune system (Fites et al. 2013), then secondary exposure to a new introduced *Bd* strain may lead to increased host mortality.

The widespread distribution of *Bd* may be due to the international trade popularity of *R. catesbeiana*. This species is a known *Bd* reservoir that likely facilitates the pathogen's spread to naïve amphibian populations (Hanselmann et al. 2004; Garner et al. 2006; Fisher & Garner 2007; Schloegel et al. 2012; Liu et al. 2013) (see Chapter 2). In Asia, *R. catesbeiana* is used as a food source and for medicinal purposes and has been introduced to China, Japan, Indonesia, Malaysia, Java, Bali, the Philippines, Taiwan, Singapore, and Thailand. Introductions began with commercial farming throughout the 1900s (Lever 2003; Diesmos et al. 2006; McLeod et al. 2008), and many places now host established wild populations, likely founded by escaped individuals from captive housing on farms or when humans released live animals from the

markets into the wild for religious reasons (Lever 2003). *Bd* has been detected in *R. catesbeiana* in Asia in established wild populations as well as on farms and in markets (Goka et al. 2009; Yang et al. 2009; Bai et al. 2010; Bai et al. 2012; Fong et al. 2015; Zhu et al. 2016). The extent of *R. catesbeiana*'s distribution and abundance in Asia is not well documented, though there is a high likelihood that their populations will continue to expand in the wild with ongoing trade and commercial farming. Therefore, *R. catesbeiana* presents a significant threat of disease spread, and it is important to identify its distribution to determine the potential threat of *Bd* epizootics.

In addition to international trade, future climate change is another anthropogenic factor that will likely influence the chytrid disease system and the distributions of both *Bd* and *R. catesbeiana*. Previous studies predicted a geographic shift towards the northern latitudes and global reductions in the geographic range of *Bd* due to climate change (Rödder et al. 2010; Xie et al. 2016). For *R. catesbeiana*, Nori et al. (2011) predicted that future climate change would cause a geographic shift and reduce the area of potentially suitable habitat for this species in South America, but no studies have looked at how the distribution of *R. catesbeiana* may change in the future in Asia. Models that incorporate future climate change impacts on distributions of *R. catesbeiana* and *Bd* in Asia would help us understand the impacts of amphibian disease spread in Asia in the future.

Accounting for environmental variables, host-pathogen dynamics, and the effects of anthropogenic activities are important when predicting vulnerability of amphibians to *Bd*. Previous model predictions for *Bd* distribution in Asia are limited because they were created using no occurrence data from Asia (Rödder et al. 2009; Ron 2005) or few, localized occurrence data (Moriguchi et al. 2015; Liu et al. 2013, Xie et al. 2016), and none incorporated the role of

specific *Bd* carriers. Here we use climatic and land-use variables to create habitat suitability models (HSMs) for both *Bd* and *R. catesbeiana*. We combine these HSMs and, because increased amphibian richness could lead to increased disease spread when a competent reservoir is present (Power & Mitchell 2004; Keesing et al. 2010), we incorporate amphibian richness with the combined distribution of *Bd* and *R. catesbeiana* to refine our estimations. We also show the potential threat of *Bd* to threatened species and predict potential impacts of future climate change on disease spread. Our goal is to address the following questions:

1. Where are the areas of highest relative vulnerability to *Bd*?
2. Are threatened species at high relative *Bd* risk?
3. How do *Bd* habitat suitability, *R. catesbeiana* distribution, and amphibian richness contribute to relative *Bd* risk?
4. How does climate change affect relative *Bd* risk?

Materials and Methods

Habitat suitability models for Bd and R. catesbeiana

We created presence-only HSMs (30 arc-second resolution, ~1 km) using climate and land use factors with Maxent version 3.3.3k (Phillips et al. 2004). Initial HSMs were trained on species occurrence data and 23 environmental factors relevant to the establishment of *Bd* and *R. catesbeiana*. We then used a subset of the most important parameters to create pruned models for analysis.

For our models we obtained 19 bioclimatic variables from the Worldclim database (http://www.worldclim.org/bioclim), which are a set of interpolated temperature and

precipitation conditions based on monthly averages measured at weather stations across the globe from the years 1950 to 2000, latitude, longitude, and elevation (Hijmans et al. 2005). In addition, we used mean potential evapotranspiration (PET), mean aridity (AI), and mean actual evapotranspiration (AET), or soil-water balance, from the CGIAR-CSI Consortium for Spatial Information (http://www.cgiar-csi.org/data/undefined/), all of which use climate data from WorldClim as primary input. PET is a measure of the ability of the atmosphere to remove water from the surface through evapotranspiration, and it was calculated using mean monthly temperature, temperature range, and radiation from above the atmosphere (Zomer et al. 2007). AI is a function of precipitation, temperature, and PET, and it quantifies the level of dryness at a given location (Zomer et al. 2008). AET is the effective quantity of water that is removed from the surface by evapotranspiration based on climatic conditions, and it was calculated using PET and soil moisture content (Trabucco & Zomer 2010). To incorporate land use patterns, we used the global human footprint (HF) from the Wildlife Conservation Society (http://sedac.ciesin.columbia.edu/data/set/wildareas-v2-human-footprint-geographic), which quantifies anthropogenic influences on land cover based on accessibility, land transformation, human population density, and electrical power infrastructure between the years 1995 to 2004 (Sanderson et al. 2011).

To reduce the chances of overfitting the model due to multicollinearity of the model predictors, we ran an initial model for each species with all 23 continuous variables. We conducted jack-knife tests to determine the relative importance of each predictor to the model. We also calculated Spearman's rank correlations (r) among all the variables to determine which variables were highly correlated with each other. Using the results of the jackknife tests, we

chose the top-ranking model parameters that together contributed to approximately 90% of the full model for each pathogen. When variable pairs had an $r^2 > 0.75$ we chose the higher ranking factor. We then used the subsets of environmental variables to create pruned HSMs for *Bd* and *R. catesbeiana.*

Modeling invasive species is challenging because it requires the extrapolation of information from a known environmental range to unknown, non-native geographic regions. It is important to consider biases that may over-influence model outcomes, such as sampling bias, which can lead to increased spatial autocorrelation and pseudoreplication. This can cause the model to overfit to environmental biases associated with the occurrence data. Boria et al. (2014) showed that applying a spatial filter to presence data reduces overfitting; therefore, we applied a spatial filter by randomly choosing one occurrence site from every 10 arc-minute (~12 km) area using R dismo (Hijmans et al. 2013) and maptools (Bivand & Lewin-Koh 2014) packages. We further minimized sampling bias for the *Bd* samples by restricting the background sampling areas. For *Bd*, since we do not know the extent of its distribution in Asia, we used a minimum convex hull polygon around clusters of the occurrence points (Appendix 4.1A) (Rödder et al. 2009; Phillips & Elith 2013; Thorne et al. 2012; Mainali et al. 2015). For *R. catesbeiana*, we limited the background areas to the known native and non-native ranges within the US, as designated by the US Geological Survey (USGS) (Appendix 4.1B). These data are based on historical presence and the most current field surveys.

Another concern is that correlative models assume the species is in an equilibrium state of distribution, which may not be the case when dealing with invasive species (Mainali et al. 2015; Thuiller et al. 2005). The lack of a presence point in a given locality does not necessarily

indicate unsuitable habitat; it may be that the species was not yet there at the time of surveillance or that it was missed. We address this by restricting the background sampling areas to the specified training areas. In addition, by default, Maxent randomly chooses 10,000 background points from the designated training area, which could potentially inflate the chances of false absences. To further minimize the chances of the model misidentifying unsuitable habitat, we limited the number of background points to be equal to the number of presence points (Mainali et al. 2015; Liu et al. 2005).

To account for variability and other uncertainties inherent in modeling, we ran 20 replicates for each species using crossvalidation; occurrence data were divided into 20 equal-sized folds, or groups, and for each replicate 19 folds were used for model training and 1 fold was used for model testing. We used 20 replicates to account for model variability (Araújo & New 2007). The results were averaged by Maxent to produce a final probability density function of potentially suitable habitat.

Maxent calculates multiple threshold values for each model run to aid in model interpretation. Areas with values above these thresholds can be interpreted as a reasonable estimate of a species distribution or suitable habitat, depending on the quality of the data. For our analyses, we used the minimum training presence logistic threshold for *Bd*, which is the mean of the lowest probabilities that the training points (i.e., true positives) fall on for each of the 20 replicates. We chose this threshold for *Bd* because we wanted to encompass any potentially suitable habitat of the limited number of occurrence data we have in Asia. For *R. catesbeiana*, we used the fixed cumulative value 5 logistic threshold, which is the probability at which the omission rate of test data (i.e., occurrence points that do not fall within predicted suitability) is

less than 5%. We chose this threshold for *R. catesbeiana* because of ample test data and our knowledge that this species prefers warmer climates (Lillywhite 1970; Graves & Anderson 1987) and likely would not occur in the higher latitudes.

Areas where Maxent extrapolated the probability of suitable habitat were excluded from analyses. These areas had environmental variables with values outside of the range of the training data.

Bd habitat suitability model

For the *Bd* HSM we used 100 *Bd*-positive sites within Asia, including China, Indonesia, Japan, Krygyzstan, Laos, Malaysia, North Korea, South Korea, the Philippines, Sri Lanka, Taiwan, and Vietnam. These data are all known data from previous studies (Swei et al. 2011; Moriguchi et al. 2015; Goka et al. 2009; Yang et al. 2009; Fong et al. 2015) and unpublished data (Vredenburg et al. unpublished). After applying the 10 arc minute spatial filter, 83 sites with environmental data remained for model training (Appendix 4.1A). Previous *Bd* HSMs in Asia used few *Bd*-positive sites (Liu et al. 2013, Moriguchi et al. 2015; Xie et al. 2016) or no sites (Rödder, et al. 2009). Our pruned model included four temperature variables, three precipitation variables, and one land-use variable (Table 4.1). These bioclimatic variables are physiologically relevant, as *Bd* requires water for dispersal, can survive freezing temperatures, has optimal growth at 17-25°C, and dies at temperatures ≥ 30°C (Piotrowski et al 2004). These variables have also been shown to perform well in HSMs for *Bd* (Rödder et al. 2009; La Marca et al. 2005; Murray et al. 2011; James et al. 2015; Xie et al. 2016).

R. catesbeiana habitat suitability model

We created a presence-only HSM for *R. catesbeiana* in Asia using occurrence data from the US. While *R. catesbeiana* now has a global distribution and has been documented in the wild in Asia, including in Japan, China, and South Korea (Goka et al. 2009; Bai et al. 2010; Bai et al. 2012; Fong et al. 2015), there are few georeferenced locations outside of the US that are publicly available, and its current distribution in Asia is unknown. Its native range is in the eastern US, though its range has expanded and data are well-dispersed throughout the entire US. Using occurrence data from established invasive populations in addition to those from a species' native range has been shown to improve model accuracy (Mainali et al. 2015); therefore, for our model we used *R. catesbeiana* occurrences within its native and invasive range in the US (including the islands of Hawaii and Puerto Rico). We obtained 1,401 *R. catesbeiana* occurrence points from the USGS and 6,611 records from VertNet (http://vertnet.org/) for a total of 8,012 records. We removed records with coordinate uncertainty greater than 15 km and applied a 10 arc-minute spatial filter (~12km), which resulted in 1,940 unique *R. catesbeiana* sites within its native and non-native range for model training (Appendix 4.1B).

Our pruned *R. catesbeiana* HSM included five temperature variables, four precipitation variables, and one land-use variable (Table 4.1). These bioclimatic variables are physiologically relevant to *R. catesbeiana*. Adults are mostly aquatic and prefer warmer lentic habitats and summer temperatures above 26°C (Lillywhite 1970; Graves & Anderson 1987). Below 15°C adults become inactive, eggs do not hatch, and larvae do not develop (Viparina & Just 1975; Harding 1997). In addition, *R. catesbeiana* requires standing water for reproduction; larvae can take a few months to 3 years to develop (Lannoo 2005), and in general they overwinter in water

and require more than one year for metamorphosis (Ryan 1943; Willis et al. 1956; Govindarajulu et al. 2006). Also, *R. catesbeiana* has been shown to be positively associated with modified land use, such as increased permanent ponds created for agricultural or recreational purposes (Ficetola et al. 2007; Ficetola et al. 2010; Rubbo and Kiesecker 2005; Maret et al 2006).

Amphibian species richness

We estimated amphibian richness in Asia by overlaying 1,669 range maps from the IUCN Red List. IUCN range maps can be limited by lack of species and habitat information from newly described or understudied species; however, these ranges are based on expert knowledge and are the best estimated representations of species distributions in their native ranges globally. We also created 41 maps using primary literature, available occurrence data from VertNet, and expert opinion. This resulted in a total of 1,710 unique species ranges for Asia. We created a grid of the tally of intersecting ranges per cell using R dplyr (Wickham & Francois 2014) and raster (Hijmans 2014) packages to build a species richness model. We normalized the richness model so that values were between 0 and 1. Spatial data for produced or modified range maps are available at https://github.com/AmphibiaWeb and all range maps are viewable on AmphibiaWeb by species (http://amphibiaweb.org).

Bd vulnerability model

We combined the *Bd* and *R. catesbeiana* HSMs to determine the areas with suitable habitat for both species. In areas where both *Bd* and *R. catesbeiana* have suitable habitat, we wanted to ensure that areas with high relative suitability for *Bd* and low relative suitability for *R. catesbeiana* held more weight in relative disease risk compared to areas with high relative

suitability for *R. catesbeiana* and low suitability for *Bd*. Therefore, we calculated the product of the *Bd* HSM and the square root of the *R. catesbeiana* HSM. To compare the effects of an invasive carrier species with the effects of species richness on *Bd* risk, we calculated the product of the *Bd* HSM and the square root of our normalized species richness model, under the same assumption that *Bd* suitability should hold more weight than species richness. We then calculated the product of the *Bd* HSM, the square root of the *R. catesbeiana* HSM, and the square root of the species richness model to estimate overall *Bd* vulnerability in Asia. We also calculated the product of the *R. catesbeiana* HSM and the amphibian richness model to evaluate the performance of the *Bd* HSM alone.

To test our assumptions and the predictive performance of our models, we compared the probability density function values of the 83 spatially filtered *Bd* sites in Asia from the *Bd* HSM, the *Bd*/*R. catesbeiana* HSM, the *Bd*/amphibian richness model, the *R. catesbeiana*/amphibian richness model, and the *Bd* vulnerability model (Bd*R. catesbeiana*amphibian richness). To do this, we applied the Jenks natural breaks classification (Jenks 1967) to our model data, which clusters values into classes in such a way that most similar values are grouped together, reducing the variance within each class while maximizing the variance between classes. We created four relative risk classes and calculated the percentage of points that fell within each relative risk class for each model. We define high relative risk as areas that include the top two relative risk classes. Although these are not statistical tests, they provide insight as a general evaluation of our models, which have high levels of uncertainty due to limited data relevant to determining *Bd* spread in Asia, including *Bd* occurrences, *R. catesbeiana* occurrences, and international amphibian trade.

Identifying risk to threatened species

Asia harbors approximately one quarter of the world's amphibian diversity. Many of these species have been designated as threatened with extinction, largely because of their small ranges, which heightens their vulnerability to changes in their environment. To determine the threat of *Bd* exposure to 410 threatened Asian species (IUCN 2016), we calculated the area and percent overlap of each species range map with predicted risk (low to high relative risk) and just high relative risk of our overall *Bd* vulnerability model. See Appendix 4.2 for a list of threatened species in Asia.

Climate change predictions

We obtained the most recent global climate change projections created by the National Oceanic and Atmospheric Administration's Geophysical Fluid Dynamics Lab (GFDL CM3) using the global climate models (GCMs) provided by the 2014 Intergovernmental Panel on Climate Change (IPCC) Fifth Assessment Report from WorldClim. These projections were downscaled and calibrated using WorldClim data as the baseline current climate. The IPCC adopted four new emission scenarios called representative concentration pathways (RCPs), which cover a possible range of radiative forcing (i.e., global annual greenhouse gas emissions) values in the year 2100 relative to pre-industrial values: 2.6, 4.5, 6.0, and 8.5. There are data for these four RCPs for the years 2050 and 2070. We used the best- and worst-case scenarios (RCP 2.6 and RCP 8.5, respectively) for both 2050 and 2070 at the highest resolution available (30 arc-second resolution, ~1 km) to predict the future potential distributions of *Bd* and *R. catesbeiana* in Asia. Because there are no future predictions for human footprint, we used the current global

human footprint version 2 (CIESIN) for future projections. We then compared the future projections with the current projections. We did not include amphibian richness predictions because those data are not available, and creating predictions based on how each species might respond to future climate change is beyond the scope of this study.

Results

Bd and R. catesbeiana habitat suitability models and amphibian species richness

The *Bd* HSM shows highest relative suitability in the mid to high latitudes and the montane regions of Asia, including the Himalayas and the mountain ranges of the Pacific Islands (Table 4.1A). Annual precipitation (Bio12), HF, precipitation of the warmest quarter (Bio18), and mean temperature of the driest quarter (Bio9) were the strongest predictors for suitable *Bd* habitat. All 83 known *Bd* localities in Asia were in predicted suitable *Bd* habitat and 41% were in high relative risk areas.

Areas highlighted as most suitable for *R. catesbeiana* are mostly in the mid and low latitudes in temperate and tropical regions (Figure 4.1B). The strongest model predictors were precipitation of the warmest quarter (Bio18), temperature seasonality (Bio4), and HF. All of the 83 known *Bd* localities in Asia were in predicted suitable *R. catesbeiana* habitat and 65% were in high relative risk areas.

Our species richness model shows higher numbers of overlapping ranges in Southeast Asia, China, and India (Figure 4.1C). The richness model also shows no amphibians in much of western China, Mongolia, and Central Asia, likely due to high elevation deserts and understudied

areas. Of the 83 known *Bd* localities in Asia, 98% were in areas where species ranges have been mapped and 40% were in high relative richness areas.

Disease vulnerability

Areas that contain suitable habitat for both *Bd* and *R. catesbeiana* occur mostly in the mid latitudes in temperate and tropical forests, including those in the mountain ranges of the Pacific Islands and western India (Figure 4.2A). When we combine *Bd* with amphibian richness, the highest relative risk is predicted to be along the east coast of Vietnam, the tropical mountains of the Pacific Islands and China, and Japan (Figure 4.2B). When we weight the combined *Bd*/*R. catesbeiana* HSM with amphibian richness, temperate and tropical montane regions are highlighted as having the highest relative disease risk (Figure 4.2C).

When we assessed the predictive performance of our combined models, proportions of documented *Bd* occurrences in high relative risk areas increased substantially with the combined *Bd*/*R. catesbeiana* HSM (54%) and the combined *Bd*/amphibian richness model (83%), compared to the *Bd* HSM alone (41%). The model with just the potential distribution of *R. catesbeiana* and amphibian richness had 40% of known *Bd* localities in high relative risk areas. With the overall *Bd* vulnerability model in which we incorporated all three individual models (the *Bd* HSM, the *R. catesbeiana* HSM and the species richness model), 82% of known *Bd* occurrences were in high relative risk areas.

Threatened species

Most threatened species have at least some part of their range in areas of predicted disease risk (96% - 394/410) and high relative disease risk (89% - 365/410) (Figure 4.3). About

90% (368/410) of threatened species have at least 25% overlap and 27% (110/410) have 100% range overlap with predicted risk. For high relative risk areas, about 80% (328/410) of threatened species have at least 25% overlap and 16% (126/410) have 100% overlap. Most of the threatened species in Asia occur in areas of high relative disease risk (Appendix 4.3).

Effects of climate change

The area of potential suitable *Bd* habitat is predicted to decrease by about 18-22% by 2050 and by about 18-31% by 2070. The ranges are based on the results for the IPCC's future climate predictions given the lowest (RCP 2.6) and highest (RCP 8.5) predicted greenhouse gas emissions. For *R. catesbeiana* potential suitable habitat expands by approximately 30-45% by 2050 and by about 39-50% by 2070. When we examine changes in the combined *Bd*/*R. catesbeiana* HSM, there is a decrease in overlapping suitable habitat of 7-9% by 2050 and 3-22% by 2070. Unsuitable *Bd* area expands mostly in the mid and low latitudes (Figure 4.4A), while potential suitability for *R. catesbeiana* increases in the upper latitudes and higher elevations (Figure 4.4B). Much of the areas previously designated as high relative *Bd* risk zones, including the temperate and tropical forests in the mountains of China and Southeast Asia, become unsuitable, though there is some expanded combined potential suitability in the higher latitudes and some higher elevations (Figure 4.4C). Figure 4.4 shows only 2070 RCP 8.5 as an example, as spatial patterns of expanded suitability and unsuitability are similar for the various climate change scenarios. See supplemental materials (Appendix 4.4) for figures regarding the other climate change scenarios.

Discussion

We show that temperate and tropical mountain forests in China, Southeast Asia, and the Pacific Islands as well as areas in Taiwan, Japan and northern Asia are most vulnerable to *Bd* spread (Figure 4.2C). This differs substantially from previous *Bd* models (Ron 2005; Rödder et al. 2009; Liu et al. 2013; Moriguchi et al. 2015; Xie et al. 2016) that highlight only areas of China and Japan as most suitable for *Bd*. These differences are primarily due to how we integrated the potential distribution of *R. catesbeiana* and amphibian richness.

Liu et al. (2013) had the most similar approach to ours by using trade data, amphibian richness, the presence of introduced hosts, climate, and land use data; however, they used all these data as predictors for their HSM, whereas we created an HSM using only climate and land use as predictors (Figure 4.1A) and incorporated richness and the potential presence of *R. catesbeiana* separately (Figure 4.2C). We argue that amphibian richness should be incorporated separate from the HSM because if climate and land use conditions are conducive to *Bd* survival, then the potential presence of native and/or introduced suitable hosts in areas of environmental suitability could increase its chances of establishment regardless of whether or not *Bd* has been detected there yet. And by using the potential distribution of *R. catesbeiana* in Asia instead of just the limited data on their occurrence, as Liu et al. (2013) did, we were able to further extrapolate from human activities to determine where *Bd*'s most widely transported carrier may already be established or where they could establish in the future. This ultimately helps to identify not only where *Bd* could potentially be brought to, but also where *Bd* could potentially be sustained by a competent reservoir species. And because high amphibian richness could

indicate an increased number of potentially available hosts (DiRenzo et al. 2014), amphibians in areas with high amphibian richness predicted to have high relative suitability for both *Bd* and *R. catesbeiana* may be at even greater risk of disease spread. Thus, incorporating amphibian richness and the potential presence of *R. catesbeiana* as separate drivers of *Bd* spread may more accurately depict where relative *Bd* threat is greatest.

The results of our model tests support these assumptions. Including both amphibian richness and the potential presence of *R. catesbeiana* led to 82% of *Bd* occurrences within high relative risk areas (Figure 4.2C) compared to just 41% when considering the *Bd* HSM alone (Figure 4.1A). When we assessed the *R. catesbeiana* HSM and amphibian richness model separately, we found 65% and 40% of *Bd* occurrences fell in high relative risk areas respectively, which could indicate that the potential presence of *R. catesbeiana* may play a bigger role in *Bd* spread compared to amphibian richness in Asia. However, amphibian richness seems to have more influence compared to *R. catesbeiana* when combined with the *Bd* HSM, as 83% of *Bd* occurrences were within high relative risk areas with the *Bd* HSM/amphibian richness model compared to 54% with the *Bd* HSM/*R. catesbeiana* HSM. Without the *Bd* HSM, the combined *R. catesbeiana*/amphibian richness model had 45% of *Bd* occurrences in high relative risk areas, which is not that different from the *Bd* HSM alone. While these are not statistical tests, they imply that amphibian richness and the potential presence of *R. catesbeiana* may influence *Bd* spread in Asia. The interactions of these factors need further investigation and more *Bd* surveys from the field are needed to test these assumptions and predictions.

Other explanations of why our *Bd* risk model differs from previous models (Ron 2005; Rödder et al. 2009; Liu et al. 2013; Moriguchi et al. 2015; Xie et al. 2016) include our use of

more *Bd* localities across a broader geography in Asia, increased resolution at 30 arc-seconds (compared to 2.5 arc-minutes), restricted background sampling areas, limited background points, and different predictors. Input data require great scrutiny to minimize pseudoreplication, multicollinearity, and overfitting, and while most attention is given to the occurrence data, the same considerations should also be given to the background data. To minimize the chances of misidentifying unsuitable habitat when only presence data are available, it is important to designate an appropriate background training area and limit the number of background points chosen (Mainali et al. 2015; Liu et al. 2005). This is especially important for invasive species that may not yet be in equilibrium distribution; without restricting background training areas, Maxent may misidentify areas where *Bd* has not been documented as unsuitable, when it could be that *Bd* may not have been introduced there yet or it was missed. Thus, the lack of appropriate treatment of the input data could result in misleading predictions about *Bd* threat as well as the factors that influence its spread.

We acknowledge that our models have a high level of uncertainty due to the paucity of data from an expansive geographic region, and we urge caution when interpreting these results. However, we believe we were able to extract useful information about *Bd* spread in Asia. We were able to incorporate both trade and an ecologically relevant host species in our *Bd* vulnerability model by predicting the potential presence of *R. catesbeiana* using extensive occurrence data from both native and invasive regions in North America. Importantly, we made sure to give the most importance to *Bd* habitat suitability by weighting the *Bd* HSM more heavily than both *R. catesbeiana* and amphibian richness when we combined the models, which may have helped make the relationship of *Bd* spread with an invasive carrier and amphibian richness

more evident. And although sufficient test data are lacking, we were able to generally evaluate how these different factors may influence *Bd* spread in Asia.

Ultimately, our models suggest that in Asia, the international trade of an invasive carrier species and amphibian richness may enhance *Bd* spread where potentially suitable *Bd* habitat exists. The presence and continuous influx of various *Bd* strains transported by *R. catesbeiana* pose a significant threat to native amphibian populations in Asia. While some populations that coexist with endemic *Bd* strains may be protected from epizootic events either through cross immunity (McMahon et al. 2014) or by host-pathogen coevolution driving native strains to outcompete the panzootic strain (Goka et al. 2009; Bataille et al. 2013), the increased virulence or pathogenicity of *Bd*-GPL may aid its ability to outcompete some endemic strains through competitive exclusion (Farrer et al. 2011; Rodriguez et al. 2014) and potentially cause outbreaks. Also, it is not yet known what impacts other introduced strains may have on native populations. *Bd* strains may behave differently in new environments or on new species, as Schloegel et al. (2012) found that *Bd*-GPL may outcompete *Bd*-Brazil on native amphibians in Japan, whereas the *Bd*-Brazil may outcompete *Bd*-GPL on *R. catesbeiana* in Japan. In addition, hybridization between *Bd*-GPL and other *Bd* strains, either endemic to Asia or otherwise, could also lead to additional *Bd* epizootics. And even if *Bd* does not cause obvious, marked declines, exposure to any of these strains could have sub-lethal costs that could translate to impacts at the population level. In fact, amphibian populations in areas where *Bd* is present may already be smaller than what they would be if *Bd* were absent (Sette et al. 2015; Vredenburg et al. 2010), though this is difficult to determine because population-level studies have not been conducted in these areas.

While the threat of *Bd* is high under current climate conditions, anthropogenic climate change may provide some relief from *Bd*. We show that the total area of overlapping suitability for *Bd* and *R. catesbeiana* decreases by 3-23% by 2070. This pattern is driven by the 18-31% decrease in suitable habitat for *Bd*, though areas of suitability expand slightly in the higher latitudes. These results are consistent with previous *Bd* studies (Rödder et al. 2010; Xie et al. 2016). The 39-50% expansion of suitable habitat for *R. catesbeiana* is consistent with conclusions from Rahel and Olden (2008), who state that climate change will favor invasive aquatic species by driving warmer water temperatures, shorter duration of ice cover, altered streamflow, increased salinization, and higher demand for water storage. Most notably, areas of China and Southeast Asia that were identified as having high relative *Bd* risk were predicted to no longer be suitable for both species. These areas also have high species richness and numerous threatened species; if those species are able to withstand climate change, they may not have to deal with *Bd* as an added stressor in the future.

Of course, like our current predictions, there are limitations with our future climate change models, and they must be interpreted with caution. Implicit in our future climate models is the assumption that the correlations between *Bd* and *R catesbeiana* and their physical environment (i.e., climate and land use) will remain constant over time, which neglects the possibility of either species adapting to changing environmental conditions. In addition, because the IPCC's GCMs have coarse resolution (>120 arc minutes, which is 7200 times greater than our 30 arc seconds resolution), the future climate change projections must be downscaled in order to consider variation at high spatial resolution. The process of downscaling is a major source of uncertainty for future projections (Chen et al. 2011); however, these projections

provide the best estimates given the information available and can still be useful at a regional scale.

We assume that potential habitat suitability for *Bd* and *R. catesbeiana* together enhances relative *Bd* risk, which is supported by our results for current *Bd* threat. However, our results also indicated that amphibian richness may strongly influence *Bd* spread, but we did not include it in the future climate models because creating a general projection about how amphibian richness might respond to climate change relies on the individual responses of all the species. This modeling has not yet been done for many species and is beyond the scope of this study. But it is important to consider that amphibians are extremely vulnerable to climate change (Foden et al. 2013), and adaptation to changes may not be quick enough to avoid extinction for many species (Bickford et al. 2010). The displacement and extinction of multiple species in the future could also decrease the abundance of potential *Bd* hosts, which could lead to further reduced *Bd* risk.

Another limitation of our future climate change models is that we used the current HF for our projections because no future HF data were available. Assuming that the global HF will likely grow and expand from what it is now, our predictions may be an underestimate of suitability since HF is positively correlated with both *Bd* and *R. catesbeiana*. However, when we consider that the decreased overlapping habitat of *Bd* and *R. catesbeiana* occurs in areas where our current predictions showed high relative risk and amphibian richness, even if the human population extends into the uninhabited regions of these areas, the net effect of these uncertainties likely leads our models to overestimate future *Bd* risk. Thus, our future climate models demonstrate that anthropogenic climate change may decrease *Bd* risk to those species that are able to adapt to climate change. However, *Bd* may remain a significant threat in the

future even if the risk is lower, as populations that may be compromised by climate change and previously unexposed to *Bd* could still be vulnerable to disease.

Our models highlight the value of incorporating abiotic, biotic and human factors when assessing disease spread in wildlife. By integrating habitat suitability for *Bd*, amphibian richness, and the potential presence of an invasive carrier species that is a major link to both *Bd* and human activities, we strengthened our ability to identify relative *Bd* risk in Asia more accurately. Given that a majority of the *Bd* occurrences in Asia were found in areas predicted to have high relative *Bd* risk and their strong association with the potential presence of *R. catesbeiana* and amphibian richness, we hypothesize that *Bd* may be newly emerging in Asia, with human influences and globalization being the main drivers of emergence. Admittedly, there are still many unanswered questions regarding the distribution, disease ecology, and host-pathogen dynamics of *Bd*. Having more field data and incorporating more detailed biotic influences would improve model predictions and aid in the conservation of amphibian biodiversity. Increased data collection and *Bd* surveillance from both wild and captive populations, particularly in areas of high relative disease risk, would be useful to monitor for outbreaks and prevent disease spread. Historical surveys using museum specimens could provide insight of an area's baseline population and community structure as well as pathogen invasion history. And more targeted studies investigating disease transmission and species susceptibility could reveal specific host-pathogen dynamics and the effects of other potentially influential variables, such as species life-history traits, host microbiome, or co-occurring pathogens.

Acknowledgements

This work was supported by NSF 1258133 (V.T.V.). We thank Vredenburg Lab collaborators, the US Geological Survey, VertNet and IUCN for providing invaluable occurrence and range data. We thank Thomas Gillespie, James Lloyd-Smith, and Richard Vance for valuable feedback and suggestions. We thank University of California, Berkeley and San Francisco State University GIS and informatics undergraduate apprentices for their species range work. And we thank the Museum of Vertebrate Zoology at University of California, Berkeley for technical support.

Figures

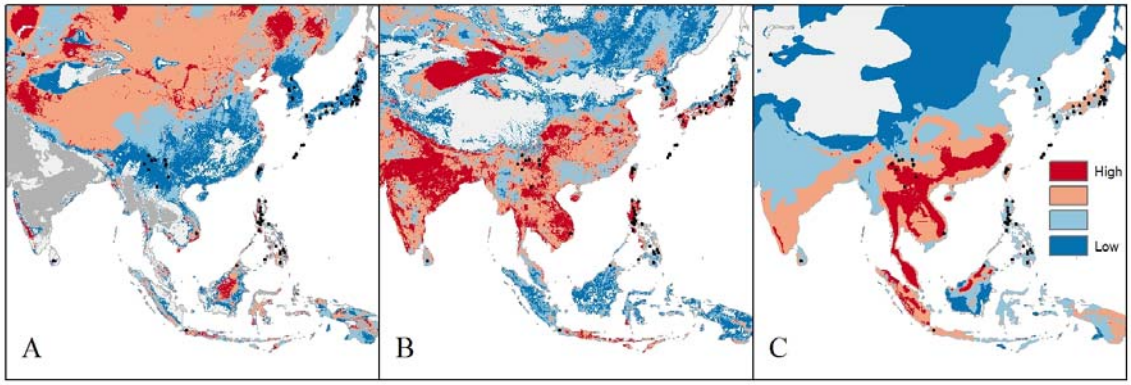

Figure 4.1 Habitat suitability models and amphibian species richness in Asia. (A) *Bd* HSM, (B) *Rana catesbeiana* HSM, and (C) amphibian richness. Light gray areas indicate no suitability for the *Bd* HSM and no data for the *R. catesbeiana* HSM. Black circles indicate *Bd*-positive sites.

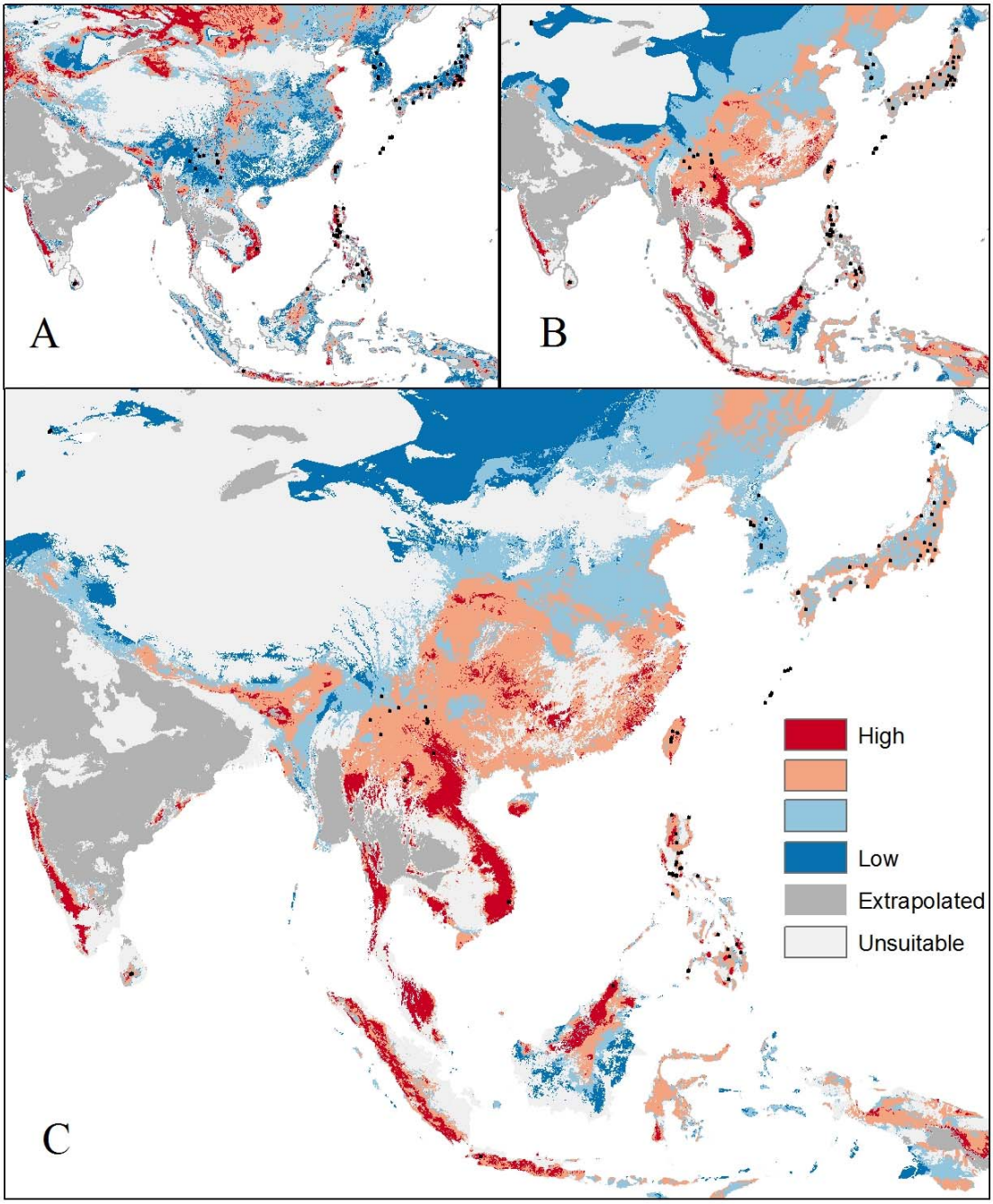

Figure 4.2 Vulnerability to *Bd* in Asia. (A) Combined *Bd*/*R. catesbeiana* HSM, (B) combined *Bd*/species richness model, and (C) overall *Bd* vulnerability. Black dots indicate *Bd*-positive sites.

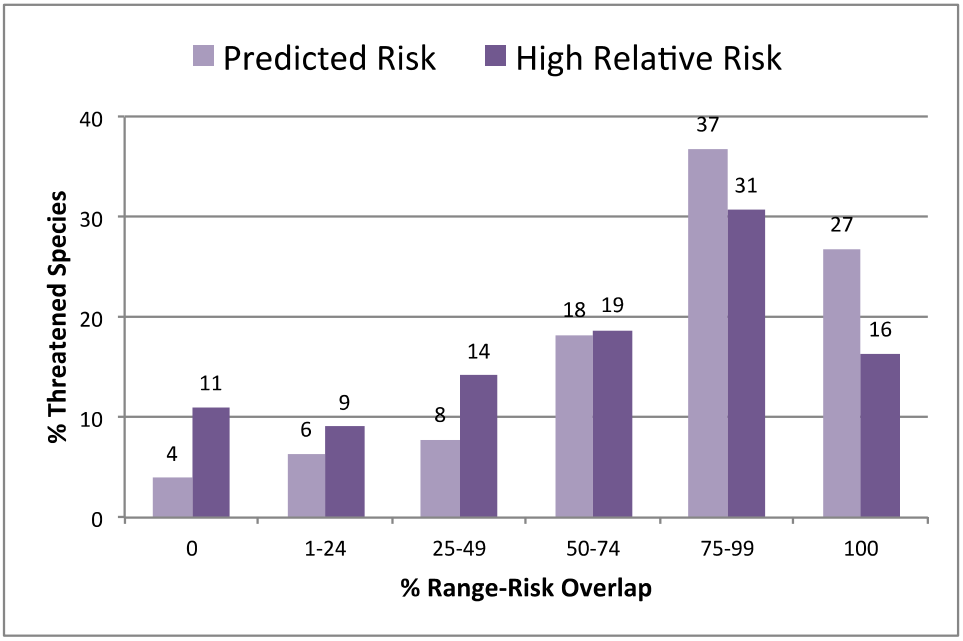

Figure 4.3 The percent of range-risk overlap of threatened species with predicted disease risk and high relative disease risk in Asia.

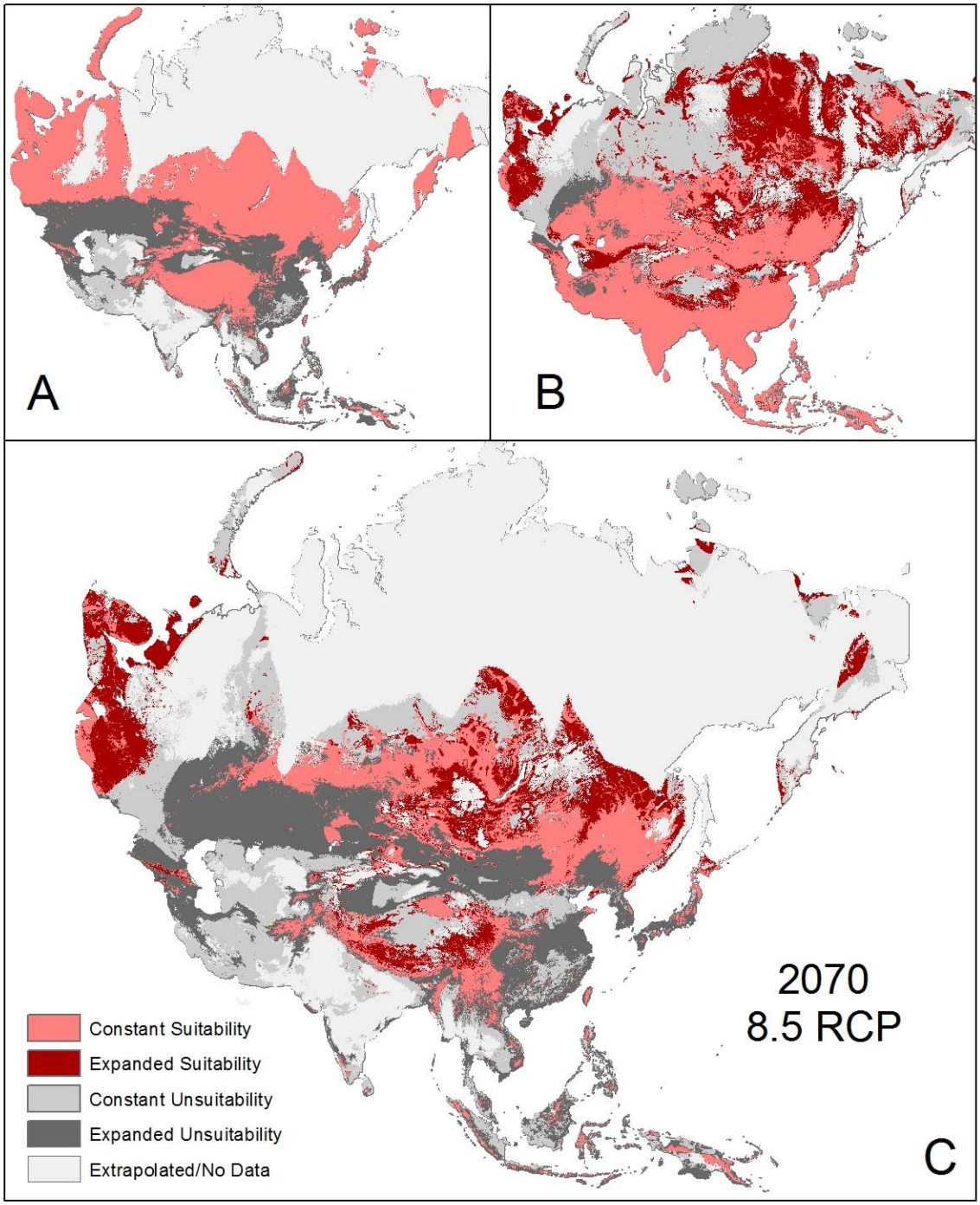

Figure 4.4 Changes in *Bd* risk in 2070 (RCP 8.5) compared to current predictions for (A) *Bd*, (B) *R. catesbeiana*, and (C) *Bd* and *R. catesbeiana*.

Tables

Table 4.1 Environmental predictors for pruned habitat suitability models for *Bd* and *R. catesbeiana* in Asia

Environmental Parameter	*Bd*	*R. catesbeiana*
Mean Diurnal Range (Bio2)	x	
Isothermality (Bio3)	x	
Temperature Seasonality (Bio4)		x
Max Temperature of Warmest Month (Bio5)	x	
Mean Temperature of Wettest Quarter (Bio8)		x
Mean Temperature of Driest Quarter (Bio9)	x	x
Mean Temperature of Warmest Quarter (Bio10)		x
Mean Temperature of Coldest Quarter (Bio11)		x
Annual Precipitation (Bio12)	x	
Precipitation of Wettest Month (Bio13)		x
Precipitation of Driest Quarter (Bio14)	x	
Precipitation Seasonality (Bio15)		x
Precipitation of Warmest Quarter (Bio18)	x	x
Precipitation of Coldest Quarter (Bio19)		x
Human Footprint (HF)	x	x

Appendices

Appendix 4.1 Training sites and background sampling areas for the habitat suitability models in Asia for (A) *Bd* and (B) *Rana catesbeiana*.

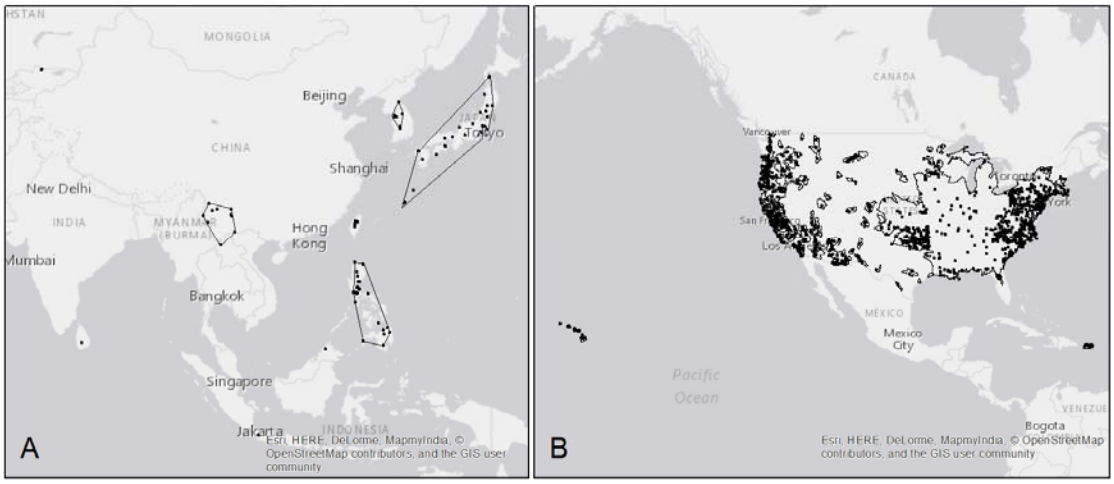

Appendix 4.2 List of threatened species in Asia according to IUCN (2016).

Order	**Species Name**
Anura	Adenomus dasi
Anura	Adenomus kandianus
Anura	Adenomus kelaartii
Anura	Amolops hainanensis
Anura	Amolops hongkongensis
Anura	Amolops jinjiangensis
Anura	Amolops kangtingensis
Anura	Amolops loloensis
Anura	Amolops torrentis
Anura	Amolops tuberodepressus
Anura	Ansonia fuliginea
Anura	Ansonia guibei
Anura	Ansonia latidisca
Anura	Ansonia mcgregori
Anura	Ansonia muelleri
Anura	Ansonia platysoma
Anura	Ansonia siamensis

Anura	Ansonia tiomanica
Anura	Ansonia torrentis
Anura	Austrochaperina novaebritanniae
Anura	Babina holsti
Anura	Babina okinavana
Anura	Babina subaspera
Anura	Barbourula busuangensis
Anura	Barbourula kalimantanensis
Anura	Bombina lichuanensis
Anura	Borneophrys edwardinae
Anura	Brachytarsophrys intermedia
Anura	Buergeria oxycephala
Anura	Bufo eichwaldi
Anura	Bufoides meghalayanus
Anura	Callulops kopsteini
Anura	Choerophryne siegfriedi
Anura	Cophixalus nubicola
Anura	Copiula minor
Anura	Cornufer akarithymus
Anura	Duttaphrynus beddomii
Anura	Duttaphrynus kotagamai
Anura	Duttaphrynus microtympanum
Anura	Duttaphrynus noellerti
Anura	Duttaphrynus sumatranus
Anura	Fejervarya nicobariensis
Anura	Gastrophrynoides borneensis
Anura	Ghatixalus variabilis
Anura	Ghatophryne ornata
Anura	Ghatophryne rubigina
Anura	Glandirana minima
Anura	Gracixalus jinxiuensis
Anura	Gracixalus quyeti
Anura	Huia masonii
Anura	Hyla suweonensis
Anura	Hylarana attigua
Anura	Hylarana aurantiaca
Anura	Hylarana mangyanum
Anura	Hylarana spinulosa
Anura	Hylarana waliesa

Anura	Indirana brachytarsus
Anura	Indirana diplosticta
Anura	Indirana gundia
Anura	Indirana leithii
Anura	Indirana leptodactyla
Anura	Indirana phrynoderma
Anura	Ingerana borealis
Anura	Ingerana charlesdarwini
Anura	Ingerana tasanae
Anura	Ingerophrynus claviger
Anura	Ingerophrynus kumquat
Anura	Kalophrynus intermedius
Anura	Kalophrynus minusculus
Anura	Kalophrynus palmatissimus
Anura	Kalophrynus punctatus
Anura	Kaloula kalingensis
Anura	Kaloula rigida
Anura	Kurixalus baliogaster
Anura	Leptobrachella baluensis
Anura	Leptobrachella brevicrus
Anura	Leptobrachella palmata
Anura	Leptobrachella parva
Anura	Leptobrachella serasanae
Anura	Leptobrachium banae
Anura	Leptobrachium boringii
Anura	Leptobrachium echinatum
Anura	Leptobrachium gunungense
Anura	Leptobrachium hainanense
Anura	Leptobrachium leishanense
Anura	Leptobrachium leucops
Anura	Leptolalax alpinus
Anura	Leptolalax arayai
Anura	Leptolalax bidoupensis
Anura	Leptolalax hamidi
Anura	Leptolalax kajangensis
Anura	Leptolalax melicus
Anura	Leptolalax pictus
Anura	Leptolalax tuberosus
Anura	Leptophryne cruentata

Anura	Limnonectes acanthi
Anura	Limnonectes arathooni
Anura	Limnonectes diuatus
Anura	Limnonectes fragilis
Anura	Limnonectes heinrichi
Anura	Limnonectes liui
Anura	Limnonectes macrodon
Anura	Limnonectes microtympanum
Anura	Limnonectes namiyei
Anura	Limnonectes nitidus
Anura	Limnonectes parvus
Anura	Limnonectes toumanoffi
Anura	Limnonectes visayanus
Anura	Litoria avocalis
Anura	Litoria becki
Anura	Litoria lutea
Anura	Litoria quadrilineata
Anura	Litoria rueppelli
Anura	Litoria wisselensis
Anura	Liuixalus ocellatus
Anura	Liuixalus romeri
Anura	Megophrys brachykolos
Anura	Megophrys giganticus
Anura	Megophrys ligayae
Anura	Megophrys nankiangensis
Anura	Megophrys stejnegeri
Anura	Melanobatrachus indicus
Anura	Meristogenys amoropalamus
Anura	Meristogenys jerboa
Anura	Micrixalus gadgili
Anura	Micrixalus kottigeharensis
Anura	Micrixalus nudis
Anura	Micrixalus phyllophilus
Anura	Micrixalus saxicola
Anura	Microhyla karunaratnei
Anura	Microhyla maculifera
Anura	Microhyla sholigari
Anura	Microhyla zeylanica
Anura	Micryletta steinegeri

Anura	Minervarya sahyadris
Anura	Nannophrys ceylonensis
Anura	Nannophrys marmorata
Anura	Nannophrys naeyakai
Anura	Nanorana liui
Anura	Nanorana maculosa
Anura	Nanorana minica
Anura	Nanorana rostandi
Anura	Nanorana unculuanus
Anura	Nanorana yunnanensis
Anura	Nasikabatrachus sahyadrensis
Anura	Nyctibatrachus aliciae
Anura	Nyctibatrachus beddomii
Anura	Nyctibatrachus dattatreyaensis
Anura	Nyctibatrachus deccanensis
Anura	Nyctibatrachus humayuni
Anura	Nyctibatrachus karnatakaensis
Anura	Nyctibatrachus major
Anura	Nyctibatrachus minor
Anura	Nyctibatrachus sanctipalustris
Anura	Nyctibatrachus vasanthi
Anura	Nyctixalus margaritifer
Anura	Nyctixalus spinosus
Anura	Occidozyga diminutiva
Anura	Odorrana amamiensis
Anura	Odorrana geminata
Anura	Odorrana hainanensis
Anura	Odorrana jingdongensis
Anura	Odorrana junlianensis
Anura	Odorrana kuangwuensis
Anura	Odorrana narina
Anura	Odorrana nasuta
Anura	Odorrana supranarina
Anura	Odorrana tormota
Anura	Odorrana utsunomiyaorum
Anura	Odorrana wuchuanensis
Anura	Oreolalax chuanbeiensis
Anura	Oreolalax granulosus
Anura	Oreolalax jingdongensis

Anura	Oreolalax liangbeiensis
Anura	Oreolalax major
Anura	Oreolalax multipunctatus
Anura	Oreolalax omeimontis
Anura	Oreolalax pingii
Anura	Oreolalax puxiongensis
Anura	Oreolalax rhodostigmatus
Anura	Oreophryne anulata
Anura	Oreophryne celebensis
Anura	Oreophryne monticola
Anura	Oreophryne variabilis
Anura	Palmatorappia solomonis
Anura	Parapelophryne scalpta
Anura	Pedostibes tuberculosus
Anura	Pelophryne albotaeniata
Anura	Pelophryne api
Anura	Pelophryne guentheri
Anura	Pelophryne lighti
Anura	Pelophryne linanitensis
Anura	Pelophryne misera
Anura	Pelophryne murudensis
Anura	Pelophryne rhopophilia
Anura	Pelophylax chosenicus
Anura	Pelophylax tenggerensis
Anura	Philautus acutirostris
Anura	Philautus acutus
Anura	Philautus amoenus
Anura	Philautus aurantium
Anura	Philautus bunitus
Anura	Philautus disgregus
Anura	Philautus erythrophthalmus
Anura	Philautus garo
Anura	Philautus gunungensis
Anura	Philautus ingeri
Anura	Philautus jacobsoni
Anura	Philautus kerangae
Anura	Philautus leitensis
Anura	Philautus neelanethrus
Anura	Philautus pallidipes

Anura	Philautus poecilius
Anura	Philautus refugii
Anura	Philautus sanctisilvaticus
Anura	Philautus saueri
Anura	Philautus schmackeri
Anura	Philautus similis
Anura	Philautus surrufus
Anura	Philautus tectus
Anura	Philautus umbra
Anura	Philautus worcesteri
Anura	Platymantis akarithymus
Anura	Platymantis banahao
Anura	Platymantis cagayanensis
Anura	Platymantis cornutus
Anura	Platymantis guentheri
Anura	Platymantis hazelae
Anura	Platymantis indeprensus
Anura	Platymantis isarog
Anura	Platymantis lawtoni
Anura	Platymantis levigatus
Anura	Platymantis montanus
Anura	Platymantis naomii
Anura	Platymantis negrosensis
Anura	Platymantis panayensis
Anura	Platymantis parkeri
Anura	Platymantis polillensis
Anura	Platymantis pseudodorsalis
Anura	Platymantis pygmaeus
Anura	Platymantis rabori
Anura	Platymantis sierramadrensis
Anura	Platymantis spelaeus
Anura	Platymantis subterrestris
Anura	Platymantis taylori
Anura	Polypedates insularis
Anura	Pseudophilautus alto
Anura	Pseudophilautus amboli
Anura	Pseudophilautus asankai
Anura	Pseudophilautus auratus
Anura	Pseudophilautus caeruleus

Anura	Pseudophilautus cavirostris
Anura	Pseudophilautus cuspis
Anura	Pseudophilautus decoris
Anura	Pseudophilautus femoralis
Anura	Pseudophilautus folicola
Anura	Pseudophilautus frankenbergi
Anura	Pseudophilautus fulvus
Anura	Pseudophilautus hallidayi
Anura	Pseudophilautus hoffmanni
Anura	Pseudophilautus limbus
Anura	Pseudophilautus lunatus
Anura	Pseudophilautus macropus
Anura	Pseudophilautus microtympanum
Anura	Pseudophilautus mittermeieri
Anura	Pseudophilautus mooreorum
Anura	Pseudophilautus nemus
Anura	Pseudophilautus ocularis
Anura	Pseudophilautus papillosus
Anura	Pseudophilautus pleurotaenia
Anura	Pseudophilautus poppiae
Anura	Pseudophilautus procax
Anura	Pseudophilautus reticulatus
Anura	Pseudophilautus sarasinorum
Anura	Pseudophilautus schmarda
Anura	Pseudophilautus silus
Anura	Pseudophilautus silvaticus
Anura	Pseudophilautus simba
Anura	Pseudophilautus singu
Anura	Pseudophilautus steineri
Anura	Pseudophilautus stuarti
Anura	Pseudophilautus tanu
Anura	Pseudophilautus wynaadensis
Anura	Pseudophilautus zorro
Anura	Pseudorana weiningensis
Anura	Pterorana khare
Anura	Quasipaa boulengeri
Anura	Quasipaa exilispinosa
Anura	Quasipaa fasciculispina
Anura	Quasipaa jiulongensis

Anura	Quasipaa robertingeri
Anura	Quasipaa shini
Anura	Quasipaa spinosa
Anura	Ramanella mormorata
Anura	Ramanella nagaoi
Anura	Ramanella palmata
Anura	Ramanella triangularis
Anura	Rana chevronta
Anura	Rana longicrus
Anura	Rana sauteri
Anura	Raorchestes bobingeri
Anura	Raorchestes bombayensis
Anura	Raorchestes chalazodes
Anura	Raorchestes charius
Anura	Raorchestes chlorosomma
Anura	Raorchestes chromasynchysi
Anura	Raorchestes dubois
Anura	Raorchestes glandulosus
Anura	Raorchestes graminirupes
Anura	Raorchestes griet
Anura	Raorchestes kaikatti
Anura	Raorchestes marki
Anura	Raorchestes munnarensis
Anura	Raorchestes nerostagona
Anura	Raorchestes ponmudi
Anura	Raorchestes resplendens
Anura	Raorchestes shillongensis
Anura	Raorchestes signatus
Anura	Raorchestes sushili
Anura	Raorchestes tinniens
Anura	Raorchestes travancoricus
Anura	Raorchestes viridis
Anura	Rhacophorus angulirostris
Anura	Rhacophorus annamensis
Anura	Rhacophorus arvalis
Anura	Rhacophorus aurantiventris
Anura	Rhacophorus bimaculatus
Anura	Rhacophorus calcadensis
Anura	Rhacophorus exechopygus

Anura	Rhacophorus fasciatus
Anura	Rhacophorus helenae
Anura	Rhacophorus kio
Anura	Rhacophorus lateralis
Anura	Rhacophorus minimus
Anura	Rhacophorus pseudomalabaricus
Anura	Rhacophorus vampyrus
Anura	Rhacophorus yaoshanensis
Anura	Rhacophorus yinggelingensis
Anura	Sanguirana igorota
Anura	Sanguirana tipanan
Anura	Scutiger chintingensis
Anura	Scutiger gongshanensis
Anura	Scutiger liupanensis
Anura	Scutiger maculatus
Anura	Scutiger muliensis
Anura	Scutiger nepalensis
Anura	Scutiger ningshanensis
Anura	Scutiger pingwuensis
Anura	Scutiger ruginosus
Anura	Scutiger tuberculatus
Anura	Taruga eques
Anura	Taruga longinasus
Anura	Taruga fastigo
Anura	Theloderma bicolor
Anura	Theloderma moloch
Anura	Xanthophryne koynayensis
Anura	Xanthophryne tigerina
Anura	Xenophrys brachykolos
Anura	Xenophrys giganticus
Anura	Xenophrys nankiangensis
Anura	Zakerana greenii
Anura	Zakerana murthii
Anura	Zakerana nilagirica
Caudata	Afghanodon mustersi
Caudata	Andrias davidianus
Caudata	Batrachuperus karlschmidti
Caudata	Batrachuperus londongensis
Caudata	Batrachuperus pinchonii

Caudata	Batrachuperus tibetanus
Caudata	Batrachuperus yenyuanensis
Caudata	Cynops ensicauda
Caudata	Cynops orphicus
Caudata	Echinotriton andersoni
Caudata	Echinotriton chinhaiensis
Caudata	Hynobius abei
Caudata	Hynobius amjiensis
Caudata	Hynobius arisanensis
Caudata	Hynobius boulengeri
Caudata	Hynobius chinensis
Caudata	Hynobius dunni
Caudata	Hynobius formosanus
Caudata	Hynobius hidamontanus
Caudata	Hynobius okiensis
Caudata	Hynobius sonani
Caudata	Hynobius stejnegeri
Caudata	Hynobius takedai
Caudata	Hynobius tokyoensis
Caudata	Hynobius yangi
Caudata	Hynobius yiwuensis
Caudata	Iranodon gorganensis
Caudata	Laotriton laoensis
Caudata	Liua tsinpaensis
Caudata	Mertensiella caucasica
Caudata	Neurergus crocatus
Caudata	Neurergus kaiseri
Caudata	Neurergus microspilotus
Caudata	Pachyhynobius shangchengensis
Caudata	Pachyhynobius yunanicus
Caudata	Paramesotriton deloustali
Caudata	Paramesotriton fuzhongensis
Caudata	Paramesotriton guanxiensis
Caudata	Pseudohynobius flavomaculatus
Caudata	Pseudohynobius shuichengensis
Caudata	Ranodon sibiricus
Caudata	Tylototriton hainanensis
Caudata	Tylototriton kweichowensis
Caudata	Tylototriton notialis

Caudata	Tylototriton wenxianensis
Gymnophiona	Ichthyophis orthoplicatus
Gymnophiona	Ichthyophis pseudangularis

Appendix 4.3 Threatened species range overlap with predicted *Bd* risk in Asia.

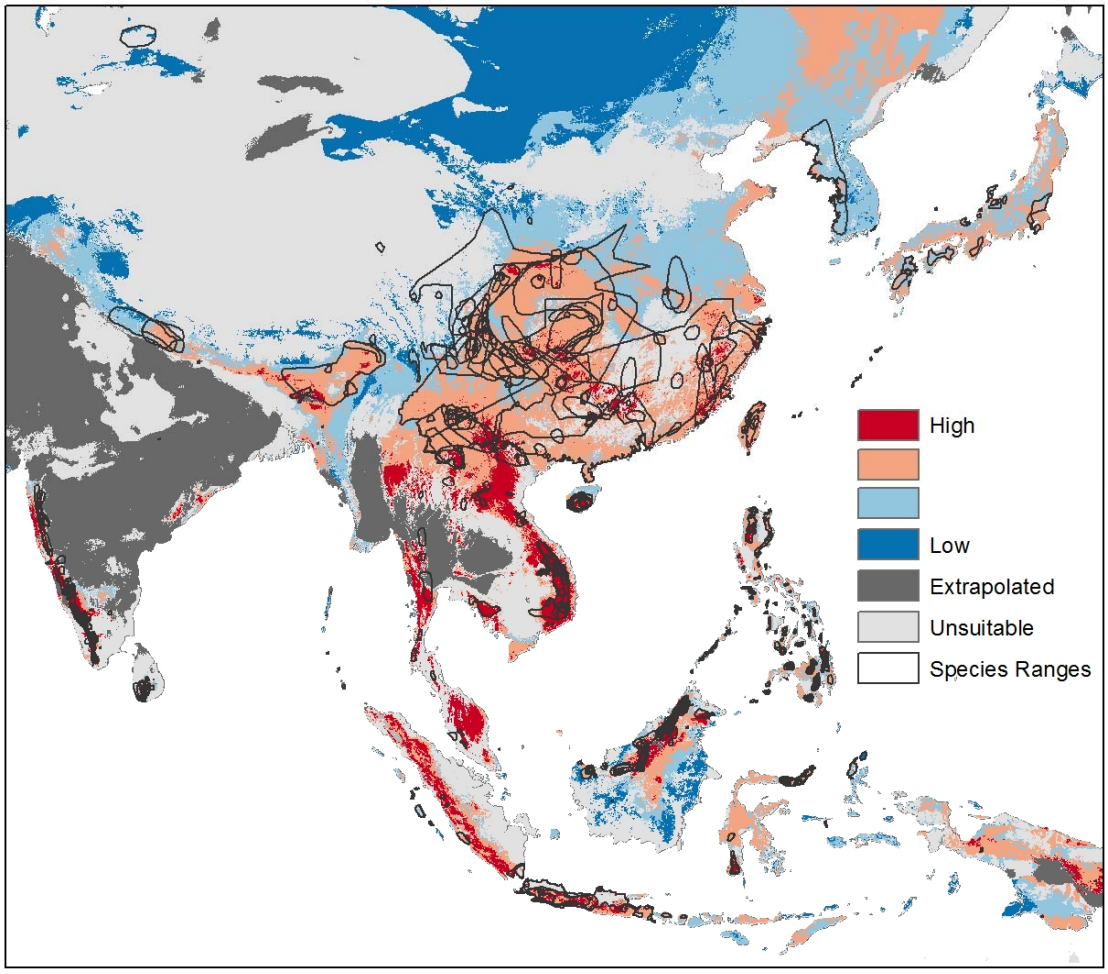

Appendix 4.4 Changes in the area of suitability due to climate change compared to current predictions in Asia for (A) *Bd*, (B) *R. catesbeiana*, and (C) *Bd* and *R. catesbeiana*.

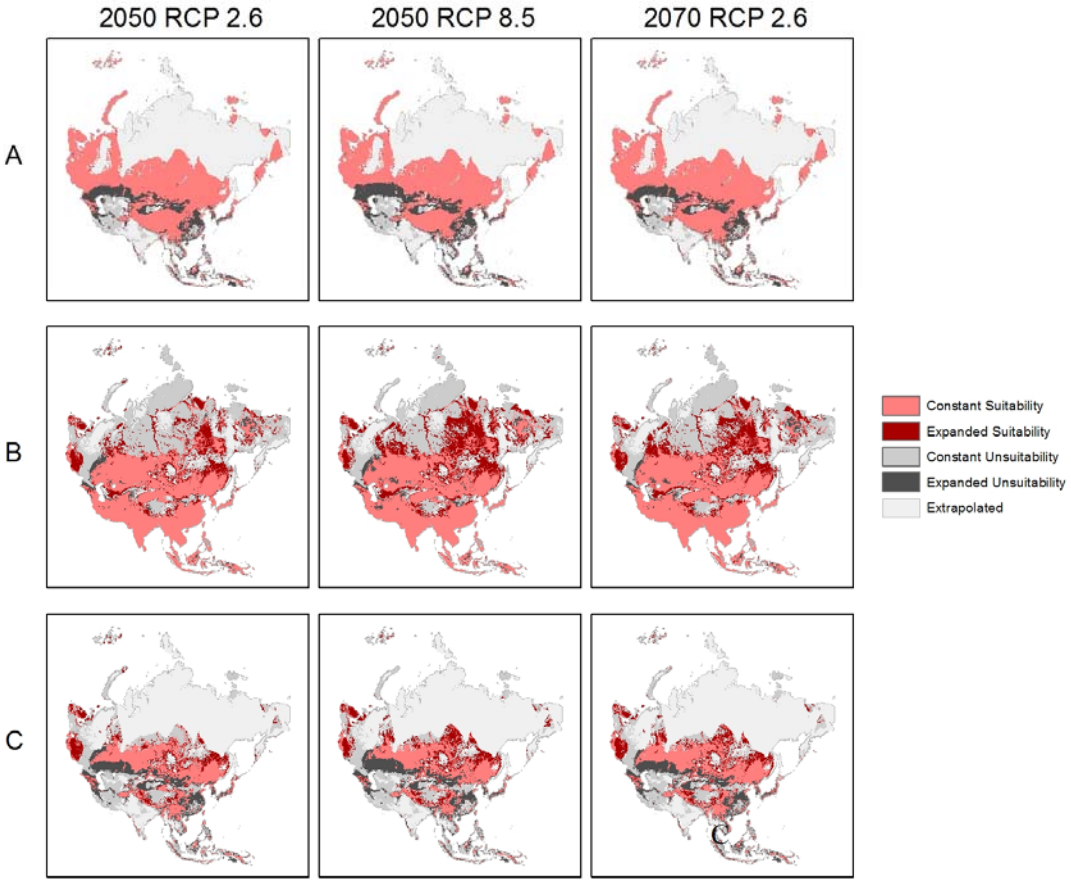

5. CHAPTER 5: Conclusions

Chytridiomycosis is a global crisis. *Bd* and associated declines have been recorded on every continent that amphibians occur on (Olson et al. 2013), and the newly arising *Bsal* expands the threat to amphibian diversity. Using habitat suitability models and vulnerability models as exploratory tools can help us understand past or present impacts of *Bd* and *Bsal* at a scale not possible using traditional field or laboratory-based studies, and they help develop hypotheses to test so we can further our knowledge of these systems. These types of models also help to predict future impacts, which can guide conservation efforts from a local to global scale.

My dissertation demonstrates that despite limited data, there is value in integrating a combination of abiotic and biotic factors with human influences and pathogen invasion history when assessing wildlife disease spread, and we reiterate that increased globalization has led to increased wildlife disease outbreaks around the world (Tompkins et al. 2015; Daszak et al. 2000). Many disease risk studies tend to focus more on abiotic factors like climate and land use conditions (Ron 2005; Lötters et al. 2009; Olson et al. 2013; James et al. 2015; Moriguchi et al. 2015), but some scientists have started to incorporate human influences, such as the presence of invasive species (Liu et al. 2013), the density of pet and pet supply stores (Richgels et al. 2016), and the density of domesticated animals in agriculture (Fuller et al. 2013). The main difficulty with including human influences is that data extending beyond land use, such as wildlife trade information or the locations of captive animals, are limited. This makes it challenging to accurately identify how and to what extent human activities are spreading emerging infectious diseases (EIDs) in wildlife, and it hinders our abilities to discern which areas and species are at greatest risk.

With limited data, correlative models such as those produced by Maxent are useful because they allow us to explore existing data and formulate hypotheses regarding pathogen spread and disease dynamics. The also allow us to estimate the potential spread of an invasive species and the threat of disease based on the best information available. However, it is important to recognize that Maxent models are very sensitive to training data (Rodda et al. 2011; Mainali et al. 2015); therefore, assumptions must be clear and input data must be scrutinized to minimize pseudoreplication, overfitting, and sampling bias while enhancing model accuracy. Without accounting for these modeling issues, predictive models can potentially be misleading. Another important factor to consider when modeling invasive species is having samples from a broad geographic distribution while keeping in mind local historical context. Using occurrence data from both native and invasive populations has been shown to improve model accuracy (Mainali et al. 2015). Also, minimizing the background area around the most concentrated areas of occurrences and limiting the number of background points to be equal to the number of presence points improve model performance (Mainali et al. 2015).

Keeping modeling issues and uncertainties in mind, sometimes innovation and creativity are needed to maximize the usefulness of existing, available data. In North America, we focused on US trade data from the US Fish and Wildlife Service (USFWS) to determine the human-induced threat of *Bsal* introduction and spread because no data were available for Canada or Mexico. We also considered local historical context of pathogen invasion by assuming the potential native range of *Bd* was similar to that of *R. catesbeiana* in the eastern US based on the assumption that *R. catesbeiana* is a known *Bd* carrier and *Bd* seems to be in an enzootic state in the eastern US, with no *Bd*-related declines, presence dating back to the 1880s, and a prevalence

of about 20% (Talley et al. 2015). This enabled us to identify areas with invasive risk in the mountains of the western US and throughout Mexico. This approach also helped us to uncover a new pattern in *Bd* dynamics that suggests that *Bd*-GPL (or its preceding strain) may have originated in the eastern US and the translocation of *R. catesbeiana* by humans may have played a major role in *Bd* spread in North America. Of course, our models only help identify potential trends in the available data; more studies are needed to test these predictions and hypotheses.

In Asia, trade data are even more limited than those in North America. Liu et al. (2013) used global trade data and frog leg trade data at the country level for their *Bd* model because live amphibian trade data were not available. However, data at such a coarse resolution may not reflect the influence of live amphibian trade and *Bd* requires live hosts to thrive. Therefore, to represent the potential impacts of live trade on *Bd* spread we used the potential presence of *R. catesbeiana* because it is a known *Bd* carrier that likely facilitates *Bd* spread (Hanselmann et al. 2004; Garner et al. 2006; Fisher & Garner 2007; Schloegel et al. 2012; Liu et al. 2013) (see Chapter 2), it is popular in trade, and *Bd* has been detected in *R. catesbeiana* in Asia in established wild populations as well as on farms and in markets (Goka et al. 2009; Yang et al. 2009; Bai et al. 2010; Bai et al. 2012; Fong et al. 2015; Zhu et al. 2016). Thus, we were able to incorporate both a highly influential human activity and an ecologically relevant host species in our *Bd* vulnerability model in Asia. We then incorporated amphibian richness under the assumption that increased richness could lead to increased disease spread when a competent reservoir is present (Power & Mitchell 2004; Keesing et al. 2010). From our analyses, we found that both the potential presence of *R. catesbeiana* and amphibian richness may play a role in *Bd* spread in Asia, with the highest relative risk occurring in the tropical montane regions of

southern China, Southeast Asia, the Pacific Islands, where most of Asia's threatened species occur. Again, additional studies are needed to test these predictions and hypotheses.

Despite limited data, it is clear that international amphibian trade has led to the globalization of *Bd* and will likely continue spreading *Bd* and *Bsal* around the world. Pathogen spread is mostly facilitated by inadequate biosecurity, which is a result of the extreme lack of infrastructure and disregard of wildlife EID management. Policy and research efforts are biased towards human zoonoses and diseases that threaten domestic livestock, as evidenced by the World Organization for Animal Health (OIE). The OIE has taken on the responsibility of fighting against animal diseases at a global level, yet very few wildlife EIDs are monitored by this agency. The OIE listed *Bd* as a "notifiable" disease a decade after it was first described and after at least 200 amphibian species experienced declines and extinctions (Alroy 2015; Fisher et al. 2009; Skerratt et al. 2007). The listing requires member countries to report the occurrence of known *Bd* infections and implement OIE recommendations. However, this delayed reaction with minimal enforcement has done little, if anything, to prevent, or even track, the continuous spread of *Bd*. There are still no requirements for amphibians to be tested for *Bd* prior to import/export, and there are no quarantine or treatment standards for infected animals in place. The same is true for *Bsal*, which has not yet been listed by the OIE as a "notifiable" disease. The shortcomings of the OIE regarding wildlife EIDs impede our abilities to effectively respond to *Bd*, *Bsal*, or other wildlife disease outbreaks.

Another source of inadequate biosecurity is unregulated and untracked international amphibian trade, which provides repeated opportunities for various *Bd* strains and *Bsal* to be introduced around the world. The only internationally recognized system that somewhat holds

countries accountable for wildlife trade is the Convention on International Trade in Endangered Species of Wild Fauna and Flora (CITES), which has limited functionality and enforcement. CITES only requires records for 146 out of over 7,500 amphibian species, and no records are required for known *Bd* or *Bsal* carriers. Countries volunteer to participate in the agreement, and instead of having a standardized protocol, each country chooses how to implement the CITES guidelines, which makes any available data incomparable for analyses. The scarcity of amphibian records combined with inconsistent documentation and poor regulation exacerbate the deficiencies in global biosecurity.

Non-existent international protocols to respond to wildlife EIDs and no international entity to implement or enforce any policies if they existed demonstrate the need for improved biosecurity. Without these, countries are left to determine the best course of action on their own with practically no international support. And because little attention is given to wildlife diseases, most countries lack relevant policies or infrastructure for risk assessment. This can lead to slow and varying responses, if any, as evidenced by the current international response to *Bsal*. In Europe, Switzerland was the first and only country to take strong preventive action, banning all salamander imports since early 2015. In the Netherlands, where the first *Bsal* outbreaks were documented, officials focus on surveillance and monitoring in the wild and only conduct passive screening of imported animals. And in Belgium, where *Bsal* outbreaks have also occurred, they have only established safety protocols and surveillance programs. The UK and Germany have yet to take official action despite discovering *Bsal* in trade animals (Cunningham et al. 2015; Sabino-Pinto et al. 2015), and in the wild (Spitzen-van der Sluijs et al. 2016). In December 2015 the European Council recommended immediate salamander trade restrictions, pre-import

screening for infectious diseases in live animal trade, the establishment of monitoring and surveillance programs, the application of biosafety rules in the field and in captive collections, and the development of emergency action plans, though it is unclear how or when these recommendations will be implemented.

In January 2016, about six months after we published Chapter 1: Averting a North American Biodiversity Crisis in *Science* (Yap et al. 2015) and over a year since *Bsal* was shown to be a significant threat to at least two salamander species in the US (Martel et al. 2014), the USFWS announced an interim rule that lists 201 salamander species as "injurious" to wildlife due to the risk of *Bsal* under the Lacey Act (USFWS 2016). The ruling states that the import or interstate trade of listed species (live, dead, or parts) is prohibited, though permits may be granted for scientific, medical, educational, or zoological purposes. This came surprisingly fast given the average time it takes the USFWS to list a species as "injurious" is over four years (Fowler et al. 2007). In fact, in 2009 Defenders of Wildlife petitioned the USFWS to list all live amphibians as "injurious" under the Lacey Act to address the *Bd* pandemic, and after seven years a decision regarding this matter has yet to be made. In addition, the Lacey Act was not written for wildlife disease prevention, and it does not allow the USFWS to list pathogens as "injurious." This is only the second time they have used the listing of vector species to prevent wildlife pathogen spread (Kolby & Daszak 2016). Thus, this unprecedented listing reflects the seriousness with which the USFWS regards the potential spread of *Bsal* in the United States.

While the listing is a breakthrough for biodiversity conservation in the US, there are still major limitations. Amphibians and pathogens do not respect administrative boundaries, and the introduction of *Bsal* via Canada or Mexico could still eventually spread to species in the US. We

have already seen this type of spread with *Bsal* in Europe, where within five years outbreaks in the wild have spread from the Netherlands to Belgium and Germany (Martel et al. 2014; Spitzen-van der Sluijs et al. 2016). This has also been seen with *Bd* spreading in a wave-like pattern in the Americas (Lips et al. 2008; Vredenburg et al. 2010; Cheng et al. 2011). And once established, it is difficult, if not impossible, to remove these pathogens. A coordinated, international effort would be more effective for both disease prevention and mitigation.

Another issue is that the USFWS listing does not include all species being imported into the US, particularly from the family Salamandridae. All Salamandrid genera tested (12 out of 20 genera) were found to be susceptible to *Bsal* infection (Martel et al. 2014), which suggests that all Salamandrid species have the potential to be at least carriers. In addition, pathogen spillover from captive salamander collections and underground salamander trade could occur. So despite the listing, there are still possible pathways for *Bsal* to spread.

Perhaps the devastating amphibian declines caused by the *Bd* pandemic have motivated some agencies to respond more quickly to the threat of *Bsal* using the legislative tools available to them. However, this piecemeal approach is not enough to safeguard against *Bd*, *Bsal*, or any other wildlife EIDs. These issues highlight the urgent need for specific national and international legislation regarding EIDs in wildlife, as well as an international agency that will hold countries accountable. Scientists must work with policymakers and the wildlife trade industry to enhance global biosecurity and help prevent the spread of chytridiomycosis and other wildlife EIDs. It may be helpful to use existing platforms for human diseases and zoonoses, such as the World Health Organization (WHO), as a template to build a wildlife disease response network. Through International Health Regulations, the WHO coordinates international collaboration and the

sharing of resources and information to prevent, detect, report, and respond to public health crises. They also support targeted research and development for human disease diagnostics and treatments. A similar system for wildlife EIDs would facilitate a more cohesive, global effort for wildlife disease management and biodiversity conservation.

Other existing infrastructure that may be helpful for wildlife EID prevention and management include those created for agricultural pests and diseases. The US Department of Agriculture's Animal and Plant Health Inspection Service (APHIS) is responsible for preventing the introduction or spread of pests, diseases, and invasive species that threaten US agriculture, and to some extent, the greater environment. They develop and implement strategies for pest and disease prevention, detection, surveillance, and mitigation through the facilitation of various management and research programs. They also work with federal and state agencies, foreign governments, industry and others to monitor and regulate the international trade of plants and animals. Perhaps the US could expand APHIS's responsibilities or establish another department that focuses on EIDs in wildlife.

Admittedly, there are still many questions regarding *Bd*, *Bsal*, and the chytrid disease system that limit our abilities to design and implement effective mitigation strategies (Kolby & Daszak 2016). This is understandable for *Bsal* because it was just recently discovered, and more time is needed to investigate its basic biology and host-pathogen dynamics. However, we may have caught *Bsal* early and so far the outbreaks appear to be isolated in Europe. With *Bd*, there are still many unanswered questions regarding its disease dynamics despite almost two decades of research. We still do not know its place of origin or the timeline of its global emergence, where and how it persists outside of the host, why some strains are more virulent than others, or

why some species succumb to disease while others remain unaffected (Kolby & Daszak 2016). These uncertainties are exacerbated by an overwhelming data gap regarding human activities. Not only has international amphibian trade been left unabated despite the known presence of highly lethal pathogens, but there is also little record of how globalization has spread and continues to spread *Bd*, *Bsal*, and other wildlife pathogens. Regardless of this uncertainty, there is undeniable evidence that *Bd* and *Bsal* are a significant threat to amphibians, with human globalization as a primary driver of their spread. Therefore, we must start prioritizing the proactive prevention and management of EIDs in wildlife.

References

Alroy, J., 2015. Current extinction rates of reptiles and amphibians. *Proceedings of the National Academy of Sciences*, 2015, p.201508681. Available at: http://www.pnas.org/lookup/doi/10.1073/pnas.1508681112.

AmphibiaWeb, 2015. Information on amphibian biology and conservation [web application]. Available at: http://amphibiaweb.org/.

Araújo, M.B. & New, M., 2007. Ensemble forecasting of species distributions. *Trends in Ecology and Evolution*, 22(1), pp.42–47. Available at: http://www.ncbi.nlm.nih.gov/pubmed/17011070.

Bai, C. et al., 2012. Global and endemic Asian lineages of the emerging pathogenic fungus *Batrachochytrium dendrobatidis* widely infect amphibians in China. *Diversity and Distributions*, 18(3), pp.307–318. Available at: http://doi.wiley.com/10.1111/j.1472-4642.2011.00878.x [Accessed May 28, 2014].

Bai, C., Garner, T.W.J. & Li, Y., 2010. First evidence of *Batrachochytrium dendrobatidis* in China: Discovery of chytridiomycosis in introduced American bullfrogs and native amphibians in the Yunnan Province, China. *EcoHealth*, 7, pp.127–134.

Bales, E.K. et al., 2015. Pathogenic Chytrid Fungus *Batrachochytrium dendrobatidis*, but not B. salamandrivorans, Detected on Eastern Hellbenders. *PLoS ONE*, 10(2), p.e0116405. Available at: http://dx.plos.org/10.1371/journal.pone.0116405.

Bataille, A. et al., 2013. Genetic evidence for a high diversity and wide distribution of endemic strains of the pathogenic chytrid fungus *Batrachochytrium dendrobatidis* in wild Asian amphibians. *Molecular ecology*, 22(16), pp.4196–209. Available at:

http://www.ncbi.nlm.nih.gov/pubmed/23802586 [Accessed June 19, 2014].

Best, M.L. & Welsh, Jr., H.H., 2014. The trophic role of a forest salamander: impacts on invertebrates, leaf litter retention, and the humification process. *Ecosphere*, 5(2), pp.1–19. Available at: http://www.esajournals.org/doi/abs/10.1890/ES13-00302.1.

Bickford, D. et al., 2010. Impacts of climate change on the amphibians and reptiles of Southeast Asia. *Biodiversity and Conservation*, 19(4), pp.1043–1062.

Bielby, J. et al., 2015. Host species vary in infection probability, sub-lethal effects, and costs of immune response when exposed to an amphibian parasite. *Scientific Reports*, 5(April), p.10828. Available at: http://www.nature.com/doifinder/10.1038/srep10828.

Bivand, R. & Lewin-Koh, N., 2014. maptools: Tools for reading and handling spatial objects. Available at: http://cran.r-project.org/package=maptools.

Blooi, M. et al., 2013. Duplex real-time PCR for rapid simultaneous detection of *Batrachochytrium dendrobatidis* and *Batrachochytrium salamandrivorans* in amphibian samples. *Journal of Clinical Microbiology*, 51(12), pp.4173–4177.

Blooi, M. et al., 2015. Successful treatment of *Batrachochytrium salamandrivorans* infections in salamanders requires synergy between voriconazole, polymyxin E and temperature. *Scientific Reports*, 5(March), p.11788. Available at: http://www.nature.com/doifinder/10.1038/srep11788.

Blooi, M. et al., 201. Treatment of urodelans based on temperature dependent infection dynamics of *Batrachochytrium salamandrivorans*. *Scientific Reports*, 5(8037), pp.1–4.

Boria, R.A. et al., 2014. Spatial filtering to reduce sampling bias can improve the performance of ecological niche models. *Ecological Modelling*, 275, pp.73–77. Available at:

http://dx.doi.org/10.1016/j.ecolmodel.2013.12.012.

Bradford, D.F., 1991.Mass mortality and extinction in a high-elevation population of *Rana muscosa*. *Journal of Herpetology*, 25(2), pp.174–177.

Briggs, C.J., Knapp, R.A. & Vredenburg, V.T., 2010. Enzootic and epizootic dynamics of the chytrid fungal pathogen of amphibians. *Proceedings of the National Academy of Sciences of the United States of America*, 107(21), pp.9695–9700. Available at: http://www.pubmedcentral.nih.gov/articlerender.fcgi?artid=2906864&tool=pmcentrez&rendertype=abstract [Accessed May 31, 2014].

Chan, B.H., Zhang, H. & Fischer, G., 2015. Improve customs systems to monitor global wildlife trade. *Science*, 348(6232), pp.291–292.

Chatfield, M.W.H., Moler, P. & Richards-Zawacki, C.L., 2012. The amphibian chytrid fungus, *Batrachochytrium dendrobatidis*, in fully aquatic salamanders from southeastern North America. *PLoS ONE*, 7(9), pp.1–5. Available at: http://www.pubmedcentral.nih.gov/articlerender.fcgi?artid=3439441&tool=pmcentrez&rendertype=abstract.

Chen, J., Brissette, F.P. & Leconte, R., 2011. Uncertainty of downscaling method in quantifying the impact of climate change on hydrology. *Journal of Hydrology*, 401(3-4), pp.190–202. Available at: http://dx.doi.org/10.1016/j.jhydrol.2011.02.020.

Cheng, T.L. et al., 2011. Coincident mass extirpation of neotropical amphibians with the emergence of the infectious fungal pathogen *Batrachochytrium dendrobatidis*. *Proceedings of the National Academy of Sciences of the United States of America*, 108(23), pp.9502–9507. Available at:

http://www.pubmedcentral.nih.gov/articlerender.fcgi?artid=3111304&tool=pmcentrez&rendertype=abstract [Accessed June 7, 2014].

Cunningham, A.A. et al., 2015. Emerging disease in UK amphibians. *Veterinary Record*, 176(18), pp.468–468. Available at: http://veterinaryrecord.bmj.com/cgi/doi/10.1136/vr.h2264.

Daszak, P., Cunningham, A. a. & Hyatt, A.D., 2000. Emerging infectious diseases of wildlife: threats to biodiversity and human health. *Science*, 287(January), pp.443–449. Available at: http://eprints.kingston.ac.uk/2526/.

Davidson, C. et al., 2013. Anuran population declines occur on an elevational gradient in the western hemisphere. *Herpetological Conservation and Biology*, 8(3), pp.503–518.

Davidson, C. et al., 2007. Effects of chytrid and carbaryl exposure on survival, growth and skin peptide defenses in foothill yellow-legged frogs. *Environmental Science and Technology*, 41(5), pp.1771–1776.

Diesmos, A.C., Diesmos, M.L. & Brown, R.M., 2006. Status and distribution of alien invasive frogs in the Philippines. *Journal of Environmental Science and Management*, 9(December), pp.41–53.

DiRenzo, G. V. et al., 2014. Fungal infection intensity and zoospore output of *Atelopus zeteki*, a potential acute chytrid supershedder. *PLoS ONE*, 9(3), p.e93356. Available at: http://dx.plos.org/10.1371/journal.pone.0093356 [Accessed June 2, 2014].

Farrer, R. et al., 2011. Multiple emergences of genetically diverse amphibian-infecting chytrids include a globalized hypervirulent recombinant lineage. *Proceedings of the National Academy of Sciences of the United States of America*.

Ficetola, G.F. et al., 2010. Knowing the past to predict the future: land-use change and the distribution of invasive bullfrogs. *Global Change Biology*, 16(2), pp.528–537. Available at: http://doi.wiley.com/10.1111/j.1365-2486.2009.01957.x.

Ficetola, G.F., Thuiller, W. & Miaud, C., 2007. Prediction and validation of the potential global distribution of a problematic alien invasive species - the American bullfrog. *Diversity and Distributions*, 13(4), pp.476–485. Available at: http://doi.wiley.com/10.1111/j.1472-4642.2007.00377.x [Accessed May 23, 2014].

Fisher, M.C. et al., 2012. Emerging fungal threats to animal, plant and ecosystem health. *Nature*, 484(7393), pp.186–94. Available at: http://www.pubmedcentral.nih.gov/articlerender.fcgi?artid=3821985&tool=pmcentrez&rendertype=abstract [Accessed May 27, 2014].

Fisher, M.C. et al., 2009. Proteomic and phenotypic profiling of the amphibian pathogen *Batrachochytrium dendrobatidis* shows that genotype is linked to virulence. *Molecular Ecology*, 18(3), pp.415–429.

Fisher, M.C. & Garner, T.W.J., 2007. The relationship between the emergence of *Batrachochytrium dendrobatidis*, the international trade in amphibians and introduced amphibian species. *Fungal Biology Reviews*, 21(1), pp.2–9. Available at: http://linkinghub.elsevier.com/retrieve/pii/S1749461307000085 [Accessed May 28, 2014].

Fites, J.S. et al., 2013. The invasive chytrid fungus of amphibians paralyses lymphocyte responses. *Science*, 342(2013), pp.366–369.

Foden, W.B. et al., 2013. Identifying the world's most climate change vulnerable species: A systematic trait-based assessment of all birds, amphibians and corals. *PLoS ONE*, 8(6).

Fong, J.J. et al., 2015. Early 1900s Detection of *Batrachochytrium dendrobatidis* in Korean amphibians. *PLoS ONE*, 10(3), p.e0115656. Available at: http://dx.plos.org/10.1371/journal.pone.0115656.

Fowler, A.J., Lodge, D.M. & Hsia, J.F., 2007. Failure of the Lacey Act to protect US ecosystems against animal invasions. *Frontiers in Ecology and the Environment*, 5(7), pp.353–359.

Fuller, T.L. et al., 2013. Predicting hotspots for influenza virus reassortment. *Emerging Infectious Diseases*, 19(4), pp.581–588.

Garner, T.W.., Perkins, M.W., Govindarajulu, P., Seglie, D., Walker, S., Cunningham, A.A., et al., 2006. The emerging amphibian pathogen *Batrachochytrium dendrobatidis* globally infects introduced populations of the North American bullfrog, *Rana catesbeiana*. *Biology Letters*, 2(3), pp.455–459. Available at: http://rsbl.royalsocietypublishing.org/cgi/doi/10.1098/rsbl.2006.0494.

Garner, T.W.., Perkins, M.W., Govindarajulu, P., Seglie, D., Walker, S., Cunningham, a. a, et al., 2006. The emerging amphibian pathogen *Batrachochytrium dendrobatidis* globally infects introduced populations of the North American bullfrog, *Rana catesbeiana*. *Biology Letters*, 2(3), pp.455–459. Available at: http://rsbl.royalsocietypublishing.org/cgi/doi/10.1098/rsbl.2006.0494.

Goka, K. et al., 2009. Amphibian chytridiomycosis in Japan: Distribution, haplotypes and possible route of entry into Japan. *Molecular Ecology*, 18(23), pp.4757–4774.

Govindarajulu, P., Price, S.J. & Anholt, B.R., 2006. Introduced bullfrogs (*Rana catesbeiana*) in western Canada: has their ecology diverged? *Journal of Herpetology*, 40, pp.249–260.

Grant, E.H.C. et al., 2016. Quantitative evidence for the effects of multiple drivers on

continental-scale amphibian declines. *Scientific*, 6, pp.1–9.

Graves, B.M. & Anderson, S.H., 1987. *Habitat suitability index models: bullfrog*. (No. 82/10.138). US Fish and Wildlife Service.

Hanselmann, R. et al., 2004. Presence of an emerging pathogen of amphibians in introduced bullfrogs *Rana catesbeiana* in Venezuela. *Biological Conservation*, 120(1), pp.115–119. Available at: http://linkinghub.elsevier.com/retrieve/pii/S0006320704000564 [Accessed June 4, 2014].

Harding, J.H., 1997. *Amphibians and reptiles of the Great Lakes region*, University of Michigan Press.

Hijmans, R.J. et al., 2013. dismo: Species distribution modeling. Available at: http://cran.r-project.org/package=dismo.

Hijmans, R.J., 2014. raster: Geographic data analysis and modeling. Available at: http://cran.r-project.org/package=raster.

Hijmans, R.J. et al., 2005. Very high resolution interpolated climate surfaces for global land areas. *International Journal of Climatology*, 25(15), pp.1965–1978.

Huss, M. et al., 2013. Prevalence of *Batrachochytrium dendrobatidis* in 120 archived specimens of Lithobates catesbeianus (American bullfrog) collected in California, 1924-2007. *EcoHealth*, 10(4), pp.339–343. Available at: http://www.ncbi.nlm.nih.gov/pubmed/24419668 [Accessed June 18, 2014].

IUCN, 2016. The IUCN red list of threatened species. *World Conservation Union*. Available at: www.iucnredlist.org.

James, T.Y. et al., 2015. Disentangling host, pathogen, and environmental determinants of a

recently emerged wildlife disease: lessons from the first 15 years of amphibian chytridiomycosis research. *Ecology and Evolution*, 5(18), pp.4079–4097. Available at: http://doi.wiley.com/10.1002/ece3.1672.

Jenks, G.F., 1967. The data model concept in statistical mapping. *International Yearbook of Cartography*, 7(1), pp.186–190.

Keesing, F. et al., 2010. Impacts of biodiversity on the emergence and transmission of infectious diseases. *Nature*, 468(7324), pp.647–652. Available at: http://dx.doi.org/10.1038/nature09575.

Keesing, F., Holt, R.D. & Ostfeld, R.S., 2006. Effects of species diversity on disease risk. *Ecology Letters*, 9(4), pp.485–498.

Kolby, J.E. & Daszak, P., 2016. The emerging amphibian fungal disease, chytridiomycosis: A key example of the global phenomenon of wildlife emerging infectious diseases. *Microbiology Spectrum*, 4(3), pp.1–17.

Langwig, K.E. et al., 2015. Context-dependent conservation responses to emerging wildlife diseases. *Frontiers in Ecology and the Environment*, 13(4), pp.195–202. Available at: http://www.esajournals.org/doi/10.1890/140241.

Lannoo, M.J., 2005. *Amphibian declines: the conservation status of United States species*, Unversity of California Press.

Larson, E.R. & Olden, J.D., 2012. Using avatar species to model the potential distribution of emerging invaders. *Global Ecology and Biogeography*, 21(11), pp.1114–1125.

Lever, C., 2003. *Naturalized amphibians and reptiles of the world*, New York: Oxford University Press on Demand.

Lillywhite, H.B., 1970. Behavioral temperature regulation in the bullfrog, *Rana catesbeiana*. *Copeia*, pp.158–168.

Lips, K.R. et al., 2006. Emerging infectious disease and the loss of biodiversity in a Neotropical amphibian community. *Proceedings of the National Academy of Sciences of the United States of America*, 103(9), pp.3165–3170.

Lips, K.R. et al., 2008. Riding the wave: Reconciling the roles of disease and climate change in amphibian declines. *PLoS Biology*, 6(3), pp.0441–0454.

Liu, C. et al., 2005. Selecting thresholds of occurrence in the predictions of species distribution. *Ecography*, 28(3), pp.385–393.

Liu, X., Rohr, J.R. & Li, Y., 2013. Climate, vegetation, introduced hosts and trade shape a global wildlife pandemic. *Proceedings of the Royal Society B: Biological Sciences*, 280(1753), p.20122506. Available at: http://www.pubmedcentral.nih.gov/articlerender.fcgi?artid=3574347&tool=pmcentrez&rendertype=abstract.

Lloyd-Smith, J.O. et al., 2005. Superspreading and the effect of individual variation on disease emergence. *Nature*, 438(7066), pp.355–359.

Lötters, S. et al., 2009. The link between rapid enigmatic amphibian decline and the globally emerging chytrid fungus. *EcoHealth*, 6(3), pp.358–372.

Mainali, K.P. et al., 2015. Projecting future expansion of invasive species: Comparing and improving methodologies for species distribution modeling. *Global Change Biology*, 21, pp.4464–4480. Available at: http://doi.wiley.com/10.1111/gcb.13038.

La Marca, E. et al., 2005. Catastrophic population declines and extinctions in neotropical

harlequin frogs (Bufonidae: *Atelopus*). *Biotropica*, 37(2), pp.190–201.

Martel, A. et al., 2013. *Batrachochytrium salamandrivorans* sp. nov. causes chytridiomicosis in amphibians. *Proceedings of the National Academy of Sciences of the United States of America*, 110(38), pp.15325–15329. Available at: http://www.pubmedcentral.nih.gov/articlerender.fcgi?artid=3780879&tool=pmcentrez&rendertype=abstract.

Martel, A. et al., 2014. Recent introduction of a chytrid fungus endangers Western Palearctic salamanders. *Science*, 346(6209), pp.630–631. Available at: http://www.sciencemag.org/cgi/doi/10.1126/science.1258268.

McLeod, D.S. et al., 2008. A survey for chytrid fungus in Thai amphibians. *The Raffles Bulletin of Zoology*, 56(1), pp.199–204.

McMahon, T. a. et al., 2014. Amphibians acquire resistance to live and dead fungus overcoming fungal immunosuppression. *Nature*, 511(7508), pp.224–227. Available at: http://www.nature.com/doifinder/10.1038/nature13491 [Accessed July 9, 2014].

Moriguchi, S. et al., 2015. Predicting the potential distribution of the amphibian pathogen *Batrachochytrium dendrobatidis* in East and Southeast Asia. *Diseases of Aquatic Organisms*, 113(3), pp.177–185. Available at: http://www.int-res.com/abstracts/dao/v113/n3/p177-185/.

Muletz, C. et al., 2014. Unexpected rarity of the pathogen *Batrachochytrium dendrobatidis* in Appalachian Plethodon salamanders: 1957-2011. *PLoS ONE*, 9(8), pp.1–7.

Murray, K. a. et al., 2011. Assessing spatial patterns of disease risk to biodiversity: implications for the management of the amphibian pathogen, *Batrachochytrium dendrobatidis*. *Journal*

of Applied Ecology, 48(1), pp.163–173. Available at: http://doi.wiley.com/10.1111/j.1365-2664.2010.01890.x [Accessed May 23, 2014].

Muths, E. et al., 2003. Evidence for disease-related amphibian decline in Colorado. *Biological Conservation*, 110(3), pp.357–365.

Nori, J. et al., 2011. Climate change and American bullfrog invasion: What could we expect in South America? *PLoS ONE*, 6(10), pp.1–8.

Olson, D.H. et al., 2013. Mapping the global emergence of *Batrachochytrium dendrobatidis*, the amphibian chytrid fungus. *PloS ONE*, 8(2), p.e56802. Available at: http://www.pubmedcentral.nih.gov/articlerender.fcgi?artid=3584086&tool=pmcentrez&rendertype=abstract [Accessed May 27, 2014].

Ouellet, M. et al., 2005. Historical evidence of widespread chytrid infection in North American amphibian populations. *Conservation Biology*, 19(5), pp.1431–1441.

Oye, K.A. et al., 2014. Regulating gene drives. *Science (New York, N.Y.)*, 645(6197), pp.6–9. Available at: http://www.ncbi.nlm.nih.gov/pubmed/25035410.

Padgett-Flohr, G.E. & Hopkins, R.L., 2009. *Batrachochytrium dendrobatidis*, a novel pathogen approaching endemism in central California. *Diseases of Aquatic Organisms*, 83(1), pp.1–9.

Parris, M.J. & Beaudoin, J.G., 2004. Chytridiomycosis impacts predator-prey interactions in larval amphibian communities. *Oecologia*, 140(4), pp.626–632.

Parris, M.J. & Cornelius, T.O., 2004. Fungal pathogen causes competitive and developmental stress in larval amphibian communities. *Ecology*, 85(12), pp.3385–3395.

Phillips, S.J., Dudík, M. & Schapire, R.E., 2004. A maximum entropy approach to species distribution modeling. *Proceedings of the twenty-first …*, pp.655–662. Available at:

http://dl.acm.org/citation.cfm?id=1015412.

Phillips, S.J. & Elith, J., 2013. On estimating probability of presence from use – availability or presence – background data. *Ecology*, 94(6), pp.1409–1419.

Piotrowski, J.S., Annis, S.L. & Longcore, J.E., 2004. Physiology of *Batrachochytrium dendrobatidis*, a chytrid pathogen of amphibians. *Mycologia*, 96(1), pp.9–15.

Power, A.G. & Mitchell, C.E., 2004. Pathogen spillover in disease epidemics. *The American Naturalist*, 164(S5) , pp.S79–S89.

Rachowicz, L.J. et al., 2005. The novel and endemic pathogen hypotheses: competing explanations for the origin of emerging infectious diseases of wildlife. *Conservation Biology*, 19(5), pp.1441–1448. Available at: http://doi.wiley.com/10.1111/j.1523-1739.2005.00255.x [Accessed June 4, 2014].

Rahel, F.J. & Olden, J.D., 2008. Assessing the effects of climate change on aquatic invasive species. *Conservation Biology*, 22(3), pp.521–533.

Richgels, K.L.D. et al., 2016. Spatial variation in risk and consequence of *Batrachochytrium salamandrivorans* introduction in the USA. *Royal Society of Open Science*, 3.

Rodda, G.H., Jarnevich, C.S. & Reed, R.N., 2011. Challenges in identifying sites climatically matched to the native ranges of animal invaders. *PLoS ONE*, 6(2).

Rödder, D., Kielgast, J., Bielby, J., Schmidtlein, S., Bosch, J., Garner, T.W.J., et al., 2009. Global amphibian extinction risk assessment for the panzootic chytrid fungus. *Diversity*, 1(1), pp.52–66. Available at: http://www.mdpi.com/1424-2818/1/1/52/ [Accessed June 4, 2014].

Rödder, D., Kielgast, J., Bielby, J., Schmidtlein, S., Bosch, J., Garner, T.W.J., et al., 2009.

Global amphibian extinction risk assessment for the panzootic chytrid fungus. *Diversity*, 1(1), pp.52–66.

Rödder, D., Kielgast, J. & Lötters, S., 2010. Future potential distribution of the emerging amphibian chytrid fungus under anthropogenic climate change. *Diseases of Aquatic Organisms*, 92(2-3), pp.201–7. Available at: http://www.ncbi.nlm.nih.gov/pubmed/21268982 [Accessed May 25, 2014].

Rödder, D., Schulte, U. & Toledo, L.F., 2013. High environmental niche overlap between the fungus *Batrachochytrium dendrobatidis* and invasive bullfrogs (*Lithobates catesbeianus*) enhance the potential of disease transmission in the Americas. *North-Western Journal of Zoology*, 9.

Rodriguez, D. et al., 2014. Long-term endemism of two highly divergent lineages of the amphibian-killing fungus in the Atlantic Forest of Brazil. *Molecular Ecology*, 23(4), pp.774–787. Available at: http://www.ncbi.nlm.nih.gov/pubmed/24471406 [Accessed May 27, 2014].

Ron, S.R., 2005. Predicting the Distribution of the Amphibian Pathogen *Batrachochytrium dendrobatidis* in the New World. *Biotropica*, 37(2), pp.209–221. Available at: http://www.jstor.org/stable/30043173.

Rubbo, M.J. & Kiesecker, J.M., 2005. Amphibian breeding distribution in an urbanized landscape. *Conservation Biology*, 19(2), pp.504–511.

Ryan, R.A., 1943. Growth rates of some ranids under natural conditions. *Copeia*, pp.73–80.

Sabino-Pinto, J. et al., 2015. First detection of the emerging fungal pathogen *Batrachochytrium salamandrivorans* in Germany. *Amphibia-Reptilia*, pp.1–6. Available at:

http://booksandjournals.brillonline.com/content/journals/10.1163/15685381-00003008.

Sanderson, E.W. et al., 2011. Predicting species distributions from small numbers of occurrence records: a test case using cryptic geckos in Madagascar. *Ecography*, 34(1), pp.102–117. Available at: http://www.jstor.org/stable/2461927\nhttp://dx.doi.org/10.1046/j.1461-0248.2000.00143.x\nhttp://dx.doi.org/10.1111/j.1365-2699.2006.01594.x\nhttp://dx.doi.org/10.1111/j.1600-0587.2011.06888.x\nhttp://dx.doi.org/10.1007/s10530-011-9963-4\nhttp://dx.doi.org.

Schloegel, L.M. et al., 2012. Novel, panzootic and hybrid genotypes of amphibian chytridiomycosis associated with the bullfrog trade. *Molecular Ecology*, 21(21), pp.5162–5177.

Sette, C.M., Vredenburg, V.T. & Zink, A.G., 2015. Reconstructing historical and contemporary disease dynamics: A case study using the California slender salamander. *Biological Conservation*, 192, pp.20–29. Available at: http://linkinghub.elsevier.com/retrieve/pii/S0006320715300896.

Skerratt, L.F. et al., 2007. Spread of chytridiomycosis has caused the rapid global decline and extinction of frogs. *EcoHealth*, 4(2), pp.125–134. Available at: http://link.springer.com/10.1007/s10393-007-0093-5 [Accessed May 27, 2014].

Spitzen-van der Sluijs, A. et al., 2014. Environmental determinants of recent endemism of *Batrachochytrium dendrobatidis* infections in amphibian assemblages in the absence of disease outbreaks. *Conservation Biology*, 00(0), pp.1–10. Available at: http://www.ncbi.nlm.nih.gov/pubmed/24641583 [Accessed June 8, 2014].

Spitzen-van der Sluijs, A. et al., 2016. Expanding distribution of lethal amphibian fungus

Batrachochytrium salamandrivorans in Europe. *Emerging Infectious Diseases*, 22(7).

Stuart, S.N. et al., 2004. Status and trends of amphibian declines and extinctions worldwide. *Science (New York, N.Y.)*, 306(5702), pp.1783–1786. Available at: http://www.ncbi.nlm.nih.gov/pubmed/15486254 [Accessed May 28, 2014].

Swei, A. et al., 2011. Is chytridiomycosis an emerging infectious disease in Asia? *PloS ONE*, 6(8), p.e23179. Available at: http://www.pubmedcentral.nih.gov/articlerender.fcgi?artid=3156717&tool=pmcentrez&rendertype=abstract [Accessed June 7, 2014].

Talley, B.L. et al., 2015. A century of *Batrachochytrium dendrobatidis* in Illinois amphibians (1888 – 1989). *Biological Conservation*, 182, pp.254–261. Available at: http://dx.doi.org/10.1016/j.biocon.2014.12.007.

Thorne, L.H. et al., 2012. Predictive modeling of spinner dolphin (*Stenella longirostris*) resting habitat in the main Hawaiian Islands. *PLoS ONE*, 7(8), p.e43167. Available at: http://dx.plos.org/10.1371/journal.pone.0043167.

Thuiller, W. et al., 2005. Niche-based modelling as a tool for predicting the risk of alien plant invasions at a global scale. *Global Change Biology*, 11(12), pp.2234–2250. Available at: <Go to ISI>://WOS:000234087300014\nhttp://onlinelibrary.wiley.com/store/10.1111/j.1365-2486.2005.001018.x/asset/j.1365-2486.2005.001018.x.pdf?v=1&t=i199xllm&s=9787505340c872*Bd*761a0e3b6fec2d5842072dcf.

Tompkins, D.M. et al., 2015. Emerging infectious diseases of wildlife: a critical perspective.

Trends in Parasitology, 31(4), pp.149–159. Available at: http://linkinghub.elsevier.com/retrieve/pii/S1471492215000197.

Trabucco, A. & Zomer, R.J., 2010. High-resolution global soil-water balance explicit for climate - standard vegetation and soil conditions. *CGIAR Consortium for Spatial Information*, 2010(June). Available at: http://www.cgiar-csi.org.

US Fish and Wildlife Service, 2016. Injurious wildlife species: Listing salamanders due to risk of salamander chytrid fungus. *Federal Register*, 81(8), pp.1534–1556.

Viparina, S. & Just, J.J., 1975. The life period, growth and differentiation of Rana catesbeiana larvae occurring in nature. *Copeia*, pp.103–109.

Voyles, J. et al., 2014. Moving beyond too little, too late: Managing emerging infectious diseases in wild populations requires international policy and partnerships. *EcoHealth*, pp.2008–2011. Available at: http://www.ncbi.nlm.nih.gov/pubmed/25287279.

Vredenburg, V.T. et al., 2010. Dynamics of an emerging disease drive large-scale amphibian population extinctions. *Proceedings of the National Academy of Sciences of the United States of America*, 107(21), pp.9689–94. Available at: http://www.pubmedcentral.nih.gov/articlerender.fcgi?artid=2906868&tool=pmcentrez&rendertype=abstract [Accessed May 31, 2014].

Vredenburg, V.T. et al., 2013. Prevalence of *Batrachochytrium dendrobatidis* in Xenopus Collected in Africa (1871-2000) and in California (2001-2010). *PLoS ONE*, 8(5), p.e63791. Available at: http://www.pubmedcentral.nih.gov/articlerender.fcgi?artid=3655066&tool=pmcentrez&rendertype=abstract [Accessed May 28, 2014].

Wake, D.B. & Vredenburg, V.T., 2008. Colloquium paper: are we in the midst of the sixth mass extinction? A view from the world of amphibians. *Proceedings of the National Academy of Sciences of the United States of America*, 105, pp.11466–11473.

Whittaker, R.H., 1960. Vegetation of the Siskiyou Mountains, Oregon and California. *Ecological Monographs*, 30(3), pp.279–338. Available at: http://www.esajournals.org/doi/abs/10.2307/1943563\nhttp://www.esajournals.org/action/showCitFormats?doi=10.2307/1943563.

Wickham, H. & Francois, R., 2014. dplyr: A grammar of data manipulation. Available at: http://cran.r-project.org/package=dplyr.

Willis, Y.L., Moyle, P.B. & Baskett, T.S., 1956. Emergence, breeding, hibernation, movements, and transformations of bullfrogs, Rana catesbeiana, in Missouri. *Copeia*, pp.30–35.

Xie, G.Y., Olson, D.H. & Blaustein, A.R., 2016. Projecting the Global Distribution of the Emerging Amphibian Fungal Pathogen, *Batrachochytrium dendrobatidis*, Based on IPCC Climate Futures. *PLoS ONE*, 11(8), p.e0160746. Available at: http://dx.plos.org/10.1371/journal.pone.0160746.

Yang, H. et al., 2009. First detection of the amphibian chytrid fungus *Batrachochytrium dendrobatidis* in free-ranging populations of amphibians on mainland Asia: survey in South Korea. *Diseases of Aquatic Organisms*, 86, pp.9–13. Available at: http://www.int-res.com/abstracts/dao/v86/n1/p9-13/.

Yap, T.A. et al., 2015. Averting a North American biodiversity crisis. *Science*, 349(6247), pp.481–482.

Yap, T.A. et al., 2016. Invasion of the Fungal Pathogen *Batrachochytrium dendrobatidis* on

California Islands. *EcoHealth*, 13(1), pp.145-150. Available at: http://link.springer.com/10.1007/s10393-015-1071-y.

Zhu, W. et al., 2014. A survey for *Batrachochytrium salamandrivorans* in Chinese amphibians. *Current Zoology*, 60(6), pp.729-735.

Zhu, W. et al., 2016. Filling a gap in the distribution of *Batrachochytrium dendrobatidis*: evidence in amphibians from northern China. *Diseases of Aquatic Organisms*, 118(3), pp.259–265. Available at: http://www.int-res.com/abstracts/dao/v118/n3/p259-265/.

Zomer, R.J. et al., 2008. Climate change mitigation: A spatial analysis of global land suitability for clean development mechanism afforestation and reforestation. *Agriculture, Ecosystems and Environment*, 126(1-2), pp.67–80.

Zomer, R.J. et al., 2007. *Trees and Water: Smallholder Agroforestry on Irrigated Lands in Northern India*, Colombo, Sri Lanka.